The internal color degrees of freedom for the weakly interacting quarks and gluons

Ismail Zakout

ITP and FIAS, Frankfurt university, Frankfurt am main, Germany

(Dated: March 30, 2010)

arXiv:1003.2018v2 [nucl-th] 27 Mar 2010

Abstract

When the phase transition from the hadronic matter to the deconfined quark-gluon plasma or quark-gluon liquid is reached, the color degrees of freedom become important and appear explicitly in the equation of state. Under the extreme conditions, the color degrees of freedom can not decouple from the other degrees of freedom. The conservation of color charges is maintained by introducing the color chemical potentials and their fugacities. We demonstrate the explicit role of color degrees of freedom in the hot and dense matter of the weakly interacting quarks and gluons. In order to illustrate our approach, we calculate the effective colored quark and gluon propagators as well as the hard thermal colored quark and gluon loops. The calculations are preformed under the assumption of the hard thermal loop approximation. Finally, we present the decay rate for the hard thermal colored quark. The present calculation is relevant to the quarks and gluons which are not truly deconfined quark-gluon plasma and behave as a fluid in the RHIC energy. The model can be explored in the LHC energy.

I. INTRODUCTION

The phase transition diagram from the hadronic phase to the quark-gluon plasma is very rich and non-trivial. It is thought that when the hadronic matter is compressed and cooled down at extreme baryonic densities it undergoes phase transition to new forms of strongly interacting matter such as the color superconducting quark matter and the color-flavor locked matter. On the other hand, when the hadronic matter is heated up to high temperatures at low baryonic density, it undergoes smooth phase transition or multiple phase transitions to the quark-gluon fluid at extreme temperature before explosive and true deconfined quark-gluon plasma emerges in the system [1–3] [4–6]. Moreover, it is suggested that there is a possibility for the existence of a new class of matter, namely quarkyonic, with a specific internal structure when the system is heated up at intermediate baryonic density. The quarkyonic (i.e. Hagedorn) matter corresponds to non-deconfined and weakly interacting quark and gluon blobs which maintain specific internal symmetries (with color-singlet states). It is reasonable to imagine the existence of such intermediate hadronic phases in order to soften the equation of state below the borderline of the true deconfined quark-gluon plasma. There is a strong argument that the deconfinement phase transition diagram has a critical point and underneath that point the hadronic matter undergoes a higher order phase transition to the Hagedorn matter at extreme temperature and it could be followed by multi phase transition precesses prior to the eventual deconfinement phase transition to quark-gluon plasma [1–6]. The role of the Hagedorn matter in RHIC has been considered in Refs. [7–10]

The quark-gluon plasma is found a perfect fluid with a low viscosity. This discovery means that the quark-gluon plasma is a weakly interacting matter of quarks and gluons rather to be free mobile quark-gluon plasma. Since at sufficiently high temperature the effective gauge running coupling constant is small, the system of the weakly coupled quarks and gluons can be treated by perturbative methods due to the asymptotic freedom in QCD. The thermal calculations is preformed by a version of the thermal perturbation theory that has been developed and improved by several people. A nice review of the field theory at finite temperature and density is given by Landsman and van Weert [11]. The procedure has been significantly improved and extended by Braaten and Pisarski in order to improve the convergence for the higher order loop calculations [12–17]. The physics of the ther-

mal QCD is reviewed in Ref. [18]. This theory is based on the hard thermal loop (HTL) re-summation program instead of relying on the bare Green functions. The HTL approximation is equivalent to the leading term of the high temperature expansion of the diagram under consideration. Excellent review for the collective dynamics and hard thermal loops is given by Blaizot and Iancu [19]. Fortunately, the standard version of the HTL re-summation program is sufficient to calculate the dynamical quantities such as the quasi-particle properties and the production and loss rates. However, the standard re-summation program in the thermal perturbation theory may not work at certain order of the running coupling constant because of the inherently non-perturbative effects of non-Abelian gauge theories. For instance, there are some calculations, such as the production rate of real photons in the plasma, are associated with the non-perturbative effect. In this case, the convergence of the re-summation procedure must be considered carefully [20, 21]. However, the non-perturbative effect does not affect much on the physical quantities which are considered in the present work. Consequently, the standard HTL re-summation program is sufficient to illustrate our approach how to include to color degrees of freedom explicitly in the calculation. This can be generalized to the non-perturbative calculation. The effective field at finite density [22, 23] and thermal field with a specific group symmetry in the lattice have been considered [24].

The explicit color degrees of freedom and the underlying internal color symmetry group of the quarks and gluons are supposed to be crucial in the deconfinement phase transition diagram in particular in the intermediate phases such as the Hagedorn, quarkyonic or quark-gluon fluid. Those intermediate phases are supposed to be located above the low-lying hadronic matter and just below the explosive deconfined quark-gluon plasma. Furthermore, the effect of weakly interacting colored quarks and gluons becomes important above the deconfinement phase transition borderline to quark-gluon plasma in particular when the medium becomes ultra-extreme hot and/or dense. The color degrees of freedom are the non-Abelian charges in QCD. They are parameterized by the eigenvalues of the $SU(N_c)$ symmetry group and their eigenvectors are given by diagonal generators. The quarks carry N_c fundamental color charges while the gluons carry $N_c^2 - 1$ adjoint color charges. The conservation of the fundamental and adjoint color charges is maintained by the fundamental and adjoint imaginary chemical potentials, namely, $i\,\theta_i$ and $i\,\phi^a$ for quarks and gluons, respectively. The fundamental and adjoint color indexes i and a, respectively, run over

$i = 1, \cdots, N_c$ and $a = 1, \cdots, N_c^2 - 1$, respectively. The adjoint color chemical potentials are related to the fundamental ones in the following way,

$$\begin{aligned} \phi^a &= \phi^{\underbrace{(AB)}}, \\ &= (\theta_A - \theta_B), \end{aligned} \tag{1}$$

with the adjoint representation, namely, $a = \underbrace{(AB)}$ where $A, B = 1, \cdots, N_c$ are fundamental-like indexes and they are given in order to maintain the conservation of the color charges. Furthermore, the imaginary fundamental and adjoint color chemical potentials can be transformed to real ones by applying the Wick rotation procedure as follows

$$i\,\frac{1}{\beta}\,\theta_i \;=\; \mu_{Ci}, \tag{2}$$

and

$$\begin{aligned} i\,\frac{1}{\beta}\,\phi^a &= \mu_C{}^a, \\ i\,\frac{1}{\beta}\,\phi^a &\to i\,\frac{1}{\beta}\,\phi^{\underbrace{(AB)}}, \\ &= i\,\frac{1}{\beta}\,(\theta_A - \theta_B), \\ &= (\mu_{C\,A} - \mu_{C\,B}). \end{aligned} \tag{3}$$

The fugacities of the fundamental and adjoint color charges are given by the fundamental and adjoint real (i.e. not imaginary) color chemical potentials. The real color chemical potentials μ_{Ci} where $i = 1, \cdots, N_c$ are essential to control the color charge densities in the equilibrium reaction.

It is relevant to note that the color chemical potentials are related to the Polyakov loop Φ in the following way,

$$\Phi \;=\; \frac{1}{N_c}\,\mathrm{tr}\,L(x). \tag{4}$$

The Polyakov loop matrix is given by

$$L(x) \;=\; \mathcal{P}\,\exp\left[-\int_0^\beta d\tau \mathbf{t}^a A_0^a(x,\tau)\right], \tag{5}$$

where $\mathcal{P}$ is the path ordering. The Polyakov gauge, $L \equiv L(x)$ in the mean field approximation is written as follows

$$L \;=\; \mathrm{diag}\left(\{e^{i\theta_i}\}\right) \to \mathrm{diag}\left(\{e^{\beta\,\mu_{C\,i}}\}\right). \tag{6}$$

Hence, the Polyakov loop is reduced to

$$\Phi \;=\; \frac{1}{N_c}\,\mathrm{tr}\,L \to \frac{1}{N_c}\sum_{i=1}^{N_c} e^{i\theta_i} \to \frac{1}{N_c}\sum_{i=1}^{N_c} e^{\beta\,\mu_{C\,i}}. \tag{7}$$

For the symmetric group $SU(3)$, there is two independent variables namely the Polyakov loop Φ and its complex conjugate Φ^*. Those two Polyakov variables correspond to the two independent chemical potentials in the $SU(3)$, namely, μ_{C1} and μ_{C2}. The Polyakov loop is the parameter of the spontaneous Z_3 symmetry breaking. This is associated with the deconfinement phase transition. However, the Polyakov loop parametrization becomes questionable above the deconfinement phase transition in particular when the color and flavor degrees of freedom are coupled with each other in a way that the color degrees of freedom can not be separated from the rest of the other degrees of freedom. In the deconfinement phase transition, it is naively to assume that the quarks and gluons carry explicit color degrees of freedom with specific color chemical potentials in order to control the color charges in the equilibrium.

Recently, the explicit color degrees of freedom have been considered to study the semi quark-gluon-plasma using the double line basis at finite N_c of $SU(N_c)$ symmetry group and $Z(N_c)$ interface [25–27]. The approach considered in the present work resembles to some extent that one has been considered in Ref. [25–27], though they apparently look different.

The outline of the present paper is as follows: In Section II, the Cartan sub-algebra is reviewed for the fundamental and adjoint $SU(N_c)$ symmetry group. The fundamental and adjoint constructions are essential to define the color degrees of freedom for quarks and gluons, respectively, in the QCD. In section III, the thermal field theory in the imaginary-time formalism is extended to include the color degrees of freedom explicitly. The thermal propagators for the colored quarks and gluons are introduced in the context of the mixed-time representation of the imaginary-time formulation. In section IV, the contraction and reduction of the fundamental and adjoint color indexes of the $SU(N_c)$ symmetry group are given for the quark's self-energy and the gluon's polarization tensor as illustrative examples of the present procedure. Furthermore, a special attention is given for the color contraction for the colored quark screening frequency and the colored gluon Debye mass. In section V, the HTL self-energy for the soft colored quark is calculated. The quark's external momentum is assumed soft in comparison with the hard momentum of the internal loop. In this approximation, when the soft external momentum is assumed to be of order $g\,T$, the momentum

of internal loop becomes of order T. The ratio between the soft momentum over the hard momentum is of order g (i.e. $p/k \sim g$). In the calculation course of the quark self-energy, the color degrees of freedom are considered explicitly for the fundamental quarks and adjoint gluons. The calculations of the colored plasma frequency and the effective propagator for the soft colored quark are given in detail. In section VI, the HTL polarization tensor for the soft colored gluon is calculated. The gluon's external momentum is taken soft in comparison with the hard internal loop momentum. The external momentum is considered soft and of order $p \sim gT$ while the hard internal momentum is taken of order T. The Debye mass and the effective propagator for the soft colored gluon are presented. In section VII, the effective quark-quark-gluon vertex and the effective two-quarks and two-gluons vertex up to the relevant corrections of order g^3 and g^4, respectively, are introduced. In section VIII, the effective self-energy and the decay rate for the colored (hard) quark are presented to illustrate the procedure of the HTL approximation when the color degrees of freedom is considered explicitly in the calculation and they can not be separated from the other degrees of freedom. Finally, the discussions and conclusions are given in section IX.

II. FUNDAMENTAL AND ADJOINT $SU(N_c)$ CARTAN SUB-ALGEBRA

A semi-simple Lie algebra can be written as a direct sum of simple Lie algebras. The necessary and sufficient condition to be semi-simple is that group matrix, namely, g is nonsingular, i.e.$\det(g) \neq 0$. The Cartan metric can tell us directly whether or not a Lie algebra is semi-simple. We have the freedom of taking a new basis vectors. The set of new basis vectors can be written as linear combinations of the old ones. The overt form of the commutation relation is changed when the the basis vectors are transformed from one set to another. The commutation relations look rather different, but of course they are completely equivalent to the first form. The Cartan way of presenting the commutation relation is a generalization of lowering and raising operators. In the fundamental representation, the maximal number of the commuting fundamental generators of the $SU(N_c)$ symmetry group is N_c-1 while for $U(N_c)$ is N_c. The maximal set of commuting generators $[\mathbf{t}_i, \mathbf{t}_j] = 0$ form a bases set for the Cartan sub algebra and the number of such generators is the rank of group. The simultaneous eigenvalues of the $\mathbf{t}_i$ will be used to label the states of any representation $[\mathbf{t}_i, \mathbf{t}_j] = 0$, where the lower index i refers to the fundamental index $i = 1, \cdots, N_c - 1$ for

the diagonal fundamental generators. Analogous to the lowering and raising operator in the quantum mechanics, we take linear combination $\mathbf{t}^{*\alpha}$ of the remaining $N_c^2 - N_c$ generators so that they have the property of step operators with respect to all of the $\mathbf{t}_i$, namely

$$[\mathbf{t}_i^*, \mathbf{t}^{*\alpha}] \propto \mathbf{t}^{*\alpha}. \tag{8}$$

Our objective of the Cartan sub-algebra is to write the commutation relations of the fundamental generators in order to achieve the diagonalizing of the adjoint action of $\mathbf{t}_i$. The goal is to reach a class of good quantum numbers requires that the matrix elements for $\phi^a \mathbf{T}^a$ is diagonal in the adjoint representation where $\mathbf{T}^a$ are the adjoint generators and the upper index a refers to the adjoint index $a = 1, \cdots, N_c^2 - 1$.

A. The group generators in the fundamental representation

The discussion in the present section is applicable to the theoretic symmetry group $SU(N_c)$ or $U(N_c)$ for any N_c. The focus on the theoretic symmetry group $SU(3)$ is for the sake of simplicity and to illustrate the method strategy in a visible way.

The maximal set of the commuting generators for the theoretic symmetry group $SU(3)$ with respect to fundamental generators $[\lambda^3, \lambda^8] = 0$, where $\{\lambda^a\}$ are the Gell-mann matrices, forms a bases set for the Cartan sub-algebra. The generators $\{\lambda^a\}$ are the common generators which are usually adopted in QCD. The fundamental matrices λ^3 and λ^8 are real traceless diagonal matrices. On the other hand, the rest of the fundamental generators do not commute with each others $\left[\lambda^a, \lambda^b\right] \neq 0$ for $a \neq b$ and $a, b = 1, 2, 4, 5, 6, 7$. The symmetry group $SU(N_c)$ has rank $N_c - 1$. The group rank is the number of independent real traceless diagonal fundamental matrices. It is possible to introduce a new set of fundamental generators $\mathbf{t}_i$, where $i = 1, \cdots, N_c - 1$. In the case of symmetry group $SU(3)$, we have $\{\mathbf{t}_1, \mathbf{t}_2\} \equiv \{\lambda^3, \lambda^8\}$. The non-diagonal fundamental matrices are assigned by $\mathbf{t}^{*\mathcal{J}}$ where $\mathcal{J} = 1, \cdots, N_c^2 - N_c$. In the symmetry group SU(3), the new generators $\mathbf{t}^{*\mathcal{J}}$ are written as linear combinations of the old ones, namely, $\mathbf{t}^{*\mathcal{J}} \equiv \{\lambda^1, \lambda^2, \lambda^4, \lambda^5, \lambda^6, \lambda^7\}$. It is possible to introduce $N_c^2 - N_c$ fundamental matrices for $SU(N_c)$. These new fundamental matrices are defined in the following way

$$\mathbf{t}^{*\mathcal{J}} \to \mathbf{t}^{*\underbrace{(AB)}}, \quad (\text{where} A \neq B), \tag{9}$$

whose entries are just a 1 in the $\underbrace{(AB)}$ place and zero elsewhere, i.e.

$$\left(\mathbf{t}^{*\underbrace{(AB)}}\right)_{kl} = \delta_{Ak}\delta_{Bl}. \tag{10}$$

The both fundamental-like indexes A and B run over $1, \cdots, N_c$. In the case of $SU(3)$ symmetry group, the fundamental generators of this transformation are related to the Gell-mann matrices, namely, $\{\lambda^i\}$ as follows

$$\begin{aligned}
\mathbf{t}^{*\underbrace{(12)}} &= (\lambda^1 + i\lambda^2),\ \mathbf{t}^{*\underbrace{(13)}} = (\lambda^4 + i\lambda^5),\ \mathbf{t}^{*\underbrace{(23)}} = (\lambda^6 + i\lambda^7), \\
\mathbf{t}^{*\underbrace{(21)}} &= (\lambda^1 - i\lambda^2),\ \mathbf{t}^{*\underbrace{(31)}} = (\lambda^4 - i\lambda^5),\ \mathbf{t}^{*\underbrace{(32)}} = (\lambda^6 - i\lambda^7).
\end{aligned} \tag{11}$$

For the definiteness, the traceless diagonal matrices $\mathbf{t}_i$ which are the bases for the Cartan sub-algebra with the index i that runs over $(i = 1, \cdots, N_c - 1)$ are defined as follows

$$(\mathbf{t}_i)_{kl} = \delta_{ik}\,\delta_{il} - \frac{1}{N_c}\,\delta_{lk}. \tag{12}$$

It is worth to note that for the $U(N_c)$ symmetry group, we have the representation $\left(\mathbf{t}^{\underbrace{(AB)}}\right)_{ij} = \delta_{Ai}\,\delta_{Bj}$ where $A, B = 1, \cdots, N_c$. Furthermore, in the $SU(N_c)$ symmetry group, we have the unimodular constraint over the $U(N_c)$ symmetry group. The complete set of fundamental generators for the $SU(N_c)$ symmetry group are reduced to following set

$$\begin{aligned}
\{\mathbf{t}^a\} &\to \left(\left\{\mathbf{t}^{*\mathcal{J}}\right\}, \mathcal{J} = 1, \cdots N_c^2 - N_c, \text{ and } \{\mathbf{t}_i\}, i = 1, \cdots, N_c - 1\right), \\
&\to \begin{pmatrix} \left\{\mathbf{t}^{*\underbrace{(AB)}}\right\}\Big|_{A\neq B}, \underbrace{(AB)} = 1, \cdots, N_c^2 - N_c \\ \{\mathbf{t}_i\}, i = 1, \cdots, N_c - 1 \end{pmatrix},
\end{aligned} \tag{13}$$

where the adjoint index runs over $a = 1, \cdots, N_c^2 - 1$. Nonetheless, it is more comfortable in the realistic calculations to define new fundamental generators that are transformed as follows

$$x_i\mathbf{t}_i = \mathrm{diag}\left(\theta_1, \theta_2, \cdots, \theta_{N_c}\right), \tag{14}$$

where the constraint $\sum_{i=1}^{N_c}\theta_i = 0$ or $\theta_{N_c} = -\sum_{i=1}^{N_c-1}\theta_i$ is imposed. The new set is related to the old one as follows

$$\begin{aligned}
x_i\mathbf{t}_i &= \sum_{i=1}^{N_c}\theta_i\tilde{\mathbf{t}}_i, \\
&= \sum_{i=1}^{N_c-1}\theta_i\tilde{\mathbf{t}}'_i.
\end{aligned} \tag{15}$$

where $\left(\tilde{\mathbf{t}}_i\right)_{nm} = \delta_{in}\,\delta_{im}$ or $\left(\tilde{\mathbf{t}}'_i\right)_{nm} = (\delta_{in} - \delta_{nN_c})\,\delta_{nm}$. For the sake of simplification, we define

$$\mathbf{t}^{\overbrace{(AA)}} = \tilde{\mathbf{t}}_A, \tag{16}$$

where the index $A = i$ acts as a fundamental-like index and it runs over $(1, \cdots, N_c)$. Hence, the new generators are related to the Gell-mann generators as follows

$$\begin{aligned}
\tilde{\mathbf{t}}_1 &= \frac{\sqrt{3}}{6}\lambda^8 + \frac{1}{2}\lambda^3 + \frac{1}{3}I, \\
\tilde{\mathbf{t}}_2 &= \frac{\sqrt{3}}{6}\lambda^8 - \frac{1}{2}\lambda^3 + \frac{1}{3}I, \\
\tilde{\mathbf{t}}_3 &= \frac{1}{3}I - \frac{\sqrt{3}}{3}\lambda^8,
\end{aligned} \tag{17}$$

where the following constraint is imposed

$$\sum_{i=1}^{N_c=3} \theta_i = 0, \quad \text{and} \quad (\theta_1, \theta_2, \theta_3). \tag{18}$$

Furthermore, it is possible to define another new set of fundamental generators in the following way

$$\begin{aligned}
\tilde{\mathbf{t}'}_1 &= \frac{1}{2}\left(\sqrt{3}\lambda^8 + \lambda^3\right), \\
\tilde{\mathbf{t}'}_2 &= \frac{1}{2}\left(\sqrt{3}\lambda^8 - \lambda^3\right), \\
I, &\qquad \text{and} \quad (\theta_1, \theta_2)\,.
\end{aligned} \tag{19}$$

This means that it is always possible to find a linear combination for the diagonal matrices from one form to another. The diagonal representation of any new set must commute with each other

$$[\mathbf{t}_i, \mathbf{t}_j] \equiv \left[\tilde{\mathbf{t}}_i, \tilde{\mathbf{t}}_j\right] \equiv \left[\tilde{\mathbf{t}'}_i, \tilde{\mathbf{t}'}_j\right] = 0. \tag{20}$$

B. Adjoint representation and the diagonalizing of the $(\theta_a\,\mathbf{T}^a)$

The simultaneous eigenvalues of the fundamental generators $\mathbf{t}_i$ will be used to label the states of any representation. The commutation relations of the Cartan sub-algebra bases can be cast as

$$[\mathbf{t}_i, \mathbf{t}_j] = 0\,\mathbf{t}_j, \quad (i, j = 1, \cdots, N_c - 1). \tag{21}$$

The diagonal representation $x_i\,\mathbf{t}_i$ commutes with any linear combination of the diagonal set $\{\mathbf{t}_i\}$ as follows

$$[x_i\mathbf{t}_i, c_j\mathbf{t}_j] = 0. \tag{22}$$

The Cartan sub-algebra for the fundamental diagonal generators gives zero eigenvalues. The remaining non-diagonal generators of the fundamental group can be transformed to another new set that is represented by

$$\mathbf{t}^{*\mathcal{J}} \rightarrow \mathbf{t}^{*\underbrace{(AB)}}, \quad (A \neq B), (A, B = 1, \cdots, N_c), \tag{23}$$

where $\mathcal{J} = 1, \cdots N_c^2 - N_c$ and $\mathcal{J} \equiv \underbrace{(AB)}$. These bases have the property of step operator with respect to all of the $\mathbf{t}_i$ and satisfy the following commutation relation

$$\left[x_i\mathbf{t}_i, \mathbf{t}^{*\mathcal{J}}\right] \propto \mathbf{t}^{*\mathcal{J}} \rightarrow \left[x_i\mathbf{t}_i, \mathbf{t}^{*\underbrace{(AB)}}\right] \propto \mathbf{t}^{*\underbrace{(AB)}}. \tag{24}$$

Furthermore, it is possible to generalize the commutation relation to include the both diagonal and non-diagonal bases as follows

$$\begin{aligned} [x_j\mathbf{t}_j, \mathbf{t}^{*a}] \;&\propto\; \mathbf{t}^{*\alpha}, \\ &=\; -\lambda\mathbf{t}^{*a}, (a = 1, \cdots, N_c^2 - 1), \end{aligned} \tag{25}$$

where the constant λ is the proportionality constant that is inverted to be the eigenvalue of the operator (it should not to be confused with the Gell-mann generators λ^a). The set of fundamental generators $\{\mathbf{t}^a\}$ with the adjoint index a runs over $1, \cdots, N_c^2 - 1$ consists of the non-diagonal fundamental generators $\{\mathbf{t}^{\mathcal{J}}\}$ where $\mathcal{J}$ runs over $1, \cdots, N_c^2 - N_c$ and the diagonal fundamental generators $\{\mathbf{t}_i\}$ with the fundamental index i runs over $1, \cdots, N_c - 1$. These commutation relations have $N_c - 1$ zero eigenvalues. The fundamental theorem of Cartan is that the nonzero eigenvalues are non degenerate.

In order to achieve the diagonalizing of the adjoint action of $x \cdot \mathbf{T}$, it is possible to write commutation relations as follows

$$\begin{aligned} [x_j\mathbf{t}_j, \mathbf{t}^{*a}] \;&=\; x_j \left[i\, f_{jab}\, \mathbf{t}^{*b}\right], \\ &=\; -x_j \left(\mathbf{T}^j\right)_{ab} \mathbf{t}^{*b}, \\ &=\; -\left(x \cdot \mathbf{T}\right)_{ab} \mathbf{t}^{*b}. \end{aligned} \tag{26}$$

The last line is derived due to the fact that the commutation constants of the fundamental generators are the adjoint generators of the group,

$$\left(\mathbf{T}^c\right)_{ab} = -i\, f_{cab}. \tag{27}$$

When a second order commutation relation is applied, the adjoint operation emerges

$$\begin{aligned}
\left[x_i\mathbf{t}_i,\, \left[x_j\mathbf{t}_j,\, \mathbf{t}^{*a}\right]\right] &= -\lambda \left[x_j\mathbf{t}_j\,,\, \mathbf{t}^{*a}\right], \\
&= -\lambda\, \delta_{ab}\, \left[x_j\mathbf{t}_j\,,\, \mathbf{t}^{*b}\right], \\
&= -\left(x\cdot\mathbf{T}\right)_{ab}\, \left[x_j\mathbf{t}_j\,,\, \mathbf{t}^{*b}\right].
\end{aligned} \tag{28}$$

The diagonalizing of the adjoint generator is done in the following way

$$\left[\left(x\cdot\mathbf{T}\right)_{ab} - \lambda\delta_{ab}\right] X = 0, \tag{29}$$

with the eigenvector

$$X = \left[x_j\mathbf{t}_j\,,\, \mathbf{t}^{*b}\right]. \tag{30}$$

This means that we are looking for the eigenvalues of the following equation

$$\det\left(\left(x\cdot\mathbf{T}\right)_{ab} - \lambda\delta_{ab}\right) = 0. \tag{31}$$

It is noted that $x_i\, f_{iab}$ is real when x_i is assumed to be real. Hence, the operator $x_i\, \left(\mathbf{T}^i\right)_{ab}$ is pure imaginary and antisymmetric and therefore it is Hermitian matrix with real eigenvalues. The eigenvalues of the adjoint matrix are identified by $N_c - 1$ zero eigenvalues and $N_c^2 - N_c$ nonzero eigenvalues. In order to determine the eigenvalues, we assume the following algebra

$$\begin{aligned}
\{\mathbf{t}^{*\mathcal{J}}\} &\equiv \{\mathbf{t}^{*\overbrace{(AB)}}\}, \quad (\text{with} \quad A \neq B, \text{ and } \mathcal{J} = 1, \cdots, N^2 - N_c), \\
\left[x_i\mathbf{t}_i, \mathbf{t}^{*\overbrace{(AB)}}\right] &= \left[x_c\mathbf{t}^c, \mathbf{t}^{*\overbrace{(AB)}}\right], \quad (\text{with} \quad i = 1, \cdots, N_c - 1).
\end{aligned} \tag{32}$$

The commutation relation is reduced to

$$\begin{aligned}
\left[x_i\mathbf{t}_i, \mathbf{t}^{*\overbrace{(AB)}}\right] &= \sum_{C=1}^{N_c} \theta_C \hat{e}_C \cdot \left(\hat{e}_A - \hat{e}_B\right) \mathbf{t}^{*\overbrace{(AB)}}, \\
&= -\left(\theta_B - \theta_A\right) \mathbf{t}^{*\overbrace{(AB)}}.
\end{aligned} \tag{33}$$

The affine transformation bases $\hat{e}_A$ and $\hat{e}_B$ are unit N_c-dimensional vectors pointing in the A and B directions respectively. The representation $\mathbf{t}^{*\overbrace{(AB)}}$ is the root generator (i.e. vector).

The summary of the commutation relations with N_c-1 zero eigenvalues and $N_c^2-N_c$ nonzero eigenvalues is given by

$$[x\cdot\mathbf{t},\mathbf{t}^a]\rightarrow\left(\begin{array}{c}\left[x\cdot\mathbf{t},\mathbf{t}^{*\overbrace{(AB)}}\right]=-(\theta_B-\theta_A)\mathbf{t}^{*\overbrace{(AB)}}\\ [x\cdot\mathbf{t},\mathbf{t}_i]=0\mathbf{t}_i\end{array}\right). \tag{34}$$

The resulting eigenvalues read

$$\lambda\equiv\{\lambda^a\}=\mathrm{diag}\left(\left\{(\theta_B-\theta_A)_{A\neq B}\right\}_{1,\cdots,N_c^2-N_c},\{0\}_{1,\cdots,N_c-1}\right), \tag{35}$$

or any permutation of the diagonal elements, where $a=1\cdots N_c^2-1$. In the realistic calculation such as $SU(3)$, the zero eigenvalues are for the generators λ^3 and λ^8 and the other eigenvalues are nonzero for the generators λ^1, λ^2, λ^4, λ^5, λ^6 and λ^7 and according to the fundamental theorem of Cartan: the nonzero eigenvalues are non degenerate. In case of $U(3)$ and $SU(3)$, the fundamental and adjoint representations read

$$x\cdot\mathbf{t}\;=\;\left(\begin{array}{ccc}\theta_1&0&0\\0&\theta_2&0\\0&0&\theta_3\end{array}\right), \tag{36}$$

and

$$x\cdot\mathbf{T}\;=\;\left(\begin{array}{cccccccc}(\theta_1-\theta_2)&0&0&0&0&0&0&0\\0&(\theta_2-\theta_1)&0&0&0&0&0&0\\0&0&0&0&0&0&0&0\\0&0&0&(\theta_1-\theta_3)&0&0&0&0\\0&0&0&0&(\theta_3-\theta_1)&0&0&0\\0&0&0&0&0&(\theta_2-\theta_3)&0&0\\0&0&0&0&0&0&(\theta_3-\theta_2)&0\\0&0&0&0&0&0&0&0\end{array}\right), \tag{37}$$

where $\theta_3=-(\theta_1+\theta_2)$ for $SU(3)$. It should be noted that the operators $x\cdot\mathbf{t}$ and $x\cdot\mathbf{T}$ can be transformed from one form to another and even the diagonal elements can be permuted in different ways but a thorough consideration must be followed in order to preserve the conservation of the color charges.

III. THE THERMAL PROPAGATORS IN THE MIXED-TIME REPRESENTATION

The Lagrangian for the non-Abelian fundamental and adjoint particles in the theoretic $SU(N_c)$ symmetry group reads,

$$\mathcal{L} = -\frac{1}{4} F^{\mu\nu a} F_{\mu\nu}{}^{a} + \sum_{f} \overline{\psi}_f \left(i\gamma^{\mu} D_{\mu} - m \right) \psi_f. \tag{38}$$

The fundamental operator acting of the fundamental field is given by

$$D_{\mu} = \partial_{\mu} - i\, g\, A_{\mu}{}^{a}\, \mathbf{t}^{a}, \tag{39}$$

while the adjoint field is given by

$$\begin{aligned} F_{\mu\nu}{}^{a} &= [D_{\mu}, D_{\nu}]/ig \\ &= \partial_{\mu} A_{\nu}{}^{a} - \partial_{\nu} A_{\mu}{}^{a} + g\, f^{abc}\, A_{\mu}{}^{b}\, A_{\nu}{}^{c}, \end{aligned} \tag{40}$$

where the adjoint index a runs over $(1, \cdots, N_c^2 - 1)$.

A. Thermal Quark propagator

The propagator, for free fundamental particle in the limit $g \to 0$, reads

$$\begin{aligned} \mathcal{S}_{0Q}(k) &= i \frac{1}{\left(\gamma_0 k_0 - \vec{\gamma} \cdot \vec{k} - m_Q \right)}, \\ \text{or} \;\; i\, \mathcal{S}_{0Q}(k) &= \frac{-1}{\left(\gamma_0 k_0 - \vec{\gamma} \cdot \vec{k} - m_Q \right)}. \end{aligned} \tag{41}$$

When the fundamental particles are embedded in the $SU(N_c)$ color symmetry group representation, it is transformed as follows

$$k_0 \to k_0 + i \frac{1}{\beta} \theta \cdot \mathbf{t}. \tag{42}$$

Under the flavor charge conservation $U(1)_{\mathrm{B}}$, it is transformed to

$$k_0 \;\to\; k_0 + \mu_Q + i \frac{1}{\beta} \theta \cdot \mathbf{t}, \tag{43}$$

where $\mu_Q = \mu_{\mathrm{B}} + \mu_{\mathrm{S}} + \cdots$ is the flavor chemical potential that is satisfying the (flavor-) charge conservation such as the baryonic and strangeness charges. In the context of the diagonal

fundamental representation transformation with fundamental operators that commute with the Hamiltonian of fundamental particles, the fundamental representation is reduced to

$$\theta\cdot\mathbf{t}=\begin{pmatrix}\theta_1 & 0 & 0\\ \vdots & \ddots & \vdots\\ 0 & 0 & \theta_{N_c}\end{pmatrix},\quad \text{with constraint}\ \sum_{i=1}^{N_c}\theta_i=0. \tag{44}$$

This leaves N_c-1 conservative color charges. It is more convenience for the practical calculation to factorize the propagator of the fundamental particle into positive and negative energy components as follows

$$\begin{aligned}\mathcal{S}_Q(k_0,\vec{k}) &= \mathcal{S}_{0Q}\left(k_0+\mu_Q+\frac{1}{\beta}i\theta\cdot\mathbf{t},\vec{k}\right),\\ &= i\frac{1}{2}\left[\gamma_0-\frac{1}{\epsilon_Q(\vec{k})}\left(\vec{k}\cdot\vec{\gamma}-m_Q\right)\right]\frac{1}{k_0-\left[\epsilon_Q(\vec{k})-\left(\mu_Q+i\frac{1}{\beta}\theta\cdot\mathbf{t}\right)\right]}\\ &\quad +i\frac{1}{2}\left[\gamma_0+\frac{1}{\epsilon_Q(\vec{k})}\left(\vec{k}\cdot\vec{\gamma}-m_Q\right)\right]\frac{1}{k_0+\left[\epsilon_Q(\vec{k})+\left(\mu_Q+i\frac{1}{\beta}\theta\cdot\mathbf{t}\right)\right]}.\end{aligned} \tag{45}$$

It can be written in terms of the Foldy-Wouthuysen decomposition:

$$\mathcal{S}_Q(k_0,\vec{k}) = i\left[\frac{\Lambda_Q^{(+)}(\vec{k})\,\gamma_0}{k_0-\left[\epsilon_Q(\vec{k})-\left(\mu_Q+i\frac{1}{\beta}\theta\cdot\mathbf{t}\right)\right]}+\frac{\Lambda_Q^{(-)}(\vec{k})\,\gamma_0}{k_0+\left[\epsilon_Q(\vec{k})+\left(\mu_Q+i\frac{1}{\beta}\theta\cdot\mathbf{t}\right)\right]}\right]. \tag{46}$$

The projections $\Lambda_Q^{(\pm)}(\vec{k})$ are the Foldy-Wouthuysen positive and negative energy projections and they are given, respectively, by

$$\begin{aligned}\Lambda_Q^{(+)}(\vec{k}) &= \frac{1}{2\epsilon_Q(\vec{k})}\left[\epsilon_Q(\vec{k})+\gamma_0\left(\vec{\gamma}\cdot\vec{k}+m_Q\right)\right],\\ \Lambda_Q^{(-)}(\vec{k}) &= \frac{1}{2\epsilon_Q(\vec{k})}\left[\epsilon_Q(\vec{k})-\gamma_0\left(\vec{\gamma}\cdot\vec{k}+m_Q\right)\right].\end{aligned} \tag{47}$$

Furthermore, under the diagonal transformation of the $SU(N_c)$ with color charges commuting with the particle energy, the fundamental particle propagator is transformed as follows

$$\mathcal{S}_{Q_{ij}}(k_0,\vec{k}) = i\,\delta_{ij}\left[\frac{\Lambda_Q^{(+)}(\vec{k})\,\gamma_0}{k_0-\left[\epsilon_Q(\vec{k})-\left(\mu_Q+i\frac{\theta_j}{\beta}\right)\right]}+\frac{\Lambda_Q^{(-)}(\vec{k})\,\gamma_0}{k_0+\left[\epsilon_Q(\vec{k})+\left(\mu_Q+i\frac{\theta_j}{\beta}\right)\right]}\right], \tag{48}$$

where i and j are the fundamental indexes of the colored particles. In order to proceed to the thermal field framework, we adopt the imaginary-time formalism. In the context of the imaginary-time formalism, the Matsubara frequency for the fermion is introduced

$$\omega_n=(2n+1)\pi/\beta. \tag{49}$$

The momentum's time-component is transformed to

$$k_0 \to i\,\omega_n + \mu_Q + i\,\frac{1}{\beta}\theta\cdot\mathbf{t}. \tag{50}$$

It is more convenience to work in the mixed-time representation in the context of the imaginary-time formalism. The quark propagator is reduced to

$$\begin{aligned}\mathcal{S}_Q(\tau,\vec{k}) \;&=\; \frac{1}{\beta}\sum_n e^{-i\omega_n\tau}\,\mathcal{S}_{0Q}(i\omega_n+\mu_Q+i\,\frac{1}{\beta}\theta\cdot\mathbf{t},\vec{k}),\\ &=\; -\oint\frac{d\omega}{2i\pi}\frac{e^{-\omega\tau}}{e^{-\beta\omega}+1}\,\mathcal{S}_{0Q}(\omega+\mu_Q+i\frac{1}{\beta}\theta\cdot\mathbf{t},\vec{k}).\end{aligned} \tag{51}$$

The above equation is equivalent to the following form

$$\mathcal{S}_Q(\tau,\vec{k}) \;=\; -\oint\frac{d\omega}{2i\pi}\frac{e^{\tau\left(\mu_Q+i\frac{1}{\beta}\theta\cdot\mathbf{t}\right)}\,e^{-\omega\tau}}{e^{\beta\left(\mu_Q+i\frac{1}{\beta}\theta\cdot\mathbf{t}\right)}\,e^{-\beta\omega}+1}\,\mathcal{S}_{0Q}(\omega,\vec{k}). \tag{52}$$

The quark propagator is decomposed into the $SU(N_c)$ fundamental color components as follows

$$\begin{aligned}\mathcal{S}_{Q_{ij}}(\tau,\vec{k}) \;&=\; -\oint\frac{d\omega}{2i\pi}\left(\frac{e^{\tau\left(\mu_Q+i\frac{1}{\beta}\theta_i\right)}e^{-\omega\tau}}{e^{\beta\left(\mu_Q+i\frac{1}{\beta}\theta_i\right)}e^{-\beta\omega}+1}\,\mathcal{S}_{0Q}(\omega,\vec{k})\right)\,\delta_{ij},\\ &\qquad\qquad\text{with the constraint }\sum_{i=1}^{N_c}\theta_i=0.\end{aligned} \tag{53}$$

The integral is evaluated using the method of the residues in the complex calculus. The two poles are found at

$$k_0 \;=\; k_0^{(+)}=\left(\epsilon_Q(\vec{k})-\mu_Q-i\frac{1}{\beta}\theta_i\right)\;\text{ and }\quad k_0=k_0^{(-)}=-\left(\epsilon_Q(\vec{k})+\mu_Q+i\frac{1}{\beta}\theta_i\right). \tag{54}$$

The quark propagator in the mixed-time representation is evaluated and projected into positive and negative energy components as follows

$$\begin{aligned}i\,\mathcal{S}_{Q_{ij}}(\tau,\vec{k}) \;=\; \delta_{ij}\,&\Big\{\Lambda_Q^{(+)}(\vec{k})\,\gamma_0\,\left[1-n_F\left(\epsilon_Q(\vec{k})-\mu_Q-i\frac{1}{\beta}\theta_i\right)\right]\\ &\qquad\times\exp\left[-\left(\epsilon_Q(\vec{k})-\mu_Q-i\frac{1}{\beta}\theta_i\right)\tau\right]\\ &+\Lambda_Q^{(-)}(\vec{k})\,\gamma_0\,\left[n_F\left(\epsilon_Q(\vec{k})+\mu_Q+i\frac{1}{\beta}\theta_i\right)\right]\\ &\qquad\times\exp\left[+\left(\epsilon_Q(\vec{k})+\mu_Q+i\frac{1}{\beta}\theta_i\right)\tau\right]\Big\}.\end{aligned} \tag{55}$$

B. Thermal gluon propagator

The gluon propagator can be introduced in several ways depending on the type of the gauge. The straightforward way is to write it as follows

$$\mathcal{G}_{\mu\nu}(k_0,\vec{k}) \;=\; \mathcal{G}(k_0,\vec{k})\widehat{g}_{\mu\nu}\left(k_0,\vec{k}\right). \tag{56}$$

The scalar propagator $\mathcal{G}(k_0,\vec{k})$ reads

$$\begin{aligned}\mathcal{G}(k_0,\vec{k}) \;&=\; \frac{-1}{k_0^2-\vec{k}^2-m_G^2},\\ &=\; \frac{-1}{2\epsilon_G(\vec{k})}\left[\frac{1}{k_0-\epsilon_G(\vec{k})}-\frac{1}{k_0+\epsilon_G(\vec{k})}\right],\end{aligned} \tag{57}$$

where $\epsilon_G(\vec{k}) = \sqrt{\vec{k}^2+m_G^2}$ and $m_G = 0$ for the gluon in the vacuum. The gluon propagator numerator $\widehat{g}_{\mu\nu}\left(k_0,\vec{k}\right)$ is gauge dependent. It can be written in the covariant gauge with a gauge-fixing $(\partial^\mu A_\mu^a)^2/2\xi$ as $[-g_{\mu\nu}+\xi k_\mu k_\nu/k^2]$. In the Feynman gauge: we have $\widehat{g}_{\mu\nu}\left(k_0,\vec{k}\right) = -g_{\mu\nu}$. Nonetheless, it has been shown the quark and gluon self-energies are gauge independent. In the sake of the calculation simplicity, we shall the present calculations in the Feynman gauge. The same procedure is also valid for the covariant gauge. Fortunately, the final results is independent on the gauge in the HTL approximation. The gluons are adjoint particles of the $SU(N_c)$ symmetry group. The adjoint representation for the gluon is given by the following transformation

$$\begin{aligned}k_0 \;&\rightarrow\; k_0+\frac{1}{\beta}\theta_i f_{iab},\\ &\rightarrow\; k_0+i\frac{1}{\beta}\left(\theta\cdot\mathbf{T}\right)_{ab}.\end{aligned} \tag{58}$$

In the imaginary-time formalism, the Matsubara frequency for gluon is introduced as follows

$$k_0 \;\rightarrow\; i\omega_n+i\frac{1}{\beta}\left(\theta\cdot\mathbf{T}\right)_{ab}, \tag{59}$$

where $\omega_n = 2n\pi\beta$ is the even Matsubara frequency. Furthermore, in the context of the mixed-time representation, the gluon propagator is transformed in the following way

$$\begin{aligned}\mathcal{G}_{\mu\nu}(\tau,\vec{k}) \;&=\; \frac{1}{\beta}\sum_n e^{-i\omega_n\tau}\mathcal{G}_{\mu\nu}\left(i\omega_n+i\frac{1}{\beta}\theta\cdot\mathbf{T},\vec{k}\right),\\ &=\; \frac{1}{(2\pi i)}\oint d\omega\frac{e^{-\omega\tau}}{e^{-\beta\omega}-1}\mathcal{G}_{\mu\nu}\left(\omega+i\frac{1}{\beta}\theta\cdot\mathbf{T},\vec{k}\right),\\ &=\; \frac{1}{(2\pi i)}\oint d\omega\frac{e^{-\left(\omega-i\frac{1}{\beta}\theta\cdot\mathbf{T}\right)\tau}}{e^{-\beta\left(\omega-i\frac{1}{\beta}\theta\cdot\mathbf{T}\right)}-1}\mathcal{G}_{\mu\nu}\left(\omega,\vec{k}\right).\end{aligned} \tag{60}$$

The adjoint representation in the theoretic $SU(N_c)$ symmetry group can be transformed into a diagonal matrix. The advantage of the diagonal adjoint representation is that it commutes with the diagonal fundamental representation beside its commutation with the adjoint particle's energy state. Furthermore, it preserves the $SU(N_c)$ fundamental color charges θ_i with the unimodular constraint $\sum_{i=1}^{N_c}\theta_i = 0$. To this end, we get the following diagonal transformation

$$\left(\theta\cdot\mathbf{T}\right)_{ab} \to \phi^a\,\delta^{ab}. \tag{61}$$

For the definiteness, the adjoint representation can be diagonalized and written in terms of the conserved fundamental color charges θ_i as follows

$$\begin{aligned}\mathrm{tr}\left[e^{i\theta\cdot\mathbf{T}}\right] &= \sum_{a=1}^{N_c^2-1} e^{i\phi^a},\\ &= \sum_{ij}^{N_c} e^{i(\theta_i-\theta_j)} - 1.\end{aligned} \tag{62}$$

The diagonal adjoint representation elements are good quantum numbers. The conserved adjoint charges depend basically on the conserved fundamental charges $\{\phi^a\} = \{(\theta_i - \theta_j)\}$ where $i,j = 1,\cdots,N_c$ are fundamental indexes while $a = \underbrace{(ij)} = 1,\cdots,(N_c^2-1)$ is the adjoint index. The gluon propagator in the mixed-time representation can be transformed to a diagonal adjoint color matrix as follows

$$\mathcal{G}_{\mu\nu}{}^{ab}(\tau,\vec{k}) = \frac{1}{(2\pi i)}\oint d\omega \frac{e^{-\left(\omega - i\frac{1}{\beta}\phi^a\right)\tau}}{e^{-\beta\left(\omega-i\frac{1}{\beta}\phi^a\right)}-1}\,\mathcal{G}_{\mu\nu}\left(\omega,\vec{k}\right)\,\delta^{ab}. \tag{63}$$

It is noted that the gluon propagator is gauge dependent and can be written as follows

$$\mathcal{G}_{\mu\nu}{}^{ab}(\tau,\vec{k}) = \frac{1}{(2\pi i)}\oint d\omega \frac{e^{-\left(\omega - i\frac{1}{\beta}\phi^a\right)\tau}}{e^{-\beta\left(\omega-i\frac{1}{\beta}\phi^a\right)}-1}\,\mathcal{G}\left(\omega,\vec{k}\right)\,\widehat{g}_{\mu\nu}(\omega,\vec{k})\,\delta^{ab}. \tag{64}$$

In the Feynman gauge, it is reduced to

$$\begin{aligned}\mathcal{G}_{\mu\nu}{}^{ab}(\tau,\vec{k}) &= \mathcal{G}^{ab}(\tau,\vec{k})g_{\mu\nu}\\ &= \frac{1}{(2\pi i)}\oint d\omega \frac{e^{-\left(\omega - i\frac{1}{\beta}\phi^a\right)\tau}}{e^{-\beta\left(\omega-i\frac{1}{\beta}\phi^a\right)}-1}\,\mathcal{G}\left(\omega,\vec{k}\right)\,\delta^{ab}\,g_{\mu\nu}.\end{aligned} \tag{65}$$

Hence, the scalar part of the gluon propagator is given by

$$\mathcal{G}^{ab}(\tau,\vec{k}) = \frac{1}{(2\pi i)}\oint d\omega \frac{e^{-\left(\omega - i\frac{1}{\beta}\phi^a\right)\tau}}{e^{-\beta\left(\omega-i\frac{1}{\beta}\phi^a\right)}-1}\,\mathcal{G}\left(\omega,\vec{k}\right)\,\delta^{ab}. \tag{66}$$

The gluon propagator in the mixed-time representation is evaluated trivially by using the complex calculus of residues. The poles are found in the following locations

$$k_0 \;=\; k_0^{(+)} = \epsilon_G(\vec{k}) - i\frac{1}{\beta}\phi^a, \text{ and } k_0 = k_0^{(-)} = -\left(\epsilon_G(\vec{k}) + i\frac{1}{\beta}\phi^a\right). \tag{67}$$

After evaluating the integral, the scalar part of the gluon propagator becomes

$$\begin{aligned}\mathcal{G}^{ab}(\tau,\vec{k}) \;=\;& \delta^{ab}\,\frac{1}{2\epsilon_G(\vec{k})}\left[1+N_G\left(\epsilon_G(\vec{k})-i\frac{1}{\beta}\phi^a\right)\right]e^{-\left(\epsilon_G(\vec{k})-i\frac{1}{\beta}\phi^a\right)\tau}\\ &+\delta^{ab}\,\frac{1}{2\epsilon_G(\vec{k})}\left[N_G\left(\epsilon_G(\vec{k})+i\frac{1}{\beta}\phi^a\right)\right]e^{+\left(\epsilon_G(\vec{k})+i\frac{1}{\beta}\phi^a\right)\tau}.\end{aligned} \tag{68}$$

It is interesting to note that it is possible to generalize the standard procedure used in the Feynman gauge to other gauge whereas the gauge does not affect the propagator singularity. The generalization of the gluon propagator is written as follows

$$\begin{aligned}{\mathcal{G}_{\mu\nu}}^{a\,b}(\tau,\vec{k}) \;=\;& \delta^{a\,b}\,{\mathcal{G}_{\mu\nu}}^{a}(\tau,\vec{k}),\\ {\mathcal{G}_{\mu\nu}}^{a}(\tau,\vec{k}) \;=\;& \frac{1}{2\epsilon_G(\vec{k})}\left[1+N_G\left(\epsilon_G(\vec{k})-i\frac{1}{\beta}\phi^a\right)\right]\exp\left[-\left(\epsilon_G(\vec{k})-i\frac{1}{\beta}\phi^a\right)\tau\right]\,\widehat{g}_{\mu\nu}\left(k_0^{(+)}\right)\\ &+\frac{1}{2\epsilon_G(\vec{k})}\left[N_G\left(\epsilon_G(\vec{k})+i\frac{1}{\beta}\phi^a\right)\right]\exp\left[\left(\epsilon_G(\vec{k})+i\frac{1}{\beta}\phi^a\right)\tau\right]\,\widehat{g}_{\mu\nu}\left(k_0^{(-)}\right).\end{aligned} \tag{69}$$

In the mixed-time representation of the imaginary-time formalism, it is useful to introduce some notations and to write the following results

$$\begin{aligned}\left[k^2\mathcal{G}\right]^{ab}\left(\tau,\vec{k}\right) \;=\;& \left(\frac{1}{2\pi i}\oint d\omega\frac{e^{i\frac{\tau}{\beta}\theta\cdot\mathbf{T}}e^{-\omega\tau}}{e^{i\theta\cdot\mathbf{T}}e^{-\beta\omega}-1}k^2{\mathcal{G}_0}^{ab}(\omega,\vec{k})\right),\\ =\;& -\,\delta(\tau)\,\delta^{ab},\end{aligned} \tag{70}$$

and

$$\begin{aligned}\left[k_0^2\mathcal{G}\right]^{ab}(\tau,\vec{k}) \;=\;& \frac{1}{2\pi i}\left(\oint d\omega\frac{e^{i\frac{\tau}{\beta}\theta\cdot\mathbf{T}}e^{-\omega\tau}}{e^{i\theta\cdot\mathbf{T}}e^{-\beta\omega}-1}\omega^2{\mathcal{G}_0}^{ab}(\omega,\vec{k})\right),\\ =\;& \frac{\epsilon_G(k)}{2}\left[1+N_G\left(\epsilon_G(k)-i\frac{1}{\beta}\phi^a\right)\right]\exp\left[-\left(\epsilon_G(k)-i\frac{1}{\beta}\phi^a\right)\tau\right]\,\delta^{ab}\\ &+\frac{\epsilon_G(k)}{2}\left[N_G\left(\epsilon_G(k)+i\frac{1}{\beta}\phi^a\right)\right]\exp\left[+\left(\epsilon_G(k)+i\frac{1}{\beta}\phi^a\right)\tau\right]\,\delta^{ab},\end{aligned} \tag{71}$$

and finally,

$$\begin{aligned}\left[k_0\mathcal{G}\right]^{ab}(\tau,\vec{k}) \;=\;& \left(\frac{1}{2\pi i}\oint d\omega\frac{e^{i\frac{\tau}{\beta}\theta\cdot\mathbf{T}}e^{-\omega\tau}}{e^{i\theta\cdot\mathbf{T}}e^{-\beta\omega}-1}\omega{\mathcal{G}_0}^{ab}(\omega,\vec{k})\right),\\ =\;& \frac{1}{2}\left[1+N_G\left(\epsilon_G(k)-i\frac{1}{\beta}\phi^a\right)\right]\exp\left[-\left(\epsilon_G(k)-i\frac{1}{\beta}\phi^a\right)\tau\right]\,\delta^{ab}\\ &-\frac{1}{2}\left[N_G\left(\epsilon_G(k)+i\frac{1}{\beta}\phi^a\right)\right]\exp\left[+\left(\epsilon_G(k)+i\frac{1}{\beta}\phi^a\right)\tau\right]\,\delta^{ab}.\end{aligned} \tag{72}$$

IV. COLOR CONTRACTION

A. Quark self-energy

In the calculations of the quark-self energy and the quark plasma frequency (i.e. Landau frequency), the color structure for the plasma Landau frequency is displayed as follows

$$\begin{aligned}\left(\omega_{0\,Q}^2\right)_{ij} &= \mathbf{t}_{in}^a\,\mathbf{t}_{mj}^b\left(\omega_{0\,Q}^2\right)_{nm}^{ab},\\ &= \mathbf{t}_{in}^a\,\mathbf{t}_{mj}^b\,\delta^{ab}\,\delta_{nm}\left(\omega_{0\,Q}^2\right)_{n}^{a},\\ &= \mathbf{t}_{in}^a\,(\mathbf{t}^{b\dagger})_{mj}\,\delta^{ab}\,\delta_{nm}\left(\omega_{0\,Q}^2\right)_{n}^{a},\\ &= \mathbf{t}_{in}^a\,\mathbf{t}_{mj}^b\left[\left(\omega_{0\,Q(Q)}^2\right)_{n}+\left(\omega_{0\,Q(G)}^2\right)^{a}\right]\delta^{ab}\,\delta_{nm}. \end{aligned}\tag{73}$$

The contraction of the fundamental indexes reduces the quark plasma frequency to

$$\left(\omega_{0\,Q}^2\right)_{nm}^{ab} = \left(\omega_{0\,Q}^2\right)_{n}^{a}\delta^{ab}\,\delta_{nm},\tag{74}$$

where

$$\left(\omega_{0\,Q}^2\right)_{n}^{a} = \left[\left(\omega_{0\,Q(G)}^2\right)^{a}+\left(\omega_{0\,Q(Q)}^2\right)_{n}\right].\tag{75}$$

The fundamental generators are defined in the following way

$$\begin{aligned}\mathbf{t}^a &= \frac{1}{\sqrt{2}}\tau^a,\\ &= \frac{1}{\sqrt{2}}\tau^{\underbrace{(AB)}},\ \text{where } a\equiv\underbrace{(AB)},\end{aligned}\tag{76}$$

where the matrix elements are expressed as follows

$$\mathbf{t}_{ij}^{\underbrace{(AB)}} = \frac{1}{\sqrt{2}}\left[\delta_{Ai}\,\delta_{Bj}-\frac{1}{N_c}\,\delta_{AB}\,\delta_{ij}\right].\tag{77}$$

The Hermitian fundamental matrices are represented by

$$\begin{aligned}(\mathbf{t}^{\underbrace{(AB)}\dagger})_{ij} &= \mathbf{t}_{ij}^{\underbrace{(BA)}},\\ &= \frac{1}{\sqrt{2}}\left[\delta_{Bi}\,\delta_{Aj}-\frac{1}{N_c}\,\delta_{AB}\,\delta_{ij}\right].\end{aligned}\tag{78}$$

The color contraction of the quark segment of the quark self-energy is reduced to

$$\begin{aligned}\mathbf{t}_{in}^a\,\mathbf{t}_{mj}^b\left(\omega_{0\,Q(Q)}^2\right)_{n}\delta_{nm}\,\delta^{ab} &\equiv \frac{1}{2}\tau_{in}^a\,(\tau^{a\dagger})_{nj}\left(\omega_{0\,Q(Q)}^2\right)_{n},\\ &= \frac{1}{2}\tau_{in}^{\underbrace{(AB)}}\,\tau_{nj}^{\underbrace{(BA)}}\left(\omega_{0\,Q(Q)}^2\right)_{n}.\end{aligned}\tag{79}$$

It becomes

$$\mathbf{t}^a_{in}\,\mathbf{t}^b_{mj}\,\left(\omega^2_{0\,Q(Q)}\right)_n\,\delta_{nm}\,\delta^{ab}\;=\;\frac{N_c^2-1}{2N_c}\,\delta_{ij}\,\left(\omega^{*2}_{0\,Q(Q)}\right)_i, \tag{80}$$

where

$$\begin{aligned}\left(\omega^{*2}_{0\,Q(Q)}\right)_i\;&=\;\frac{1}{N_c^2-1}\,\left[N_c\sum_{n=1}^{N_c}\left(\omega^2_{0\,Q(Q)}\right)_n-\left(\omega^2_{0\,Q(Q)}\right)_i\right],\\&=\;\frac{N_c}{N_c^2-1}\,\left[\sum_{n=1}^{N_c}\left(1-\frac{\delta_{in}}{N_c}\right)\,\left(\omega^2_{0\,Q(Q)}\right)_n\right],\\&=\;\frac{N_c}{N_c^2-1}\sum_{n=1}^{N_c}\sum_{m=1}^{N_c}\,\left[\left(1-\frac{\delta_{nm}}{N_c}\right)\,\delta_{mi}\,\left(\omega^2_{0\,Q(Q)}\right)_n\right].\end{aligned} \tag{81}$$

Furthermore, the color contraction of the gluon segment of the quark self-energy is reduced to

$$\begin{aligned}\mathbf{t}^a_{in}\,\mathbf{t}^b_{mj}\,\left(\omega^2_{0\,Q(G)}\right)^a\,\delta_{nm}\,\delta^{ab}\;&\equiv\;\frac{1}{2}\tau^a_{in}\,\left(\tau^{a\dagger}\right)_{nj}\,\left(\omega^2_{0\,Q(G)}\right)^a,\\&\equiv\;\frac{1}{2}\,\tau_{in}\underbrace{(AB)}\,\tau_{nj}\underbrace{(BA)}\,\left(\omega^2_{0\,Q(G)}\right)\underbrace{(AB)},\\&=\;\frac{1}{2N_c}\,\delta_{ij}\,\left[N_c\sum_{n=1}^{N_c}\left(\omega^2_{0\,Q(G)}\right)\underbrace{(in)}-\left(\omega^2_{0\,Q(G)}\right)\underbrace{(ii)}\right].\end{aligned} \tag{82}$$

It is reduced to

$$\mathbf{t}^a_{in}\,\mathbf{t}^b_{mj}\,\left(\omega^2_{0\,Q(G)}\right)^a\,\delta_{nm}\,\delta^{ab}\;=\;\frac{N_c^2-1}{2N_c}\,\delta_{ij}\,\left(\omega^{*2}_{0\,Q(G)}\right)_i, \tag{83}$$

where

$$\begin{aligned}\left(\omega^{*2}_{0\,Q(G)}\right)_i\;&=\;\frac{1}{N_c^2-1}\,\left[N_c\sum_{n=1}^{N_c}\left(\omega^2_{0\,Q(G)}\right)\underbrace{(in)}-\left(\omega^2_{0\,Q(G)}\right)\underbrace{(ii)}\right],\\&=\;\frac{N_c}{N_c^2-1}\sum_{n=1}^{N_c}\sum_{m=1}^{N_c}\left[\left(1-\frac{\delta_{nm}}{N_c}\right)\,\delta_{mi}\left(\omega^2_{0\,Q(G)}\right)\underbrace{(mn)}\right].\end{aligned} \tag{84}$$

The adjoint color indexes are represented in terms of the fundamental color indexes as follows

$$a\rightarrow\underbrace{(AB)}\rightarrow\underbrace{(ij)}\,. \tag{85}$$

The quark Landau frequency is coupled with two fundamental generators as follows,

$$\begin{aligned}\mathbf{t}^a_{in}\,\mathbf{t}^a_{nj}\,\left(\omega^2_{0\,Q}\right)^a_n\;&=\;\mathbf{t}^a_{in}\,\mathbf{t}^a_{nj}\,\left[\left(\omega^2_{0\,Q(Q)}\right)_n+\left(\omega^2_{0\,Q(G)}\right)^a\right],\\&=\;\frac{N_c^2-1}{2N_c}\,\delta_{ij}\,\left(\omega^{*2}_{0\,Q}\right)_i,\end{aligned} \tag{86}$$

where

$$\begin{aligned}\left(\omega^{*2}_{0\,Q}\right)_i &= \left[\left(\omega^{*2}_{0\,Q(Q)}\right)_i + \left(\omega^{*2}_{0\,Q(G)}\right)_i\right], \\ &= \frac{N_c}{N_c^2-1}\sum_{n=1}^{N_c}\sum_{m=1}^{N_c}\left(1-\frac{\delta_{nm}}{N_c}\right)\delta_{mi}\left[\left(\omega^2_{0\,Q(Q)}\right)_n + \left(\omega^2_{0\,Q(G)}\right)\underbrace{(mn)}\right]. \end{aligned} \tag{87}$$

In the case that the quark Landau frequency is decoupled from the color degree of freedom, the plasma frequency components for the quark and gluon segments (i.e. lines) of the quark self-energy are reduced to

$$\begin{aligned}\left(\omega^2_{0\,Q(Q)}\right)_n &\to \overline{\omega}^2_{0\,Q(Q)}, \\ \left(\omega^2_{0\,Q(G)}\right)\underbrace{(mn)} &\to \overline{\omega}^2_{0\,Q(G)}, \end{aligned} \tag{88}$$

respectively. Hence, the quark Landau frequency is reduced to

$$\left(\omega^{*\,2}_{0\,Q}\right)_i = \overline{\omega}^2_{0\,Q(Q)} + \overline{\omega}^2_{0\,Q(G)}. \tag{89}$$

The coupling of the internal Landau frequency, namely, $\left(\omega^2_{0\,Q}\right)^a_n$ with the fundamental generators contracts the color indexes in the following way

$$\mathbf{t}^a_{in}\,\mathbf{t}^a_{nj}\left(\omega^2_{0\,Q}\right)^a_n = \frac{N_c^2-1}{2N_c}\,\delta_{ij}\,\left[\overline{\omega}^2_{0\,Q(Q)} + \overline{\omega}^2_{0\,Q(G)}\right]. \tag{90}$$

B. Gluon Polarization tensor

1. *Gluon Polarization tensor: the color indexes for gluon and ghost loops and tadpole*

The multiplication of two adjoint matrices appears in the Feynman diagrams for the gluon self-energy. It is given by

$$(\mathbf{T}^{a'})_{c'b'}(\mathbf{T}^a)_{bc} \equiv (\mathbf{T}^{a'})_{c'b'}(\mathbf{T}^{a\dagger})_{bc}. \tag{91}$$

The adjoint matrix can be represented in terms of the fundamental representations as follows,

$$\begin{aligned}(\mathbf{T}^a)_{bc} &= -if^{abc}, \\ &= -2\mathrm{tr}\left(\left[\mathbf{t}^a,\mathbf{t}^b\right]\mathbf{t}^c\right). \end{aligned} \tag{92}$$

The adjoint conjugate matrix becomes

$$\left(\mathbf{T}^{a\dagger}\right)_{bc} = -2\mathrm{tr}\left([\mathbf{t}^{a\dagger},\mathbf{t}^{b\dagger}]\mathbf{t}^{c\dagger}\right). \tag{93}$$

The multiplication of two adjoint matrices is written in terms of fundamental matrices as follows,

$$
\begin{aligned}
(\mathbf{T}^{a'})_{c'b'}(\mathbf{T}^{a\dagger})_{bc} &= 4\mathrm{tr}\left([\mathbf{t}^{a'},\mathbf{t}^{c'}]\mathbf{t}^{b'}\right)\times \mathrm{tr}\left([\mathbf{t}^{a\dagger},\mathbf{t}^{b\dagger}]\mathbf{t}^{c\dagger}\right), \\
&= -4\mathrm{tr}\left([\mathbf{t}^{a'},\mathbf{t}^{b'}]\mathbf{t}^{c'}\right)\times \mathrm{tr}\left([\mathbf{t}^{a\dagger},\mathbf{t}^{b\dagger}]\mathbf{t}^{c\dagger}\right), \\
&= -4\mathrm{tr}\left([\mathbf{t}^{a'},\mathbf{t}^{c'}]\mathbf{t}^{b'}\right)\times \mathrm{tr}\left([\mathbf{t}^{a\dagger},\mathbf{t}^{c\dagger}]\mathbf{t}^{b\dagger}\right). \qquad (94)
\end{aligned}
$$

The $\delta^{c'\,c}$ index contraction is performed in the following way,

$$
\begin{aligned}
(\mathbf{T}^{a'})_{c'b'}\,(\mathbf{T}^{a\dagger})_{bc}\,\delta^{c'c} &= -2[\mathbf{t}^{a'},\mathbf{t}^{b'}]_{in}\,[\mathbf{t}^{a\dagger},\mathbf{t}^{b\dagger}]_{jm}\,\tau_{ni}\underbrace{(AB)}\,\tau_{mj}\underbrace{(BA)}, \\
&= -2\left([\mathbf{t}^{a'},\mathbf{t}^{b'}]_{ij}\,[\mathbf{t}^{a\dagger},\mathbf{t}^{b\dagger}]_{ji}-\frac{1}{N_c}\,[\mathbf{t}^{a'},\mathbf{t}^{b'}]_{ii}\,[\mathbf{t}^{a\dagger},\mathbf{t}^{b\dagger}]_{jj}\right), \\
&= -2\left([\mathbf{t}^{a'},\mathbf{t}^{b'}]_{ij}\,[\mathbf{t}^{a\dagger},\mathbf{t}^{b\dagger}]_{ji}\right). \qquad (95)
\end{aligned}
$$

In a similar manner, the contraction over $\delta^{b'\,b}$ leads to the following result

$$
(\mathbf{T}^{a'})_{c'b'}\,(\mathbf{T}^{a\dagger})_{bc}\,\delta^{b'b} = -2\left([\mathbf{t}^{a'},\mathbf{t}^{c'}]_{ij}\,[\mathbf{t}^{a\dagger},\mathbf{t}^{c\dagger}]_{ji}\right). \qquad (96)
$$

Therefore, the contraction over either $\delta^{b'\,b}\left(\mathbf{m}^2_{D\,(G)}\right)^b$ for Eq. (95) or $\delta^{c'\,c}\left(\mathbf{m}^2_{D\,(G)}\right)^c$ for Eq. (96) leads, respectively, to

$$
(\mathbf{T}^{a'})_{c'b'}\,(\mathbf{T}^{a\dagger})_{bc}\,\delta^{c'c}\,\delta^{b'b}\left(\mathbf{m}^2_{D\,(G)}\right)^b = -2\left([\mathbf{t}^{a'},\mathbf{t}^{b}]_{ij}\,[\mathbf{t}^{a\dagger},\mathbf{t}^{b\dagger}]_{ji}\right)\left(\mathbf{m}^2_{D\,(G)}\right)^b, \qquad (97)
$$

or

$$
(\mathbf{T}^{a'})_{c'b'}\,(\mathbf{T}^{a\dagger})_{bc}\,\delta^{b'b}\,\delta^{c'c}\left(\mathbf{m}^2_{D\,(G)}\right)^c = -2\left([\mathbf{t}^{a'},\mathbf{t}^{c}]_{ij}\,[\mathbf{t}^{a\dagger},\mathbf{t}^{c\dagger}]_{ji}\right)\left(\mathbf{m}^2_{D\,(G)}\right)^c. \qquad (98)
$$

The results of Eqns. (97) and (98) leads to the folowing symmetry relation

$$
\begin{aligned}
(\mathbf{T}^{a'})_{c'b'}\,(\mathbf{T}^{a\dagger})_{bc}\,\delta^{c'c}\,\delta^{b'b}\left(\mathbf{m}^2_{D\,(G)}\right)^b &= (\mathbf{T}^{a'})_{c'b'}\,(\mathbf{T}^{a\dagger})_{bc}\,\delta^{b'b}\,\delta^{c'c}\left(\mathbf{m}^2_{D\,(G)}\right)^c, \\
&= (\mathbf{T}^{a'})_{cb}\,(\mathbf{T}^{a\dagger})_{bc}\,\left(\mathbf{m}^2_{D\,(G)}\right)^b, \\
&= (\mathbf{T}^{a'})_{cb}\,(\mathbf{T}^{a\dagger})_{bc}\,\left(\mathbf{m}^2_{D\,(G)}\right)^c, \\
&\qquad \text{(sum over the repeated adjoint color indexes)} \qquad (99)
\end{aligned}
$$

when the summation over the internal adjoint color indexes b and c is taken for the Debye mass that is weighted by the Casimir-like operator, namely, $(\mathbf{T}^{a'})_{cb}\,(\mathbf{T}^{a\dagger})_{bc}$. Moreover, the

term $\left(\Delta \mathbf{m}^2_{D\,(G)}\right)^b$ which generates the quadratic temperature has the following symmetry relations with respect to the interchange of adjoint color indexes b and c:

$$(\mathbf{T}^{a'})_{cb}\,(\mathbf{T}^{a\dagger})_{bc}\,\left(\Delta \mathbf{m}^2_{D\,(G)}\right)^b \;=\; (\mathbf{T}^{a'})_{cb}\,(\mathbf{T}^{a\dagger})_{bc}\,\left(\Delta \mathbf{m}^2_{D\,(G)}\right)^c\,,$$

(sum over the repeated adjoint color indexes). (100)

Evidently, the symmetry in Eq. (100) eliminates the quadratic temperature terms from gluon polarization tensor with the external line legs those are labeled by the external adjoint color indexes, namely, $a'\,a$. These quadratic temperature terms usually appear in the internal loop segments which are associated with the three gluon vertexes and they are usually labelled by the internal adjoint color indexes.

The adjoint color index c is replaced with the fundamental-like A and B indexes using the following relation,

$$c \equiv \underbrace{(AB)} \;\text{ or }\; \underbrace{(ij)} \;\text{ or }\; \underbrace{(nm)}\,. \tag{101}$$

The $\delta^{c'c}$ and $\delta^{b'b}$ contractions with the coefficient $\left(\mathbf{m}^2_{D\,(G)}\right)^b$ reduce the multiplication of the two adjoint matrices to

$$\begin{aligned}(\mathbf{T}^{a'})_{c'b'}\,(\mathbf{T}^{a\dagger})_{bc}\,\delta^{c'c}\,\delta^{b'b}\,\left(\mathbf{m}^2_{D\,(G)}\right)^b \;&=\; -2\,\Big(\mathbf{t}^{a'}_{in}\,\mathbf{t}^{b}_{nj}\,\mathbf{t}^{a\dagger}_{jm}\,\mathbf{t}^{b\dagger}_{mi} \;-\; \mathbf{t}^{a'}_{in}\,\mathbf{t}^{b}_{nj}\,\mathbf{t}^{b\dagger}_{jm}\,\mathbf{t}^{a\dagger}_{mi} \\ &\qquad -\,\mathbf{t}^{b}_{in}\,\mathbf{t}^{a'}_{nj}\,\mathbf{t}^{a\dagger}_{jm}\,\mathbf{t}^{b\dagger}_{mi} \;+\; \mathbf{t}^{b}_{in}\,\mathbf{t}^{a'}_{nj}\,\mathbf{t}^{b\dagger}_{jm}\,\mathbf{t}^{a\dagger}_{mi}\Big)\,\left(\mathbf{m}^2_{D\,(G)}\right)^b, \\ &=\; 4\,\Big(\mathbf{t}^{a'}_{in}\,\mathbf{t}^{b}_{nj}\,\mathbf{t}^{b\dagger}_{jm}\,\mathbf{t}^{a\dagger}_{mi} \;-\; \mathbf{t}^{a'}_{in}\,\mathbf{t}^{b}_{nj}\,\mathbf{t}^{a\dagger}_{jm}\,\mathbf{t}^{b\dagger}_{mi}\Big)\,\left(\mathbf{m}^2_{D\,(G)}\right)^b.\end{aligned} \tag{102}$$

It is useful to derive the contraction relation over the adjoint index b for the following fundamental matrices operation

$$\begin{aligned}\mathbf{t}^{b}_{nj}\,\mathbf{t}^{b\dagger}_{jm}\,\left(\mathbf{m}^2_{D\,(G)}\right)^b \;&=\; \frac{1}{2}\tau_{nj}^{\underbrace{(AB)}}\,\tau_{jm}^{\underbrace{(BA)}}\,\left(\mathbf{m}^2_{D\,(G)}\right)^{\underbrace{(AB)}}, \\ &=\; \frac{1}{2}\left[\delta_{nm}\,\sum_{l=1}^{N_c}\left(\mathbf{m}^2_{D\,(G)}\right)^{\underbrace{(nl)}} - \frac{1}{N_c}\delta_{nm}\,\left(\mathbf{m}^2_{D\,(G)}\right)^{\underbrace{(00)}}\right].\end{aligned} \tag{103}$$

Furthermore, we have the following contraction relation,

$$\begin{aligned}\mathbf{t}^{b}_{nj}\,\mathbf{t}^{b\dagger}_{mi}\,\left(\mathbf{m}^2_{D\,(G)}\right)^b \;&=\; \frac{1}{2}\,\tau_{nj}^{\underbrace{(AB)}}\,\tau_{mi}^{\underbrace{(BA)}}\,\left(\mathbf{m}^2_{D\,(G)}\right)^{\underbrace{(AB)}}, \quad \left(\text{where}\, b \,\equiv\, \underbrace{(AB)}\right), \\ &=\; \frac{1}{2}\left[\delta_{in}\,\delta_{jm}\left(\mathbf{m}^2_{D\,(G)}\right)^{\underbrace{(ij)}} - \frac{1}{N_c}\delta_{mi}\,\delta_{nj}\,\left(\mathbf{m}^2_{D\,(G)}\right)^{\underbrace{(00)}}\right].\end{aligned} \tag{104}$$

Using Eq. (103), the first term in Eq. (102) is reduced to

$$\mathbf{t}^{a'}_{in}\,\mathbf{t}^{a\dagger}_{mi}\,\mathbf{t}^{b}_{nj}\,\mathbf{t}^{b\dagger}_{jm}\,\left(\mathbf{m}^{2}_{D\,(G)}\right)^{b} \;=\; \frac{1}{2}\left[\mathbf{t}^{a'}_{in}\,\mathbf{t}^{a\dagger}_{ni}\,\sum_{l=1}^{N_c}\underbrace{\left(\mathbf{m}^{2}_{D\,(G)}\right)}^{(nl)} - \frac{1}{N_c}\mathbf{t}^{a'}_{in}\,\mathbf{t}^{a\dagger}_{ni}\,\underbrace{\left(\mathbf{m}^{2}_{D\,(G)}\right)}^{(00)}\right] \quad (105)$$

While using Eq. (104) reduces the second term in Eq. (102) to

$$\mathbf{t}^{a'}_{in}\,\mathbf{t}^{a\dagger}_{jm}\,\mathbf{t}^{b}_{nj}\,\mathbf{t}^{b\dagger}_{mi}\,\left(\mathbf{m}^{2}_{D\,(G)}\right)^{b} \;=\; \frac{1}{2}\left[\mathbf{t}^{a'}_{ii}\,\mathbf{t}^{a\dagger}_{jj}\,\underbrace{\left(\mathbf{m}^{2}_{D\,(G)}\right)}^{(ij)} - \frac{1}{N_c}\mathbf{t}^{a'}_{ij}\,\mathbf{t}^{a\dagger}_{ji}\,\underbrace{\left(\mathbf{m}^{2}_{D\,(G)}\right)}^{(00)}\right]. \quad (106)$$

Furthermore, the contraction relations of the fundamental matrices which are given by Eqns. (105) and (106) reduce Eq. (102) to

$$(\mathbf{T}^{a'})_{cb}\,(\mathbf{T}^{a})^{\dagger}_{bc}\,\left(\mathbf{m}^{2}_{D\,(G)}\right)^{b} \;=\; 2\left(\mathbf{t}^{a'}_{ij}\,\mathbf{t}^{a\dagger}_{ji}\,\sum_{l=1}^{N_c}\underbrace{\left(\mathbf{m}^{2}_{D\,(G)}\right)}^{(jl)} - \mathbf{t}^{a'}_{ii}\,\mathbf{t}^{a\dagger}_{jj}\,\underbrace{\left(\mathbf{m}^{2}_{D\,(G)}\right)}^{(ij)}\right). \quad (107)$$

The first term on the right hand side of Eq. (107) is reduced to

$$\begin{aligned}
2\,\mathbf{t}^{a'}_{in}\,\mathbf{t}^{a\dagger}_{ni}\,\sum_{l=1}^{N_c}\underbrace{\left(\mathbf{m}^{2}_{D\,(G)}\right)}^{(nl)} \;&=\; 2\,\underbrace{\mathbf{t}_{in}}^{(A'B')}\,\underbrace{\mathbf{t}_{ni}}^{(BA)}\,\sum_{l=1}^{N_c}\underbrace{\left(\mathbf{m}^{2}_{D\,(G)}\right)}^{(nl)},\\
&=\; \delta_{A'A}\delta_{B'B}\,\sum_{l=1}^{N_c}\underbrace{\left(\mathbf{m}^{2}_{D\,(G)}\right)}^{(Bl)}\\
&\quad -\frac{1}{N_c}\,\delta_{A'B'}\delta_{AB}\,\left[\sum_{l=1}^{N_c}\underbrace{\left(\mathbf{m}^{2}_{D\,(G)}\right)}^{(B'l)} + \sum_{l=1}^{N_c}\underbrace{\left(\mathbf{m}^{2}_{D\,(G)}\right)}^{(Bl)}\right.\\
&\quad \left. -\frac{1}{N_c}\sum_{k=1}^{N_c}\sum_{l=1}^{N_c}\underbrace{\left(\mathbf{m}^{2}_{D\,(G)}\right)}^{(kl)}\right].
\end{aligned} \quad (108)$$

The second term in Eq. (107) reads

$$\begin{aligned}
2\,\mathbf{t}^{a'}_{ii}\,\mathbf{t}^{a\dagger}_{jj}\,\underbrace{\left(\mathbf{m}^{2}_{D\,(G)}\right)}^{(ij)} \;&=\; 2\,\sum_{ij}^{N_c}\underbrace{\mathbf{t}_{ii}}^{(A'B')}\,\underbrace{\mathbf{t}_{jj}}^{(BA)}\,\underbrace{\left(\mathbf{m}^{2}_{D\,(G)}\right)}^{(ij)},\\
&=\; \delta_{A'B'}\delta_{AB}\,\underbrace{\left(\mathbf{m}^{2}_{D\,(G)}\right)}^{(A'A)}\\
&\quad -\frac{1}{N_c}\,\delta_{A'B'}\delta_{AB}\,\left[\sum_{l=1}^{N_c}\underbrace{\left(\mathbf{m}^{2}_{D\,(G)}\right)}^{(A'l)} + \sum_{l=1}^{N_c}\underbrace{\left(\mathbf{m}^{2}_{D\,(G)}\right)}^{(lA)}\right.\\
&\quad \left. -\frac{1}{N_c}\sum_{k=1}^{N_c}\sum_{l=1}^{N_c}\underbrace{\left(\mathbf{m}^{2}_{D\,(G)}\right)}^{(kl)}\right].
\end{aligned} \quad (109)$$

By considering the results of Eq. (108) and (109), Eq. (107) becomes

$$\begin{aligned}
(\mathbf{T}^{a'})_{cb}\,(\mathbf{T}^{a})^{\dagger}_{bc}\,\left(\mathbf{m}^{2}_{D\,(G)}\right)^{b} \;&=\; \delta_{A'A}\delta_{B'B}\,\sum_{l=1}^{N_c}\underbrace{\left(\mathbf{m}^{2}_{D\,(G)}\right)}^{(Bl)} - \delta_{A'B'}\delta_{AB}\,\underbrace{\left(\mathbf{m}^{2}_{D\,(G)}\right)}^{(B'B)}\\
&\quad -\;\frac{1}{N_c}\delta_{A'B'}\delta_{AB}\,\left[\sum_{l=1}^{N_c}\left(\underbrace{\left(\mathbf{m}^{2}_{D\,(G)}\right)}^{(Bl)} - \underbrace{\left(\mathbf{m}^{2}_{D\,(G)}\right)}^{(lB)}\right)\right].
\end{aligned} \quad (110)$$

The term $\left(\mathbf{m}^2_{D\,(G)}\right)\overbrace{}^{(ij)}$ is symmetric over the fundamental-like indexes i and j. Furthermore, the second term on the right hand side of Eq. (110) can be averaged as follows

$$\left(\mathbf{m}^2_{D\,(G)}\right)\overbrace{}^{(B'B)}\,\delta_{A'B'}\delta_{AB} \;\equiv\; \frac{1}{N_c}\sum_{l=1}^{N_c}\left(\mathbf{m}^2_{D\,(G)}\right)\overbrace{}^{(Bl)}\,\delta_{A'B'}\delta_{AB}. \tag{111}$$

Therefore, Eq. (110) is reduced to

$$\begin{aligned}(\mathbf{T}^{a'})_{c\,b}\,(\mathbf{T}^{a})^{\dagger}_{b\,c}\,\left(\mathbf{m}^2_{D\,(G)}\right)^{b} \;&=\; \left(\delta_{A'A}\delta_{B'B}-\frac{1}{N_c}\delta_{A'B'}\delta_{AB}\right)\sum_{l=1}^{N_c}\left(\mathbf{m}^2_{D\,(G)}\right)\overbrace{}^{(Bl)},\\ &=\; N_c\,\delta^{a'a}\,\left(\mathbf{m}^2_{D\,(G)}\right)^{a},\end{aligned} \tag{112}$$

where

$$\left(\mathbf{m}^2_{D\,(G)}\right)^{a} \;\equiv\; \frac{1}{N_c}\sum_{l=1}^{N_c}\left(\mathbf{m}^2_{D\,(G)}\right)\overbrace{}^{(Bl)}, \quad \text{(note that } a\equiv\underbrace{(AB)}\text{)}. \tag{113}$$

Eq. (113) is re-written as follows

$$\left(\mathbf{m}^2_{D\,(G)}\right)^{a} \;=\; \frac{1}{N_c}\left[\sqrt{2}\sum_{ij}^{N_c}\sum_{n}^{N_c}(\mathbf{t}^{a})_{in}\left(\mathbf{m}^2_{D\,(G)}\right)\overbrace{}^{(nj)}+\frac{1}{N_c}\delta_{AB}\sum_{ij}^{N_c}\left(\mathbf{m}^2_{D\,(G)}\right)\overbrace{}^{(ij)}\right]. \tag{114}$$

The last term with the Kronecker delta δ_{AB} corresponds the diagonal fundamental generators with the fundamental index $i=1,\cdots,N_c-1$ which commute with the entire fundamental generator set $[\mathbf{t}_i,\mathbf{t}^a]=0$ where the adjoint index $a=1,\cdots,N_c^2-1$ and they commute with the energy eigenstates as well. Furthermore, the Kronecker delta δ_{AB} can be replaced by δ_{ai}. Hence, the above equation becomes

$$\left(\mathbf{m}^2_{D\,(G)}\right)^{a} \;\equiv\; \frac{1}{N_c}\left[\sqrt{2}\sum_{ij}^{N_c}\sum_{n}^{N_c}(\mathbf{t}^{a})_{in}\left(\mathbf{m}^2_{D\,(G)}\right)\overbrace{}^{(nj)}+\frac{1}{N_c}\delta_{ai}\sum_{ij}^{N_c}\left(\mathbf{m}^2_{D\,(G)}\right)\overbrace{}^{(ij)}\right], \tag{115}$$

where i is the fundamental index that represents the diagonal fundamental generators where its off-diagonal elements are identical to zero.

2. Gluon Polarization tensor: quark-loop color indexes

The multiplication of the two fundamental color matrices which appears in the quark loop is usually given by

$$\mathbf{t}^{a'}_{i'j'}\,\mathbf{t}^{a\dagger}_{ji}\,\delta_{j'j}\,\delta_{i'i}\,\left(\mathbf{m}^2_{D\,(Q)}\right)_{i} \;=\; \mathbf{t}^{a'}_{ij}\,(\mathbf{t}^{a\dagger})_{ji}\,\left(\mathbf{m}^2_{D\,(Q)}\right)_{i}. \tag{116}$$

It can be written as follows

$$\begin{aligned}
\mathbf{t}^{a'}_{ij}\,(\mathbf{t}^{a\dagger})_{ji}\,\left(\mathbf{m}^2_{D\,(Q)}\right)_i \;&=\; \mathbf{t}\underbrace{_{ij}}_{(A'B')}\,\mathbf{t}\underbrace{_{ji}}_{(BA)}\,\left(\mathbf{m}^2_{D\,(Q)}\right)_i\,,\\
&=\; \frac{1}{2}\left(\delta_{A'A}\,\delta_{B'B}-\frac{1}{N_c}\,\delta_{A'B'}\,\delta_{AB}\right)\,\left(\mathbf{m}^2_{D\,(Q)}\right)_A\,,\\
&=\; \frac{1}{2}\,\delta^{a'a}\,\left(\mathbf{m}^2_{D\,(Q)}\right)_A\,,\\
&=\; \frac{1}{2}\delta^{a'a}\,\left(\mathbf{m}^2_{D\,(Q)}\right)^a\,. \qquad (117)
\end{aligned}$$

where

$$\left(\mathbf{m}^2_{D\,(Q)}\right)^a \;=\; \left(\mathbf{m}^2_{D\,(Q)}\right)_A\,,\quad \text{(note that } a\equiv\underbrace{(AB)}\text{)}\,. \qquad (118)$$

The quark-loop part of the Debye mass with an external adjoint color index a is written as follows

$$\left(\mathbf{m}^2_{D\,(Q)}\right)^a \;=\; \left[\sqrt{2}\sum_{ij}^{N_c}(\mathbf{t}^a)_{ij}\,\left(\mathbf{m}^2_{D\,(Q)}\right)_i+\frac{1}{N_c}\delta_{AB}\,\left(\mathbf{m}^2_{D\,(Q)}\right)_i\right]. \qquad (119)$$

The second term comes from the diagonal elements of the representation that represents the N_c-1 fundamental generators which commute with the energy states. The fundamental generators are given by $\mathbf{t}_i$ where $[\mathbf{t}_i,\mathbf{t}^a]=0$. The Kronecker delta δ_{AB} is replaced by δ_{ai} where $a=1,\cdots,N_c^2-1$ is the adjoint color index for the entire set of generators while $i=1,\cdots,N_c-1$ is the fundamental color index for fundamental generators which their off-diagonal elements are identical to zero. They commute with energy eigenstates as well as the rest of fundamental color generators. Hence, Eq. (119) becomes

$$\left(\mathbf{m}^2_{D\,(Q)}\right)^a \;=\; \left[\sqrt{2}\sum_{ij}^{N_c}(\mathbf{t}^a)_{ij}\,\left(\mathbf{m}^2_{D\,(Q)}\right)_i+\frac{1}{N_c}\delta_{ai}\,\left(\mathbf{m}^2_{D\,(Q)}\right)_i\right]. \qquad (120)$$

It is worth to remind the reader to the following dual,

$$\mathbf{t}^a_{i'\,j'}\,\mathbf{t}^b_{j\,i}\to\mathbf{t}^a_{i'\,j'}\,(\mathbf{t}^{b\dagger})_{j\,i}, \qquad (121)$$

3. Gluon self-energy: quark, gluon, ghost loops and tadpole

The colored gluon Debye mass is given by adding the contributions of quark loop, gluon loop, ghost loop and tadpole Feynman diagrams. The colored Debye mass is reduced to

$$\delta^{a'a}\left(\mathbf{m}^2_D\right)^a \;=\; \left[(\mathbf{T}^{a'})_{cb}\,(\mathbf{T}^a)^\dagger_{bc}\,\left(\mathbf{m}^2_{D\,(G)}\right)^b+\mathbf{t}^{a'}_{ij}\,(\mathbf{t}^{a\dagger})_{ji}\,\left(\mathbf{m}^2_{D\,(Q)}\right)_i\right], \qquad (122)$$

where

$$\left(\mathbf{m}_D^2\right)^a \;=\; N_c\,\left(\mathbf{m}_{D\,(G)}^2\right)^a + \frac{1}{2}\,\left(\mathbf{m}_{D\,(Q)}^2\right)^a . \tag{123}$$

V. QUARK SELF-ENERGY

Fig. (1) depicts the Feynman diagrams for the quark self-energy. The fundamental indexes for the quark segment and adjoint indexes for the gluon segment in the quark-gluon loop are shown explicitly. The quark self-energy is calculated as follows,

$$\begin{aligned}
\Sigma_{Q\,ij}(p) \;&=\; \Sigma_{Q\,ij}(p_0,\vec{p}),\\
&=\; \int \frac{dk_0}{(2\pi)} \int \frac{d^3\vec{k}}{(2\pi)^3}\,\Sigma_{Q\,ij}(p,k),\\
&=\; \int \frac{dk_0}{(2\pi)} \int \frac{d^3\vec{k}}{(2\pi)^3}\,\Sigma_{Q\,ij}\left(p_0,\vec{p},k_0,\vec{k}\right),
\end{aligned} \tag{124}$$

where p and k are the external and internal momentum, respectively. The fundamental indexes $i\,j$ refer to the quark line (i.e. two external legs). The conservation of color charges leads to color contraction δ_{ij} for the quark line and make the quark line to have a conserved color charge with fundamental index i. The quark self-energy kernel part for the quark-gluon loop is furnished as follows,

$$\begin{aligned}
\Sigma_{Q\,ij}(p,k) \;&=\; \left[-g\,\gamma^\mu(\mathbf{t}^a)_{in}\right]\,i\,\mathcal{S}_{Q\,nm}\left(p_0-k_0,\vec{p}-\vec{k}\right)\,\left[-g\,\gamma^\nu(\mathbf{t}^b)_{mj}\right]\\
&\quad\times\mathcal{G}_{\mu\nu}{}^{ab}\left(-k_0,-\vec{k}\right),\\
&=\; (\mathbf{t}^a)_{in}\,\left(\mathbf{t}^b\right)_{mj}\,\Sigma_{Q\,nm}^{ab}\left(p_0,\vec{p},k_0,\vec{k}\right),\\
&=\; (\mathbf{t}^a)_{in}\,\left(\mathbf{t}^b\right)_{mj}\,\Sigma_{Q}{}_{nm}^{ab}(p,k),
\end{aligned} \tag{125}$$

where p and k are the external and internal momenta, respectively. The internal quark-gluon loop kernel, where the quark segment carries the fundamental color indexes n and m and the gluon segment carries the adjoint color indexes a and b, is given by

$$\Sigma_{Q}{}_{nm}^{ab}(p_0,\vec{p},k_0,\vec{k}) \;=\; g^2\,\left[\gamma^\mu\,i\,\mathcal{S}_{Q\,nm}\left(p_0-k_0,\vec{p}-\vec{k}\right)\,\gamma^\nu\,\mathcal{G}_{\mu\nu}{}^{ab}\left(-k_0,-\vec{k}\right)\right]. \tag{126}$$

It is naturally to anticipate that the conservation of color charge contracts the gluon segment to δ^{ab} while the quark segment to δ_{nm} and subsequently the internal quark and gluon segments have the fundamental color index n and the adjoint color index a, respectively.

The quark self-energy can be projected with respect to the quark-quark-gluon vertexes $(\mathbf{t}^a)_{in}$ and $(\mathbf{t}^b)_{mj}$ as follows

$$\Sigma_{Q\,ij}(p_0,\vec{p}) \;=\; (\mathbf{t}^a)_{in}\,\left(\mathbf{t}^b\right)_{mj}\,\Sigma_{Q\,nm}^{\;ab}(p_0,\vec{p}), \tag{127}$$

where the integration over the internal momentum k (i.e. k_0 and $\vec{k}$) is given by

$$\Sigma_{Q\,nm}^{\;ab}(p_0,\vec{p}) \;=\; \int \frac{d^4k}{(2\pi)^4}\,\Sigma_{Q\,nm}^{\;ab}(p_0,\vec{p},k_0,\vec{k}). \tag{128}$$

The quark self-energy kernel which is given by Eq. (126) is written in the mixed-time representation of the imaginary-time formalism as follows,

$$\begin{aligned}\Sigma_{Q\,nm}^{\;ab}(p_0,\vec{p},k_0,\vec{k}) \;=\; & \int_0^\beta d\tau \int_0^\beta d\tau' \exp\left(\left[(p_0-k_0)-\mu_Q-i\frac{1}{\beta}\theta_n\right]\tau'\right)\,\exp\left(\left[k_0-i\frac{1}{\beta}\phi^a\right]\tau\right)\\ & \times\,\widetilde{\Sigma}_{Q\,nm}^{\;ab}(\tau,\tau',\vec{p},\vec{k}).\end{aligned} \tag{129}$$

It is re-written as follows

$$\begin{aligned}\Sigma_{Q\,ij}(p_0,\vec{p},k_0,\vec{k}) \;=\; & (\mathbf{t}^a)_{in}\,\left(\mathbf{t}^b\right)_{mj}\int_0^\beta d\tau\int_0^\beta d\tau'\,\exp\left(\left[k_0-i\frac{1}{\beta}\phi^a\right][\tau-\tau']\right)\\ & \times\exp\left(\left[p_0-\mu_Q-i\frac{1}{\beta}\theta_n-i\frac{1}{\beta}\phi^a\right]\tau'\right)\,\widetilde{\Sigma}_{Q\,nm}^{\;ab}(\tau,\tau',\vec{p},\vec{k}).\end{aligned} \tag{130}$$

The last term under the integral in Eqns. (129) and (130) is given by

$$\widetilde{\Sigma}_{Q\,nm}^{\;ab}(\tau,\tau',\vec{p},\vec{k}) \;=\; g^2\,\gamma^\mu\,i\,\mathcal{S}_{Q_{nm}}\left(\tau',\vec{p}-\vec{k}\right)\,\gamma^\nu\,\mathcal{G}_{\mu\nu}{}^{ab}\left(\tau,\vec{k}\right). \tag{131}$$

After evaluating the integral over the internal time-momentum k_0, Eq. (130) is reduced to

$$\begin{aligned}\Sigma_{Q\,ij}(p_0,\vec{p},\vec{k}) \;=\; & \int\frac{dk_0}{(2\pi)}\,\Sigma_{Q\,ij}(p_0,\vec{p},k_0,\vec{k}),\\ =\; & (\mathbf{t}^a)_{in}\,\left(\mathbf{t}^b\right)_{mj}\int_0^\beta d\tau\exp\left(\left[p_0-\mu_Q-i\frac{1}{\beta}\theta_n-i\frac{1}{\beta}\phi^a\right]\tau\right)\\ & \times\widetilde{\Sigma}_{Q\,nm}^{\;ab}(\tau,\tau,\vec{p},\vec{k}).\end{aligned} \tag{132}$$

In order to evaluate Eq. (131), the quark and gluon propagators are decomposed to the energy plane components. The quark propagator part that is sandwiched by gamma matrices,

namely, $\gamma^\mu \otimes \gamma^\nu$ in Eq. (131) is decomposed in the following way,

$$\begin{aligned} S_{Q\ nm}^{\mu\nu}(\tau,\vec{q}) &= \gamma^\mu\, i\,\mathcal{S}_{Q nm}(\tau,\vec{q})\,\gamma^\nu, \\ &= \left[1 - n_F\left(\epsilon_Q(\vec{q}) - \mu_Q - \frac{1}{\beta} i\theta_n\right)\right] \exp\left(-\left(\epsilon_Q(\vec{q}) - \mu_Q - \frac{1}{\beta} i\theta_n\right)\tau\right) \\ &\quad \times \left[\gamma^\mu\, \Lambda_Q^{(+)}(\vec{q})\,\gamma_0\,\gamma^\nu\right]\,\delta_{nm} \\ &+ \left[n_F\left(\epsilon_Q(\vec{q}) + \mu_Q + \frac{1}{\beta} i\theta_n\right)\right] \exp\left(\left(\epsilon_Q(\vec{q}) + \mu_Q + \frac{1}{\beta} i\theta_n\right)\tau\right) \\ &\quad \times \left[\gamma^\mu\, \Lambda_Q^{(-)}(\vec{q})\,\gamma_0\,\gamma^\nu\right]\,\delta_{nm}, \end{aligned} \tag{133}$$

where $n_F(x) = \frac{1}{e^x+1}$ is the Fermi-Dirac partition function, $\vec{q} = \vec{p} - \vec{k}$ and $\epsilon_Q = \sqrt{\vec{p}^2 + m_Q^2} \approx |\vec{p}|$. The Foldy-Wouthuysen positive and negative energy projectors read

$$\Lambda_Q^{(\pm)}(\vec{q}) \;=\; \frac{1}{2\epsilon_Q(\vec{q})}\left[\epsilon_Q(\vec{q}) \pm \gamma_0\,\left(\vec{\gamma}\cdot\vec{q} + m_Q\right)\right]. \tag{134}$$

In the case that color degree of freedom is decoupled, the quark screening mass (i.e. the plasma Landau frequency) is shown to be gauge independent in the HTL approximation. The result is also gauge independent in the HTL approximation for the case that the color degree of freedom is not decoupled. Hence, it is sufficient to work in the Feynman gauge to derive the gauge independent result. The gluon propagator for the gluon segment in Eq. (131) is given by

$$\mathcal{G}_{\mu\nu}{}^{ab}(\tau,\vec{k}) \;=\; g_{\mu\nu}\,\mathcal{G}^a\left(\tau,\vec{k}\right)\,\delta^{ab}. \tag{135}$$

The color contracted gluon propagator with an adjoint index a is reduced to

$$\begin{aligned} \mathcal{G}^a\left(\tau,\vec{k}\right) &= \frac{1}{2\epsilon_G(\vec{k})}\left[1 + N_G\left(\epsilon_G(\vec{k}) - i\frac{1}{\beta}\phi^a\right)\right]\,\exp\left[-\left(\epsilon_G(\vec{k}) - i\frac{1}{\beta}\phi^a\right)\tau\right] \\ &\quad + \frac{1}{2\epsilon_G(\vec{k})}\left[N_G\left(\epsilon_G(\vec{k}) + i\frac{1}{\beta}\phi^a\right)\right]\exp\left[+\left(\epsilon_G(\vec{k}) + i\frac{1}{\beta}\phi^a\right)\tau\right], \end{aligned} \tag{136}$$

where $N_G(x) = \frac{1}{e^x-1}$ is Bose-Einstein partition function and $\epsilon_G(\vec{k}) = \sqrt{\vec{k}^2} = |\vec{k}|$. The quark self-energy is calculated by integrating out the internal momentum as follows

$$\Sigma_{Q\,ij}(p_0,\vec{p}) \;=\; (\mathbf{t}^a)_{in}\,\left(\mathbf{t}^b\right)_{mj}\,\Sigma_{Q\,nm}^{ab}(p_0,\vec{p}), \tag{137}$$

where

$$\begin{aligned} \Sigma_{Q\,nm}^{ab}(p_0,\vec{p}) &= \int\frac{d^3\vec{k}}{(2\pi)^3}\int_0^\beta d\tau\,\exp\left[\left(p_0 - \mu_Q - i\frac{1}{\beta}\theta_n - i\frac{1}{\beta}\phi^a\right)\tau\right] \\ &\quad \times\; \widetilde{\Sigma}_{Q\,nm}^{ab}(\tau,\tau,\vec{p},\vec{k}). \end{aligned} \tag{138}$$

The term $\Sigma_Q{}^{ab}_{nm}(p_0,\vec{p})$ that is appeared in Eq. (138) can be projected using the Foldy-Wouthuysen transformation to positive and negative energy components. It is reduced to the following superposition function,

$$\begin{aligned}\Sigma_Q{}^{ab}_{nm}(p_0,\vec{p}) &= \sum_{r=\pm}^{\pm}\sum_{s=\pm}^{\pm}\Sigma_Q^{(rs)}{}^{ab}_{nm}(p_0,\vec{p}),\\ &= \sum_{r=\pm}^{\pm}\sum_{s=\pm}^{\pm}\Sigma_Q^{(rs)}{}^{a}_{n}(p_0,\vec{p})\,\delta_{nm}\,\delta^{ab}. \end{aligned} \tag{139}$$

It is evident that Eq. (139) is diagonalized with respect to the adjoint and fundamental color indexes alike. This result is a natural one since the fundamental color index n represents the internal quark segment with the fundamental color charge conservation $\delta_{n\,m}$ while the adjoint color index a represents the internal gluon segment with the adjoint color charge conservation $\delta^{a\,b}$. The Foldy-Wouthuysen energy components of Eq. (139) is calculated as follows

$$\Sigma_Q^{(rs)}{}^{a}_{n}(p_0,\vec{p}) = g^2\left(\int\frac{d^3\vec{k}}{(2\pi)^3}\,g_{\mu\nu}\,\mathbf{S}_Q^{(r)\mu\nu}(\vec{p}-\vec{k})\mathbf{D}_Q^{(rs)a}{}_{n}(p,\vec{k})\right), \tag{140}$$

where $r=\pm$, $s=\pm$ are the positive and negative energy components. The sandwiched Foldy-Wouthuysen projectors by the gamma matrices $\gamma^\mu\otimes\gamma^\nu$ are given by,

$$\mathbf{S}_Q^{(r)\mu\nu}(\vec{p}-\vec{k}) = \left[\gamma^\mu\,\Lambda_Q^{(r)}(\vec{p}-\vec{k})\gamma_0\,\gamma^\nu\right]. \tag{141}$$

The explicit expressions for $\mathbf{D}_Q^{(rs)a}{}_{n}(p,\vec{k})$ are reduced to

$$\left(\mathbf{D}_Q^{(++)a}{}_{n}(p,\vec{k})\right) = -\frac{\left[1-n_F\left(\epsilon_Q(\vec{p}-\vec{k})-\mu_Q-i\tfrac{1}{\beta}\theta_n\right)+N_G\left(\epsilon_G(\vec{k})-i\tfrac{1}{\beta}\phi^a\right)\right]}{2\epsilon_G(\vec{k})\left[p_0-\left(\epsilon_G(\vec{k})+\epsilon_Q(\vec{p}-\vec{k})\right)\right]}, \tag{142}$$

$$\left(\mathbf{D}_Q^{(+-)a}{}_{n}(p,\vec{k})\right) = -\frac{\left[n_F\left(\epsilon_Q(\vec{p}-\vec{k})-\mu_Q-i\tfrac{1}{\beta}\theta_n\right)+N_G\left(\epsilon_G(\vec{k})+i\tfrac{1}{\beta}\phi^a\right)\right]}{2\epsilon_G(\vec{k})\left[p_0+\left(\epsilon_G(\vec{k})-\epsilon_Q(\vec{p}-\vec{k})\right)\right]}, \tag{143}$$

$$\left(\mathbf{D}_Q^{(-+)a}{}_{n}(p,\vec{k})\right) = -\frac{\left[n_F\left(\epsilon_Q(\vec{p}-\vec{k})+\mu_Q+i\tfrac{1}{\beta}\theta_n\right)+N_G\left(\epsilon_G(\vec{k})-i\tfrac{1}{\beta}\phi^a\right)\right]}{2\epsilon_G(\vec{k})\left[p_0-\left(\epsilon_G(\vec{k})-\epsilon_Q(\vec{p}-\vec{k})\right)\right]}, \tag{144}$$

and

$$\left(\mathbf{D}_Q^{(--)a}{}_{n}(p,\vec{k})\right) = -\frac{\left[1-n_F\left(\epsilon_Q(\vec{p}-\vec{k})+\mu_Q+i\tfrac{1}{\beta}\theta_n\right)+N_G\left(\epsilon_G(\vec{k})+i\tfrac{1}{\beta}\phi^a\right)\right]}{2\epsilon_G(\vec{k})\left[p_0+\left(\epsilon_G(\vec{k})+\epsilon_Q(\vec{p}-\vec{k})\right)\right]}, \tag{145}$$

for the positive-positive, positive-negative, negative-positive and negative-negative energy components, respectively. In the derivation of Eq. (138), we have considered the following relations for the Matsubara frequency for the momentum time-component in the imaginary-time formalism,

$$\begin{aligned} & p_0 - \mu_Q - i\tfrac{1}{\beta}\theta_n - i\tfrac{1}{\beta}\phi^a = i\tfrac{(2m+1)\pi}{\beta}, \\ & \exp\left(p_0 - \mu_Q - i\tfrac{1}{\beta}\theta_n - i\tfrac{1}{\beta}\phi^a\right) = -1, \end{aligned} \tag{146}$$

where the Fermion Matsubara frequency is given by $\omega = (2m+1)\pi/\beta$ and $m = 1, 2, \cdots$. The HTL are one-loop diagrams for which only the contribution from hard loop momenta of the order T or larger is considered. In this approximation, the external momentum is soft $p \sim g\,T$, while the internal momentum is hard $k \sim T$. Hence, the internal momentum k is assumed relatively large in comparison with the external one (i.e. $p/k \sim g$). In order to simplify the calculations, it is useful to adopt the following approximations

$$\begin{aligned} g_{\mu\nu}\,\mathbf{S}_Q^{(\pm)\,\mu\nu}(\vec{p}-\vec{k}) \;&=\; g_{\mu\nu}\,\left[\gamma^\mu\,\Lambda_Q^{(\pm)}(\vec{p}-\vec{k})\gamma_0\gamma^\nu\right], \\ &\approx\; -\left[\gamma_0 \pm \vec{\gamma}\cdot\hat{k}\right]. \end{aligned} \tag{147}$$

It is also useful to introduce the following approximation for the composites with the hard internal momentum $k \sim T$ and the soft external momentum $p \sim g\,T$,

$$\epsilon_G(\vec{k}) + \epsilon_Q(\vec{p}-\vec{k}) \;\approx\; 2\,|\vec{k}| \sim 2\,T, \tag{148}$$

and

$$\begin{aligned} \epsilon_G(\vec{k}) - \epsilon_Q(\vec{p}-\vec{k}) \;&\approx\; \hat{k}\cdot\vec{p} = |\vec{p}|\cos\theta, \\ &\sim\; gT\cos\theta. \end{aligned} \tag{149}$$

Therefore, under the assumption of the HTL approximation, the positive-positive energy component of the quark-gluon loop part of the quark self-energy is reduced to

$$\begin{aligned} \Sigma_Q^{(++)\,a}{}_n(p_0,\vec{p}) \;&=\; g^2\int\frac{d^3\vec{k}}{(2\pi)^3}\,\frac{1}{2\epsilon_G(\vec{k})}\,\frac{\left(\gamma_0+\vec{\gamma}\cdot\hat{k}\right)}{\left(p_0-\epsilon_Q(\vec{p}-\vec{k})-\epsilon_G(\vec{p})\right)} \\ &\quad\times\left[-n_F\left(\epsilon_Q(\vec{p}-\vec{k})-\mu_Q-i\frac{1}{\beta}\theta_n\right)+N_G\left(\epsilon_G(\vec{k})-i\frac{1}{\beta}\phi^a\right)\right], \\ &\approx\; g^2\int\frac{d^3\vec{k}}{(2\pi)^3}\frac{1}{4|\vec{k}|^2}\left(\gamma_0-\vec{\gamma}\cdot\hat{k}\right) \\ &\quad\times\left[n_F\left(\epsilon_Q(\vec{k})-\mu_Q-i\frac{1}{\beta}\theta_n\right)-N_G\left(\epsilon_G(\vec{k})-i\frac{1}{\beta}\phi^a\right)\right]. \end{aligned} \tag{150}$$

The sum of the positive-positive and negative-negative energy components is approximated to

$$\left[\Sigma_Q^{(++)\,a}{}_n(p_0,\vec{p}) + \Sigma_Q^{(--)\,a}{}_n(p_0,\vec{p})\right] \approx 0. \tag{151}$$

The results for the positive-negative and negative-positive energy components are finite in the HTL approximation. The positive-negative energy component reads

$$\begin{aligned}\Sigma_Q^{(+-)\,a}{}_n(p_0,\vec{p}) \;=\; g^2 \int \frac{d^3\vec{k}}{(2\pi)^3}\,\frac{1}{2\epsilon_G(\vec{k})}\,\frac{\left(\gamma_0+\vec{\gamma}\cdot\hat{k}\right)}{\left(p_0-\epsilon_Q(\vec{p}-\vec{k})+\epsilon_G(\vec{p})\right)} \\ \times\left[n_F\left(\epsilon_Q(\vec{p}-\vec{k})-\mu_Q-i\frac{1}{\beta}\theta_n\right)+N_G\left(\epsilon_G(\vec{k})+i\frac{1}{\beta}\phi^a\right)\right].\end{aligned} \tag{152}$$

The $(+-)$-component with the assumptions of the soft external momentum p and the hard internal momentum k is simplified to

$$\begin{aligned}\Sigma_{Q\,n}^{\;a\,(+-)}(p_0,\vec{p}) \;\approx\; g^2 \int \frac{d^3\vec{k}}{(2\pi)^3}\,\frac{1}{2|\vec{k}|}\left[\frac{\gamma_0-\vec{\gamma}\cdot\hat{k}}{p_0-\hat{k}\cdot\vec{p}}\right] \\ \times\left[n_F\left(\epsilon_Q(\vec{k})-\mu_Q-i\frac{1}{\beta}\theta_n\right)+N_G\left(\epsilon_G(\vec{k})+i\frac{1}{\beta}\phi^a\right)\right].\end{aligned} \tag{153}$$

Furthermore, the symmetry over the polar integration for the negative-positive and positive-negative energy components leads to

$$\int\frac{d\Omega}{4\pi}\left[\frac{\gamma_0+\vec{\gamma}\cdot\hat{k}}{p_0+\vec{p}\cdot\hat{k}}\right] \;=\; \int\frac{d\Omega}{4\pi}\left[\frac{\gamma_0-\vec{\gamma}\cdot\hat{k}}{p_0-\vec{p}\cdot\hat{k}}\right]. \tag{154}$$

The sum of the positive-negative and negative-positive energy components is found finite while the sum of positive-positive and negative-negative components is approximated to zero. Therefore, the quark self-energy component, namely, $\Sigma_{Q\,n}^{\;a}(p_0,\vec{p})$ is reduced to

$$\begin{aligned}\Sigma_{Q\,n}^{\;a}(p_0,\vec{p}) \;&=\; \Sigma_Q^{(+-)\,a}{}_n(p_0,\vec{p}) + \Sigma_Q^{(-+)\,a}{}_n(p_0,\vec{p}),\\ &=\; \left(\omega_{0\,Q}^2\right)_n^a \int\frac{d\Omega}{4\pi}\left[\frac{\gamma_0-\vec{\gamma}\cdot\hat{k}}{p_0-\hat{k}\cdot\vec{p}}\right].\end{aligned} \tag{155}$$

The quark plasma frequency that is labeled by the internal quark and gluon color indexes namely n and a, respectively, is defined by

$$\left(\omega_{0\,Q}^2\right)_n^a \;=\; \left[\left(\omega_{0\,Q(Q)}^2\right)_n + \left(\omega_{0\,Q(G)}^2\right)^a\right]. \tag{156}$$

The contributions of quark and gluon segments of the quark-gluon loop to the fermion Landau frequency are given by,

$$\begin{aligned}\left(\omega_{0\,Q(Q)}^{2}\right)_{n} &= \frac{1}{2}g^{2}\int\frac{d|\vec{k}||\vec{k}|}{2\pi^{2}}\left[n_{F}\left(\epsilon_{Q}(\vec{k})-\mu_{Q}-i\frac{1}{\beta}\theta_{n}\right)+n_{F}\left(\epsilon_{Q}(\vec{k})+\mu_{Q}+i\frac{1}{\beta}\theta_{n}\right)\right],\\ &= \frac{g^{2}}{4\pi^{2}}\left[\frac{\pi^{2}}{6\,\beta^{2}}+\frac{1}{2}\left(\mu_{Q}+i\,\frac{1}{\beta}\theta_{n}\right)^{2}\right],\end{aligned}\tag{157}$$

and

$$\begin{aligned}\left(\omega_{0\,Q(G)}^{2}\right)^{a} &= \frac{1}{2}g^{2}\int\frac{d|\vec{k}||\vec{k}|}{2\pi^{2}}\left[N_{G}\left(\epsilon_{G}(\vec{k})-i\frac{1}{\beta}\phi^{a}\right)+N_{G}\left(\epsilon_{G}(\vec{k})+i\frac{1}{\beta}\phi^{a}\right)\right],\\ &= \frac{g^{2}}{4\pi^{2}}\left[\frac{\pi^{2}}{3\,\beta^{2}}-\frac{1}{2}\left(i\,\frac{1}{\beta}\phi^{a}\right)^{2}+i\,\frac{\pi}{\beta}\left(i\,\frac{1}{\beta}\phi^{a}\right)\right],\\ &= \frac{g^{2}}{4\pi^{2}\,\beta^{2}}\left[\frac{1}{2}\left(\phi^{a}\right)^{2}-\pi\left(\phi^{a}\right)+\frac{\pi^{2}}{3}\right],\end{aligned}\tag{158}$$

respectively. In the case of real color chemical potentials, the fundamental and adjoint color chemical potentials are reduced to $i\,\frac{1}{\beta}\theta_{n}\rightarrow\mu_{C_{n}}$ and $i\,\frac{1}{\beta}\phi^{a}\equiv i\,\frac{1}{\beta}\phi\overbrace{\qquad}^{(AB)}\rightarrow\mu_{C}{}^{a}\equiv(\mu_{C_{A}}-\mu_{C_{B}})$, respectively. Hence, the quark and gluon contributions to the Landau fermion frequency which are given by Eqns. (157) and (158), are reduced to

$$\left(\omega_{0\,Q(Q)}^{2}\right)_{n} = \frac{g^{2}}{4\pi^{2}}\left[\frac{\pi^{2}}{6\,\beta^{2}}+\frac{1}{2}\left(\mu_{Q}+\mu_{C_{n}}\right)^{2}\right],\tag{159}$$

and

$$\begin{aligned}\left(\omega_{0\,Q(G)}^{2}\right)^{a} &= \frac{g^{2}}{4\pi^{2}}\left[\frac{\pi^{2}}{3\,\beta^{2}}-\frac{1}{2}\left(\mu_{C}{}^{a}\right)^{2}+i\,\frac{\pi}{\beta}\left(\mu_{C}{}^{a}\right)\right]\\ &\equiv \frac{g^{2}}{4\pi^{2}}\left[\frac{\pi^{2}}{3\,\beta^{2}}-\frac{1}{2}\left(\mu_{C_{A}}-\mu_{C_{B}}\right)^{2}+i\,\frac{\pi}{\beta}\left(\mu_{C_{A}}-\mu_{C_{B}}\right)\right],\end{aligned}\tag{160}$$

respectively. Finally, it is worth to mention that it is possible to transform the real flavor chemical potential μ_{Q} to an imaginary chemical potential $\mu_{Q}\rightarrow i\,\frac{1}{\beta}\,\theta_{fl_{Q}}$. In this case, Eq. (157) is reduced to

$$\left(\omega_{0\,Q(Q)}^{2}\right)_{n} = \frac{g^{2}}{4\pi^{2}}\left[\frac{\pi^{2}}{6\,\beta^{2}}-\frac{1}{2}\frac{1}{\beta^{2}}\left(\theta_{fl_{Q}}+\theta_{n}\right)^{2}\right].\tag{161}$$

Hereinafter, the real chemical potentials for the flavor and color degrees of freedom will be considered in the discussion of the physical aspects of the weakly interacting quark-gluon plasma above the critical point of deconfinement phase transition. The quark self-energy

with the external quark line indexes i and j is written as follows

$$\begin{aligned}\Sigma_{Q\,ij}(p_0,\vec{p}) &= (\mathbf{t}^a)_{in}\,\left(\mathbf{t}^b\right)_{mj}\,\Sigma_{Q\,nm}^{\;ab}(p_0,\vec{p})\,,\\ &= \left(\omega^2_{0\,Q}\right)_{ij}\,\left[\int\frac{d\Omega}{4\pi}\,\frac{\gamma_0-\vec{\gamma}\cdot\hat{k}}{p_0-\hat{k}\cdot\vec{p}}\right].\end{aligned}\tag{162}$$

The quark plasma frequency that is labeled by the external quark line (i.e. the external two legs of the internal quark-gluon loop) color indexes i and j is given by

$$\begin{aligned}\left(\omega^2_{0\,Q}\right)_{ij} &= (\mathbf{t}^a)_{in}\left(\mathbf{t}^b\right)_{mj}\delta_{nm}\delta_{ab}\left(\omega^2_{0\,Q}\right)^a_n\,,\\ &= (\mathbf{t}^a)_{in}\left(\mathbf{t}^b\right)_{mj}\delta_{nm}\delta_{ab}\left[\left(\omega^2_{0\,Q}\right)_n+\left(\omega^2_{0\,Q}\right)^a\right],\end{aligned}\tag{163}$$

where the elements $(\mathbf{t}^a)_{in}$ and $\left(\mathbf{t}^b\right)_{mj}$ are the vertexes which connect the external quark line with the internal quark and gluon loop segments. The conservation of quark (line) color charge contracts the external color indexes i and j for the quark plasma frequency to $\delta_{ij}\left(\omega^2_{0\,Q}\right)_i$. The adjoint color index a is set to $a=\underbrace{(AB)}$ where $a=1\ldots N_c^2-1$ while the fundamental-like indexes A and B run over $1\cdots N_c$. For example, the adjoint color index set $a=(1,2,3,4,5,6,7,8)$ corresponds to $a=\left(\underbrace{(11)},\underbrace{(12)},\underbrace{(13)},\underbrace{(21)},\underbrace{(22)},\underbrace{(23)},\underbrace{(31)},\underbrace{(32)}\right)$. The quark screening mass (i.e. Landau frequency) is defined as follows

$$\begin{aligned}\left(\omega^2_{0\,Q}\right)_{ij} &= (\mathbf{t}^a)_{in}\left(\mathbf{t}^b\right)_{mj}\delta_{nm}\delta_{ab}\left[\left(\omega^2_{0\,Q(Q)}\right)_n+\left(\omega^2_{0\,Q(G)}\right)^a\right],\\ &\sim \frac{1}{2}\left(\tau^{\underbrace{(AB)}}\right)_{in}\left(\tau^{\underbrace{(BA)}}\right)_{nj}\left[\left(\omega^2_{0\,Q(Q)}\right)_n+\left(\omega^2_{0\,Q(G)}\right)^{\underbrace{(AB)}}\right].\end{aligned}\tag{164}$$

The contraction over the fundamental color indexes $i\,j$ in the $SU(N_c)$ representation is reduced to

$$\begin{aligned}\left(\omega^2_{0\,Q}\right)_{ij} &= \left(\omega^2_{0\,Q(Q)}\right)_{ij}+\left(\omega^2_{0\,Q(G)}\right)_{ij}\,,\\ &= \delta_{ij}\,\left(\left(\omega^2_{0\,Q(Q)}\right)_j+\left(\omega^2_{0\,Q(G)}\right)_j\right),\\ &= \delta_{ij}\,\left(\omega^2_{0\,Q}\right)_j\,.\end{aligned}\tag{165}$$

The quark and gluon segments of the quark-gluon loop part of the quark self-energy gives the following Landau frequency elements, respectively,

$$\left(\omega^2_{0\,Q(Q)}\right)_i = \frac{1}{2N_c}\left(N_c\sum_{n=1}^{N_c}\left(\omega^2_{0\,Q}\right)_n-\left(\omega^2_{0\,Q}\right)_i\right),\tag{166}$$

and

$$\left(\omega^2_{0\,Q(G)}\right)_i \;=\; \frac{1}{2N_c}\left(N_c\sum_{n=1}^{N_c}\left(\omega^2_{0\,Q}\right)\overbrace{\qquad}^{(in)} - \left(\omega^2_{0\,Q}\right)\overbrace{\qquad}^{(ii)}\right). \tag{167}$$

Hence, the quark plasma frequency is given by

$$\left(\omega^2_{0\,Q}\right)_i \;=\; \left(\omega^2_{0\,Q(Q)}\right)_i + \left(\omega^2_{0\,Q(G)}\right)_i. \tag{168}$$

The quark self-energy becomes

$$\Sigma_{Q\,ij}(p_0,\vec{p}) \;=\; \delta_{ij}\;\left(\omega^2_{0\,Q}\right)_j\int\frac{d\Omega}{4\pi}\left[\frac{\gamma_0-\vec{\gamma}\cdot\hat{k}}{p_0-\hat{k}\cdot\vec{p}}\right]. \tag{169}$$

Under certain circumstances, it possible to take the average over external color indexes to calculate the mean value of the Landau frequency over the color charges. The color mean value of the quark plasma frequency is given by

$$\begin{aligned}\left(\omega^2_{0\,Q}\right) \;&=\; \frac{1}{N_c}\sum_{i=1}^{N_c}\left(\omega^2_{0\,Q}\right)_i,\\ &=\; \frac{1}{2N_c}\sum_{n=1}^{N_c}\sum_{m=1}^{N_c}\left(1-\frac{\delta_{nm}}{N_c}\right)\left[\left(\omega^2_{0\,Q}\right)_n + \left(\omega^2_{0\,Q}\right)\overbrace{\qquad}^{(nm)}\right].\end{aligned} \tag{170}$$

A. The imaginary part

The analytic continuation of the momentum time-component $p_0 = p_0 + i\eta$ develops an imaginary part for the space-like energy domain $(p_0^2-\vec{p}^2)\leq 0$. This imaginary part describes the Landau-damping of the soft fermion field. The analytic continuation of p_0 develops real and imaginary parts for the quark self-energy as follows

$$\begin{aligned}\Sigma_{Q\,ij}\,(p_0,\vec{p}) \;&=\; \delta_{ij}\;\left(\omega^2_{0\,Q}\right)_j\;\left[\int\frac{d\Omega}{4\pi}\,\frac{\left(\gamma_0-\vec{\gamma}\cdot\hat{k}\right)}{\left(p_0-\hat{k}\cdot\vec{p}+i\eta\right)}\right],\\ &=\; \Re e\left(\Sigma_{Q\,ij}\,(p_0,\vec{p})\right) + i\,\Im m\left(\Sigma_{Q\,ij}\,(p_0,\vec{p})\right).\end{aligned} \tag{171}$$

The real and imaginary parts are not developed simultaneously but rather the real part is developed in the time-like energy domain $(p_0^2-\vec{p}^2)>0$ and then the real part is suppressed and is replaced by the imaginary part when the time-like energy turns to space-like energy.

Therefore, the real part is developed in the time-like energy domain $\vec{p}^2 < p_0^2$. It is reduced to

$$\begin{aligned}\Re e\left(\Sigma_{Q\,ij}\left(p_0,\vec{p}\right)\right) &= \delta_{ij}\,\left(\omega_{0\,Q}^2\right)_j\,\mathrm{P}\left[\int\frac{d\Omega}{4\pi}\,\frac{\gamma_0-\vec{\gamma}\cdot\hat{k}}{\left(p_0-\hat{k}\cdot\vec{p}\right)}\right],\\ &= \delta_{ij}\,\left[\Re e\left(\Sigma_{Q\,j}\left(p_0,\vec{p}\right)\right)\right],\\ &\qquad\left(\text{with the time-like energy } p_0^2>\vec{p}^2\right).\end{aligned}\tag{172}$$

After evaluating the principal value integral, the real part becomes

$$\begin{aligned}\Re e\left(\Sigma_{Q\,j}\left(p_0,\vec{p}\right)\right) &= \left(\omega_{0\,Q}^2\right)_j\,\left[\frac{1}{p_0}\,Q\left(\frac{p_0}{|\vec{p}|}\right)\,\gamma_0-\frac{1}{|\vec{p}|}\left[-1+Q\left(\frac{p_0}{|\vec{p}|}\right)\right]\,\vec{\gamma}\cdot\hat{p}\right],\\ &\qquad\left(\text{with the time-like energy } p_0^2>\vec{p}^2\right).\end{aligned}\tag{173}$$

The imaginary part is developed in the space-like energy domain, $\vec{p}^2 \geq p_0^2$, and it is reduced to

$$\begin{aligned}\Im m\left(\Sigma_{Q\,ij}\left(p_0,\vec{p}\right)\right) &= \delta_{ij}\,\left(\omega_{0\,Q}^2\right)_j\,\left[-\pi\int\frac{d\Omega}{4\pi}\,\left(\gamma_0-\vec{\gamma}\cdot\hat{k}\right)\,\delta\left(p_0-\hat{k}\cdot\vec{p}\right)\right],\\ &= \delta_{ij}\,\left[\Im m\left(\Sigma_{Q\,j}\left(p_0,\vec{p}\right)\right)\right],\\ &\qquad\left(\text{with the space-like energy } \vec{p}^2\geq p_0^2\right).\end{aligned}\tag{174}$$

After evaluating the integral over the Dirac-delta function, the imaginary part becomes

$$\begin{aligned}\Im m\left(\Sigma_{Q\,ij}\left(p_0,\vec{p}\right)\right) &= \delta_{ij}\,\left(\omega_{0\,Q}^2\right)_j\,\left[-\frac{\pi}{2|\vec{p}|}\,\left(\gamma_0-\frac{p_0}{|\vec{p}|}\vec{\gamma}\cdot\hat{p}\right)\,\theta\left(\frac{|\vec{p}|}{|p_0|}-1\right)\right],\\ &\qquad\left(\text{with the space-like energy } \vec{p}^2\geq p_0^2\right).\end{aligned}\tag{175}$$

B. Effective propagator for the soft quark

In order to find the quark propagator inverse, it is more convenience to decompose the quark self-energy to the Foldy-Wouthuysen positive and negative energy components as follows

$$\Sigma_{Q\,ij}(p_0,\vec{p}) = \delta_{ij}\,\left[\Sigma_Q^{(+)}{}_j(p_0,\vec{p})\,\gamma_0\,\Lambda_Q^{(+)}(\vec{k})-\Sigma_Q^{(-)}{}_j(p_0,\vec{p})\,\gamma_0\,\Lambda_Q^{(-)}(\vec{k})\right],\tag{176}$$

where the positive and negative energy components, respectively, read

$$\Sigma_Q^{(+)}{}_j(p_0,\vec{p}) = \left(\omega_{0\,Q}^2\right)_j\,\left[\frac{1}{|\vec{p}|}+\left(\frac{1}{p_0}-\frac{1}{|\vec{p}|}\right)\,Q\left(\frac{p_0}{|\vec{p}|}\right)\right],\tag{177}$$

and

$$\Sigma_{Q}^{(-)}{}_{j}(p_0,\vec{p}) \;=\; \left(\omega_{0\,Q}^{2}\right)_{j}\,\left[\frac{1}{|\vec{p}|}-\left(\frac{1}{p_0}+\frac{1}{|\vec{p}|}\right)\,Q\left(\frac{p_0}{|\vec{p}|}\right)\right]. \tag{178}$$

The inverse of the effective soft quark propagator is calculated by adding the quark self-energy to the inverse of the bar quark propagator as follows

$$\begin{aligned} {}^{*}\mathcal{S}_{Q}^{-1}{}_{ij}(p_0,\vec{p}) \;&=\; \mathcal{S}_{Q}^{-1}{}_{ij}(p_0,\vec{p}) + i\,\Sigma_{Q\,ij}(p_0,\vec{p}), \\ \text{or}\quad i\,{}^{*}\mathcal{S}_{Q}^{-1}{}_{ij}(p_0,\vec{p}) \;&=\; i\,\mathcal{S}_{Q}^{-1}{}_{ij}(p_0,\vec{p}) - \Sigma_{Q\,ij}(p_0,\vec{p}). \end{aligned} \tag{179}$$

The bar quark propagator is decomposed to the Foldy-Wouthuysen positive and negative energy components as follows

$$\mathcal{S}_{Q\,ij}(p_0,\vec{p}) \;=\; i\,\delta_{ij}\,\left[\frac{\Lambda_{Q}^{(+)}(\vec{k})\gamma_0}{p_0-\epsilon_Q(\vec{k})}+\frac{\Lambda_{Q}^{(-)}(\vec{k})\gamma_0}{p_0+\epsilon_Q(\vec{k})}\right]. \tag{180}$$

The inverse of the bar quark propagator is straightforward and it is reduced to

$$\mathcal{S}_{Q}^{-1}{}_{ij}(p_0,\vec{p}) \;=\; -i\,\delta_{ij}\,\left[\left(p_0-\epsilon_Q(\vec{k})\right)\gamma_0\,\Lambda_{Q}^{(+)}(\vec{k})+\left(p_0+\epsilon_Q(\vec{k})\right)\gamma_0\,\Lambda_{Q}^{(-)}(\vec{k})\right]. \tag{181}$$

The effective soft quark propagator is found as follows,

$$\begin{aligned} {}^{*}\mathcal{S}_{Q\,ij}\,(p_0,\vec{p}) \;&=\; i\,\delta_{ij}\,\left[\frac{\Lambda_{Q}^{(+)}(\vec{p})\,\gamma_0}{p_0-\left(\epsilon_Q(\vec{p})+\Sigma_{Q}^{(+)}{}_{j}(p_0,\vec{p})\right)}+\frac{\Lambda_{Q}^{(-)}(\vec{p})\,\gamma_0}{p_0+\left(\epsilon_Q(\vec{p})+\Sigma_{Q}^{(-)}{}_{j}(p_0,\vec{p})\right)}\right], \\ &=\; i\,\delta_{ij}\,\sum_{r}^{\pm}\left({}^{*}\Delta_{Q}^{(r)}{}_{j}(p_0,\vec{p})\right)\,h_{Q}^{(r)}(\vec{p}), \end{aligned} \tag{182}$$

where the following positive and negative energy projectors are introduced

$$h_{Q}^{(r)}(\vec{p}) = \Lambda_{Q}^{(r)}(\vec{p})\,\gamma_0, \qquad (\text{where } r=\pm). \tag{183}$$

The positive and negative energy decompositions, respectively, read,

$${}^{*}\Delta_{Q}^{(+)}{}_{j}\,(p_0,\vec{p}) \;=\; \frac{1}{p_0-\left(\epsilon_Q(\vec{p})+\Sigma_{Q}^{(+)}{}_{j}(p_0,\vec{p})\right)}, \tag{184}$$

and

$${}^{*}\Delta_{Q}^{(-)}{}_{j}\,(p_0,\vec{p}) \;=\; \frac{1}{p_0+\left(\epsilon_Q(\vec{p})+\Sigma_{Q}^{(-)}{}_{j}\,(p_0,\vec{p})\right)}. \tag{185}$$

In order to be able to work in the mixed-time representation of the imaginary-time formalism of the thermal field theory, we need to find all the poles of the effective soft quark propagator. The positive and negative energy poles are found in the following locations

$$\begin{aligned} p_0 = \overline{\omega}_{+j}: \quad & \left(\overline{\omega}_{+j} - \left(\epsilon_Q(\vec{p}) + \Sigma_Q^{(+)}{}_j(\overline{\omega}_{+j}, \vec{p})\right)\right) \;=\; 0, \\ p_0 = \overline{\omega}_{-j}: \quad & \left(\overline{\omega}_{-j} + \left(\epsilon_Q(\vec{p}) + \Sigma_Q^{(-)}{}_j(\overline{\omega}_{-j}, \vec{p})\right)\right) \;=\; 0, \end{aligned} \tag{186}$$

for the positive and negative Foldy-Wouthuysen energy components. Therefore, positive and negative energy poles are written, respectively, as follows

$$\varepsilon_Q^{(+)}{}_j(\vec{p}) \;=\; \left(\epsilon_Q(\vec{p}) + \Sigma_Q^{(+)}{}_j(\overline{\omega}_{+j}, \vec{p})\right), \; \overline{\omega}_{+j} = \varepsilon_Q^{(+)}{}_j(\vec{p}), \text{ and } p_0 = \overline{\omega}_{+j}, \tag{187}$$

and

$$\varepsilon_Q^{(-)}{}_j(\vec{p}) \;=\; \left(\epsilon_Q(\vec{p}) + \Sigma_Q^{(-)}{}_j(\overline{\omega}_{-j}, \vec{p})\right), \; \overline{\omega}_{-j} = -\varepsilon_Q^{(-)}{}_j(\vec{p}), \text{ and } p_0 = \overline{\omega}_{-j}. \tag{188}$$

After introducing the flavor and color chemical potentials, we can write the effective positive and negative energy poles as follows,

$$\begin{aligned} p_0 \to \; & \varepsilon_Q^{*(+)}{}_j(\vec{p}) \;=\; \varepsilon_Q^{(+)}{}_j(\vec{p}) - \mu_Q - i\,\frac{\theta_j}{\beta}, \\ p_0 \to \; & -\varepsilon_Q^{*(-)}{}_j(\vec{p}) \;=\; -\varepsilon_Q^{(-)}{}_j(\vec{p}) - \mu_Q - i\,\frac{\theta_j}{\beta}. \end{aligned} \tag{189}$$

The effective soft quark propagator in the mixed-time representation is reduced to

$$\begin{aligned} i\,{}^*\mathcal{S}_{ij}(\tau, \vec{p}) \;&=\; \delta_{ij} \;\left[i\,{}^*\mathcal{S}_j(\tau, \vec{p})\right], \\ &=\; \delta_{ij} \;\left[\Lambda_Q^{(+)}(\hat{p})\,\gamma_0\;{}^*\Delta_{Q\,j}^{(+)}(\tau, \vec{p}) + \Lambda_Q^{(-)}(\hat{p})\,\gamma_0\;{}^*\Delta_{Q\,j}^{(-)}(\tau, \vec{p})\right], \end{aligned} \tag{190}$$

where

$${}^*\Delta_{Q\,j}^{(+)}(\tau, \vec{p}) \;=\; \left[1 - n_F\left(\varepsilon_Q^{(+)}{}_j(\vec{p}) - \mu_Q - i\,\frac{\theta_j}{\beta}\right)\right] \exp\left[-\tau\,\left(\varepsilon_Q^{(+)}{}_j(\vec{p}) - \mu_Q - i\,\frac{\theta_j}{\beta}\right)\right], \tag{191}$$

and

$${}^*\Delta_{Q\,j}^{(-)}(\tau, \vec{p}) \;=\; n_F\left(\varepsilon_Q^{(-)}{}_j(\vec{p}) + \mu_Q + i\,\frac{\theta_j}{\beta}\right) \exp\left[\tau\,\left(\varepsilon_Q^{(-)}{}_j(\vec{p}) + \mu_Q + i\,\frac{\theta_j}{\beta}\right)\right]. \tag{192}$$

The mixed-time representation in the imaginary-time formalism in the thermal field theory is represented in the following way

$$\mathcal{S}\left(i\omega_n + \mu_Q + i\frac{\theta_j}{\beta}\right) = \int_0^\beta d\tau e^{i\omega_n\tau}\mathcal{S}_j^{>}(\tau), \quad (\text{where } \; \tau \geq 0), \tag{193}$$

and

$$\mathcal{S}_j(\tau) = \frac{1}{\beta}\sum_n \exp[-i\omega_n\tau]\mathcal{S}\left(i\omega_n + \mu_Q + i\frac{\theta_j}{\beta}\right). \tag{194}$$

VI. GLUON SELF-ENERGY: FEYNMAN DIAGRAMS

The soft gluon polarization tensor, namely, $\Pi^{\alpha'\alpha\,a'a}(p_0,\vec{p})$ is calculated up to the one loop approximation and the Feynman diagrams for the gluon-loop, tadpole, ghost-loop and quark-loop are depicted in Figs. (2 a), (2 b), (2 c) and (2 d), respectively. Hereinafter, the soft gluon polarization tensor is decomposed to two parts which are the gluon's part, namely, $\Pi^{\alpha'\alpha\,a'a}_{(gp)}(p_0,\vec{p})$ and the quark's part, namely, $\Pi^{\alpha'\alpha\,a'a}_{(ql)}(p_0,\vec{p})$. The gluon's part of the soft gluon polarization tensor, $\Pi^{\alpha'\alpha\,a'a}_{(gp)}(p_0,\vec{p})$, consists the gluon-loop, tadpole and ghost-loop that are displayed in Figs. (2 a), (2 b) and (2 c), respectively. Furthermore, the contributions of the gluon-loop, tadpole and ghost-loop to the soft gluon polarization tensor are represented by $\Pi^{\alpha'\alpha\,\,a'a}_{(g-l)}(p_0,\vec{p})$, $\Pi^{\alpha'\alpha\,a'a}_{(tp)}(p_0,\vec{p})$, and $\Pi^{\alpha'\alpha\,\,a'a}_{(gh)}(p_0,\vec{p})$, respectively. On the other hand, the quark's part of the soft gluon polarization tensor, namely, $\Pi^{\alpha'\alpha\,a'a}_{(ql)}(p_0,\vec{p})$, consists only the quark-loop that is depicted in Fig. (2 d). The color indexes are shown explicitly in the figures. These diagrams are evaluated in the HTL approximation. In the context of the HTL approximation the external gluon line is assumed soft and carries soft momentum and energy of order $p \sim g\,T$ (i.e. $|\vec{p}| \sim g\,T$ and $p_0 \sim g\,T$) while the internal momentum is considered hard one and is of oder $k \sim T$. The hard internal and soft external momenta have the following relationship,

$$p \sim gT \ll k \sim T \text{ and } g \ll 1. \tag{195}$$

The polarization tensor in the HTL approximation is shown to be gauge independent. It is straightforward to construct the gluon polarization tensor in the Feynman gauge where the final result is concluded to be gauge fixing independent. It is known that in the four space-time dimensions, the gluon polarization tensor expression develops an ultraviolet divergence. Such divergence is eliminated by the gluon wave-function renormalization. Moreover, the thermal contribution of the soft gluon polarization tensor

$$\Pi^{\alpha'\alpha\,a'a}(p_0,\vec{p})\Big|_T \;=\; \Pi^{\alpha'\alpha\,a'a}(p_0,\vec{p}) - \Pi^{\alpha'\alpha\,a'a}(p_0,\vec{p})\Big|_{T=0}, \tag{196}$$

has no ultraviolet divergence, since the statistical factors which are given by $n_F(\epsilon_Q(\vec{k}))$ for quark and $N_G(\epsilon_G(\vec{k}))$ for gluon are exponential decreasing. Hence, it is sufficient to evaluated the thermal soft gluon polarization in the standard 4 space-time dimensions and retaining only the thermal terms while dropping any term does not have an explicit temperature term. There is no need for any renormalization scheme in the present calculations.

A. Gluon-loop kernel $\Pi_{(g-l)}\,(p,k)$

The gluon loop part of the soft gluon polarization tensor is depicted in Fig. (2 a). It is furnished as follows

$$\begin{aligned}
\Pi_{(g-l)\,\alpha'\alpha}{}^{a'a}(p,k) &= \Pi_{(g-l)_{\alpha'\alpha}}{}^{a'a}(p_0,\vec{p},k_0,\vec{k}),\\
&= \frac{1}{2}\Big(-i\,g\,f^{a'c'b'}\,\Gamma^{(\rm out)}_{\alpha'\gamma'\beta'}(p,-k,-p+k)\Big)\;\mathcal{G}^{\gamma'\gamma\,c'c}(k_0,\vec{k})\\
&\quad\times\Big(-i\,g\,f^{cab}\,\Gamma^{(\rm in)}_{\gamma\alpha\beta}(-k,p,-p+k)\Big)\;\mathcal{G}^{\beta\beta'\,b'b}(p_0-k_0,\vec{p}-\vec{k}),\\
&= \frac{1}{2}\Big(+i\,g\,f^{a'c'b'}\,\Gamma_{\alpha'\gamma'\beta'}\,(-p,k,p-k)\Big)\;\mathcal{G}^{\gamma'\gamma\,c'c}(k_0,\vec{k})\\
&\quad\times\big(-i\,g\,f^{cab}\,\Gamma_{\gamma\alpha\beta}(-k,p,-p+k)\big)\;\mathcal{G}^{\beta\beta'\,b'b}(p_0-k_0,\vec{p}-\vec{k}). \qquad (197)
\end{aligned}$$

The inward-vertex $\Gamma^{(\rm in)}_{\gamma\alpha\beta}(-k,p,-p+k)=\Gamma_{\gamma\alpha\beta}\,(-k,p,-p+k)$ has the inward momentum, while the outward-vertex $\Gamma^{(\rm out)}_{\alpha'\gamma'\beta'}(p,-k,-p+k)\;=\;-\Gamma_{\alpha'\gamma'\beta'}\,(-p,k,p-k)$ has an outward momentum. The gluon vertexes that are appearing in the gluon-loop are given by

$$\begin{aligned}
\Gamma_{\beta\gamma\alpha}\,(-k,p,-p+k) &= \left[g_{\beta\gamma}(-p+2k)_\alpha+g_{\gamma\alpha}(-k-p)_\beta+g_{\alpha\beta}(2p-k)_\alpha\right],\\
\Gamma_{\gamma'\beta'\alpha'}\,(-p,k,p-k) &= -\left[g_{\gamma'\beta'}(-2k+p)_{\alpha'}+g_{\beta'\alpha'}(-2p+k)_{\gamma'}+g_{\alpha'\gamma'}(p+k)_{\beta'}\right], \qquad (198)
\end{aligned}$$

for the in- and out-vertexes, respectively. The gluon-loop kernel which is given by Eq. (197) is re-written as follows,

$$\begin{aligned}
\Pi_{(g-l)\,\alpha'\alpha}{}^{a'a}(p,k) &= +\frac{g^2}{2}\,f^{a'c'b'}\,f^{abc}\,\Gamma_{\alpha'\gamma'\beta'}\,(-p,k,p-k)\;\Gamma_{\gamma\alpha\beta}\,(-k,p,-p+k)\;g^{\gamma'\gamma'}\,g^{\beta\beta'}\\
&\quad\times\mathcal{G}^{c'c}(k_0,\vec{k})\,\mathcal{G}^{b'b}(p_0-k_0,\vec{p}-\vec{k}),\\
&= -\frac{g^2}{2}(\mathbf{T}^{a'})_{c'b'}(\mathbf{T}^{a})_{bc}\Gamma_{\alpha'\gamma'\beta'}\,(-p,k,p-k)\;\Gamma_{\gamma\alpha\beta}\,(-k,p,-p+k)\;g^{\gamma'\gamma'}\,g^{\beta\beta'}\\
&\quad\times\mathcal{G}^{c'c}(k_0,\vec{k})\,\mathcal{G}^{b'b}(p_0-k_0,\vec{p}-\vec{k}). \qquad (199)
\end{aligned}$$

Moreover, under the assumption of the HTL approximation where the hard internal momentum is supposed to be much bigger than the soft external gluon momentum by a ratio $p/k\;\sim\;g$ (i.e. $k\sim T\;\gg\;p\sim g\,T$), it is useful to introduce the following approximation,

$$\Gamma_{\alpha'\gamma'\beta'}\,(-k,p,-p+k)\;\Gamma_{\gamma\alpha\beta}\,(-p,k,p-k)\;g^{\gamma'\gamma'}\,g^{\beta\beta'}\approx 10\,k_\alpha\,k_{\alpha'}\;+\;2\,g_{\alpha\alpha'}\,k^2. \qquad (200)$$

The approximation, that is given by Eq. (200), reduces the gluon-loop kernel which is given by Eq. (199) to

$$\begin{aligned}
\Pi^{\alpha'\,\alpha}_{(g-l)}{}^{a'a}(p,k) &= -\frac{g^2}{2}\,(\mathbf{T}^{a'})_{c'b'}\,(\mathbf{T}^{a})_{bc}\,\Big[10\,k^\alpha\,k^{\alpha'}\;+\;2\,g^{\alpha\,\alpha'}\,k^2\Big]\\
&\quad\times\mathcal{G}^{c'c}(k_0,\vec{k})\,\mathcal{G}^{b'b}(p_0-k_0,\vec{p}-\vec{k}). \qquad (201)
\end{aligned}$$

B. Tadpole diagram kernel $\Pi_{(tp)}\,(p,k)$

The gluon tadpole contributes to the soft gluon polarization tensor. Its Feynman diagram is depicted in Fig. (2 b). The gluon tadpole kernel is constructed by the four-gluons vertex and one gluon loop as follows,

$$\begin{aligned}
\Pi_{(tp)}^{\alpha\alpha'\,a'a}(p,k) &= \Pi_{(tp)}^{\alpha\alpha'\,a'a}(p_0,\vec{p},k_0,\vec{k}),\\
&= \frac{1}{2}\,g^2\,\Gamma_{\beta'\beta}^{\alpha'\alpha\,a'a\,c'c}\,g^{\beta'\beta}\,\mathcal{G}^{c'c}(k_0,\vec{k}),\\
&= \frac{1}{2}\,g^2\,\Gamma_{\beta'\beta}^{\alpha'\alpha\,a'c'\,ca}\,g^{\beta'\beta}\,\mathcal{G}^{c'c}(k_0,\vec{k}).
\end{aligned}\tag{202}$$

The four-gluons vertex that is contracted by $g^{\beta'\beta}$ is reduced to

$$\begin{aligned}
g^{\beta'\beta}\,\Gamma_{\beta'\beta}^{\alpha'\alpha\,a'c'\,ca} &= \Big[f^{a'c'e}\,f^{eca}\,(g_{\alpha\alpha'}\,\delta_{\beta\beta}-g_{\alpha\alpha'})-f^{a'ae}\,f^{ec'c}\,(g_{\alpha\alpha'}\,\delta_{\beta\beta}-g_{\alpha\alpha'})\Big],\\
&= (\delta_{\beta\beta}-1)g_{\alpha\alpha'}\Big[f^{a'c'e}\,f^{eca}\,+\,f^{a'ae}\,f^{ecc'}\Big],\\
&= 2\,(\mathrm{dim}_4-1)\,g_{\alpha\alpha'}\,\Big[f^{a'c'e}\,f^{aec}\Big],\\
&= -6\,g_{\alpha\alpha'}\,(\mathbf{T}^{a'})_{c'e'}\,(\mathbf{T}^{a})_{ec}\,\delta_{ee'}.
\end{aligned}\tag{203}$$

The dimension of the configuration space is set to 4 ($i.e.\mathrm{dim}=4$). Therefore, the kernel of the gluon tadpole is reduced to

$$\Pi_{(tp)}^{\alpha'\alpha\,a'a}(p,k)\;\equiv\;-3\,g^2\,(\mathbf{T}^{a'})_{c'b'}\,(\mathbf{T}^{a})_{bc}\,\mathcal{G}^{c'c}(k_0,\vec{k})\,g_{\alpha\alpha'}\,\delta^{b'b},\tag{204}$$

where p and k are the soft external and the hard internal gluon momenta, respectively.

C. Ghost-loop diagram kernel $\Pi_{(gh)}(p,k)$

The Feynman diagram for the ghost-loop is depicted in Fig. (2 c). The ghost-loop's kernel as a function of the soft external and hard internal momenta, p and k, respectively, is constructed as follows

$$\begin{aligned}
\Pi_{(gh)}^{\alpha'\alpha\;\;a'a}(p,k) &= \Pi_{(gh)}^{\alpha'\alpha\;\;a'a}(p_0,\vec{p},k_0,\vec{k}),\\
&= \Big(-i\,g\,f^{b'a'c'}\,k_{\alpha'}\Big)\,\mathcal{G}^{c'c}(k_0,\vec{k})\,\Big(-i\,g\,f^{cab}\,(k-p)_{\alpha}\Big)\\
&\qquad\times\mathcal{G}^{b'b}(k_0-p_0,\vec{k}-\vec{p}).
\end{aligned}\tag{205}$$

It is approximated to

$$\begin{aligned}
\Pi_{(gh)}^{\alpha'\alpha\;\;a'a}(p,k) &\approx \Big(-i\,g\,f^{b'a'c'}\,k_{\alpha'}\Big)\,\mathcal{G}^{c'c}(k_0,\vec{k})\,\Big(-i\,g\,f^{cab}\,k_{\alpha}\Big)\,\mathcal{G}^{b'b}(k_0-p_0,\vec{k}-\vec{p}),\\
&= -g^2\,f^{a'c'b'}\,f^{abc}\,k_{\alpha'}\,k_{\alpha}\,\mathcal{G}^{c'c}(k_0,\vec{k})\,\mathcal{G}^{b'b}(k_0-p_0,\vec{k}-\vec{p}).
\end{aligned}\tag{206}$$

In terms of the adjoint $\mathbf{T}^a$ and $\mathbf{T}^{a'}$ color matrices, the kernel of the ghost-loop that is given by Eq. (206) becomes,

$$\Pi^{\alpha'\alpha\ a'a}_{(gh)}(p,k) \;=\; g^2\,(\mathbf{T}^{a'})_{c'b'}\,(\mathbf{T}^{a})_{bc}\,\Big[k^{\alpha'}\,k^{\alpha}\,\mathcal{G}^{c'c}(k_0,\vec{k})\,\mathcal{G}^{b'b}(k_0-p_0,\vec{k}-\vec{p})\Big]\,. \tag{207}$$

D. Gluon's part of the gluon's self-energy: $\Pi_{(gp)}(p_0,\vec{p}) = \Pi_{(g-l)}(p_0,\vec{p}) + \Pi_{(tp)}(p_0,\vec{p}) + \Pi_{(gh)}(p_0,\vec{p})$

The gluon's part of the gluon's self-energy consists of the gluon-loop, ghost-loop and tadpole interactions. These interactions are depicted in Figs. (2 a), (2 b) and (2 c), respectively. The energy of the gluon's part is calculated by integrating the kernel over the hard internal momentum k as follows,

$$\begin{aligned}\Pi^{\alpha'\alpha\ a'a}_{(gp)}(p) \;&=\; \Pi^{\alpha'\alpha\ a'a}_{(gp)}(p_0,\vec{p}),\\ &=\; \int\frac{dk_0}{2\pi}\int\frac{d^3\vec{k}}{(2\pi)^3}\,\Pi^{\alpha'\alpha\ a'a}_{(gp)}(p,k).\end{aligned} \tag{208}$$

The kernel is expressed in terms of the both soft external 4-momentum p and hard internal 4-momentum k and it reads,

$$\Pi^{\alpha'\alpha\ a'a}_{(gp)}(p,k) \;=\; \Pi^{\alpha'\alpha\ a'a}_{(g-l)}(p,k) + \Pi^{\alpha'\alpha\ a'a}_{(tp)}(p,k) + \Pi^{\alpha'\alpha\ a'a}_{(gh)}(p,k). \tag{209}$$

The soft external momentum line, namely, p is labeled by the external adjoint indexes $a'\,a$ while the hard internal momentum lines are labeled by the internal adjoint color indexes $b'\,b$ for one line segment and $c'\,c$ for the other line segment. The external adjoint color indexes $a'\,a$ are coupled to the internal color indexes through the elements of the adjoint color matrices (i.e. vertexes) $(\mathbf{T}^{a'})_{c'b'}$ and $(\mathbf{T}^{a})_{bc}$. Hence, the total kernel of the gluon's part of the gluon's self-energy is reduced to

$$\begin{aligned}\Pi^{\alpha'\alpha\ a'a}_{(gp)}(p,k) \;=\; (\mathbf{T}^{a'})_{c'b'}\,(\mathbf{T}^{a})_{bc}\,g^2\,\Big[&-\big(4k_{\alpha'}\,k_{\alpha}+g_{\alpha'\alpha}\,k^2\big)\;\mathcal{G}^{c'c}(k_0,\vec{k})\,\mathcal{G}^{b'b}(k_0-p_0,\vec{k}-\vec{p})\\ &-3g_{\alpha'\alpha}\,\mathcal{G}^{c'c}(k_0,\vec{k})\,\delta^{bb'}\Big]\,.\end{aligned} \tag{210}$$

It is useful to note the following relation for the integration over the time-component of the hard internal momentum k,

$$
\begin{aligned}
(\mathbf{T}^{a'})_{c'b'}\,(\mathbf{T}^{a})_{bc}\int\frac{dk_0}{2\pi}\mathcal{G}^{c'c}(k_0,\vec{k})\,\delta^{bb'} \;&\equiv\; -(\mathbf{T}^{a'})_{c'b'}\,(\mathbf{T}^{a})_{bc}\\
&\quad\times\int\frac{dk_0}{2\pi}k^2\,\mathcal{G}^{c'c}(k_0,\vec{k})\,\mathcal{G}^{b'b}(k_0-p_0,\vec{k}-\vec{p}),\\
&\equiv\; \frac{1}{2}\,(\mathbf{T}^{a'})_{c'b'}\,(\mathbf{T}^{a})_{bc}\\
&\quad\times\int\frac{dk_0}{2\pi}\left[\mathcal{G}^{c'c}(k_0,\vec{k})\,\delta^{bb'}+\mathcal{G}^{b'b}(k_0,\vec{k})\,\delta^{cc'}\right].
\end{aligned}
\tag{211}
$$

The last line in the preceding integral is to indicate the symmetry of the term $(\mathbf{T}^{a'})_{c'b'}\,(\mathbf{T}^{a})_{bc}\,\delta^{b'b}\delta^{c'c}$ over the internal adjoint indexes under the sum of the repeated indexes those are considered in Eq. (210). Therefore, the gluon's part of the gluon's self-energy is reduced to

$$
\begin{aligned}
\Pi^{\alpha'\alpha\;\,a'a}_{(gp)}(p) \;&=\; \Pi^{\alpha'\alpha\;\,a'a}_{(gp)}(p_0,\vec{p}),\\
&=\; -4(\mathbf{T}^{a'})_{c'b'}\,(\mathbf{T}^{a})_{bc}\,g^2\int\frac{d^3\vec{k}}{(2\pi)^3}\left[\int\frac{dk_0}{2\pi}k_{\alpha'}\,k_{\alpha}\,\mathcal{G}^{c'c}(k_0,\vec{k})\,\mathcal{G}^{b'b}(k_0-p_0,\vec{k}-\vec{p})\right.\\
&\qquad\left.+\,\frac{1}{2}g_{\alpha'\alpha}\int\frac{dk_0}{2\pi}\mathcal{G}^{c'c}(k_0,\vec{k})\,\delta^{bb'}\right],\\
&=\; -4(\mathbf{T}^{a'})_{c'b'}\,(\mathbf{T}^{a})_{bc}\,g^2\int\frac{d^3\vec{k}}{(2\pi)^3}\int\frac{dk_0}{2\pi}\left[k_{\alpha'}\,k_{\alpha}-\frac{1}{2}\,g_{\alpha'\alpha}\,k^2\right]\\
&\qquad\times\mathcal{G}^{c'c}(k_0,\vec{k})\,\mathcal{G}^{b'b}(k_0-p_0,\vec{k}-\vec{p}).
\end{aligned}
\tag{212}
$$

The notations for the gluon part of the gluon's self-energy is simplified to

$$
\Pi^{\alpha'\alpha\;\,a'a}_{(gp)}(p_0,\vec{p}) \;=\; -4(\mathbf{T}^{a'})_{c'b'}\,(\mathbf{T}^{a})_{bc}\left([k_{\alpha'}k_{\alpha}\Pi_{\mathcal{G}\mathcal{G}}]^{b'b\,cc'}(p_0,\vec{p})+\frac{1}{2}g_{\alpha'\alpha}\,[\Pi_{\mathcal{G}}]^{b'b\,cc'}(p_0,\vec{p})\right).
\tag{213}
$$

The two terms inside the parenthesis on the right hand side of Eq. (213) is labeled by the internal adjoint color indexes $b'\,b$ and $c'c$. Moreover, the first term on the right hand side of Eq. (213) is defined by

$$
[k_{\alpha'}k_{\alpha}\Pi_{\mathcal{G}\mathcal{G}}]^{b'b\,cc'}(p_0,\vec{p}) \;=\; g^2\int\frac{d^3\vec{k}}{(2\pi)^3}\int\frac{dk_0}{2\pi}k_{\alpha'}\,k_{\alpha}\,\mathcal{G}^{c'c}(k_0,\vec{k})\,\mathcal{G}^{b'b}(k_0-p_0,\vec{k}-\vec{p}).
\tag{214}
$$

While the second term on the right hand side of Eq. (213) is written as follows,

$$
\begin{aligned}
[\Pi_{\mathcal{G}}]^{b'b\,cc'}(p_0,\vec{p}) \;&=\; \int\frac{d^3\vec{k}}{(2\pi)^3}\int\frac{dk_0}{2\pi}\Pi_{\mathcal{G}}{}^{b'b\,cc'}(p,k),\\
&=\; -\left[k^2\Pi_{\mathcal{G}\mathcal{G}}\right]^{b'b\,cc'}(p_0,\vec{p}),
\end{aligned}
\tag{215}
$$

where

$$[\Pi_{\mathcal{G}}]^{b'b\,cc'}(p_0,\vec{p}) \;=\; g^2 \int \frac{d^3\vec{k}}{(2\pi)^3} \int \frac{dk_0}{2\pi} \mathcal{G}^{c'c}(k_0,\vec{k})\,\delta^{bb'}, \tag{216}$$

and

$$\left[k^2\Pi_{\mathcal{G}\mathcal{G}}\right]^{b'b\,cc'}(p_0,\vec{p}) \;=\; g^2 \int \frac{d^3\vec{k}}{(2\pi)^3} \int \frac{dk_0}{2\pi}\, k^2\, \mathcal{G}^{b'b}(k_0,\vec{k})\, \mathcal{G}^{c'c}(k_0-p_0,\vec{k}-\vec{p}). \tag{217}$$

The second term inside the parenthesis on the right hand side of Eq. (213) shall be evaluated at first because it is easier than the first one. The term, namely, $[k^2\Pi_{\mathcal{G}\mathcal{G}}]^{b'b\,cc'}(p_0,\vec{p})$ is written the mixed-time representation of the imaginary-time formalism as follows

$$\begin{aligned}\left[k^2\Pi_{\mathcal{G}\mathcal{G}}\right]^{b'b\,cc'}(p_0,\vec{p},\vec{k}) \;=\; -g^2 \int \frac{dk_0}{2\pi} \int_0^\beta d\tau \int_0^\beta d\tau'\, e^{\left[k_0 - i\frac{1}{\beta}\phi^b\right]\tau}\, e^{\left[(k_0-p_0) - i\frac{1}{\beta}\phi^c\right]\tau'}\,\delta(\tau) \\ \times \mathcal{G}^{c'c}(\tau',\vec{k}-\vec{p})\,\delta^{bb'}.\end{aligned} \tag{218}$$

It is evaluated as follows,

$$\begin{aligned}\left[k^2\Pi_{\mathcal{G}\mathcal{G}}\right]^{b'b\,cc'}(p_0,\vec{p},\vec{k}) \;&\equiv\; -g^2\,\mathcal{G}^{cc'}(0,\vec{k}-\vec{p})\,\delta^{bb'}, \\ &\approx\; -\frac{g^2}{2\epsilon_G(\vec{k})}\left[1 + N_G\left(\epsilon_G(\vec{k}) - i\frac{1}{\beta}\phi^c\right)\right. \\ &\qquad \left. + N_G\left(\epsilon_G(\vec{k}) + i\frac{1}{\beta}\phi^c\right)\right]\,\delta^{bb'}\,\delta^{cc'}.\end{aligned} \tag{219}$$

After integrating Eq. (219) over the hard internal momentum $\vec{k}$, we get

$$\begin{aligned}\left[k^2\Pi_{\mathcal{G}\mathcal{G}}\right]^{b'b\,cc'}(p_0,\vec{p}) \;&=\; \int \frac{d^3\vec{k}}{(2\pi)^3}\left[k^2\Pi_{\mathcal{G}\mathcal{G}}\right]^{bc}(p_0,\vec{p},\vec{k})\,\delta^{b'b}\,\delta^{cc'}, \\ &=\; \left[k^2\Pi_{\mathcal{G}\mathcal{G}}\right]^{bc}(p_0,\vec{p})\,\delta^{b'b}\,\delta^{cc'},\end{aligned} \tag{220}$$

where

$$\begin{aligned}\left[k^2\Pi_{\mathcal{G}\mathcal{G}}\right]^{bc}(p_0,\vec{p}) \;\approx\; -g^2 \int \frac{d^3\vec{k}}{(2\pi)^3}\,\frac{1}{2\epsilon_G(\vec{k})}\left[N_G\left(\epsilon_G(\vec{k}) - i\frac{1}{\beta}\phi^c\right) + N_G\left(\epsilon_G(\vec{k}) + i\frac{1}{\beta}\phi^c\right)\right] \\ +\;\text{(non-thermal part)}\,.\end{aligned} \tag{221}$$

The thermal part of the above equation is given by dropping the non-thermal part. Therefore, the second term on the right hand side of Eq. (213) is reduced to

$$\begin{aligned}[\Pi_{\mathcal{G}}]^{bc}(p_0,\vec{p}) \;&=\; -\left[k^2\Pi_{\mathcal{G}\mathcal{G}}\right]^{bc}(p_0,\vec{p}), \\ &\approx\; \frac{1}{4}\,\left(\mathbf{m}^2_{D\,(G)}\right)^{bc}.\end{aligned} \tag{222}$$

The Debye mass $\left(\mathbf{m}^2_{D\,(G)}\right)^{bc}$ which is contracted by $(\mathbf{T}^{a'})_{cb}\,(\mathbf{T}^{a})_{bc}\,\left(\mathbf{m}^2_{D\,(G)}\right)^{bc}$ $=$ $(\mathbf{T}^{a'})_{cb}\,(\mathbf{T}^{a})_{bc}\,\left(\mathbf{m}^2_{D\,(G)}\right)^{b}$ is reduced to

$$\begin{aligned}
\left(\mathbf{m}^2_{D\,(G)}\right)^{bc} &= g^2\int\frac{d|\vec{k}|}{2\pi^2}|\vec{k}|\left[N_G\left(\epsilon_G(\vec{k})-i\frac{1}{\beta}\phi^b\right)+N_G\left(\epsilon_G(\vec{k})+i\frac{1}{\beta}\phi^b\right)\right.\\
&\quad\left.+N_G\left(\epsilon_G(\vec{k})-i\frac{1}{\beta}\phi^c\right)+N_G\left(\epsilon_G(\vec{k})+i\frac{1}{\beta}\phi^c\right)\right],\\
&= 2\,g^2\int\frac{d|\vec{k}|}{2\pi^2}|\vec{k}|\left[N_G\left(\epsilon_G(\vec{k})-i\frac{1}{\beta}\phi^b\right)+N_G\left(\epsilon_G(\vec{k})+i\frac{1}{\beta}\phi^b\right)\right]. \qquad (223)
\end{aligned}$$

It is natural to symmetrize the adjoint color indexes b and c under the sum of all possible configurations. Moreover, the first term on the right hand side of Eq. (213) can be evaluated in a straightforward way. Eq. (214) is written as follows

$$\begin{aligned}
\left[k_\alpha k_{\alpha'}\Pi_{\mathcal{G}\mathcal{G}}\right]^{b'b\,cc'}(p_0,\vec{p}) &= \int\frac{d^3\vec{k}}{(2\pi)^3}\left[k_\alpha k_{\alpha'}\Pi_{\mathcal{G}\mathcal{G}}\right]^{b'b\,cc'}(p_0,\vec{p},\vec{k}),\\
&= \int\frac{d^3\vec{k}}{(2\pi)^3}\int\frac{dk_0}{2\pi}\left[k_\alpha k_{\alpha'}\Pi_{\mathcal{G}\mathcal{G}}\right]^{b'b\,cc'}(p_0,\vec{p},k_0,\vec{k}), \qquad (224)
\end{aligned}$$

where

$$\left[k_\alpha k_{\alpha'}\Pi_{\mathcal{G}\mathcal{G}}\right]^{b'b\,cc'}(p_0,\vec{p},k_0,\vec{k}) = g^2\,k_{\alpha'}\,k_\alpha\,\mathcal{G}^{b'b}(k_0,\vec{k})\,\mathcal{G}^{c'c}(k_0-p_0,\vec{k}-\vec{p}). \qquad (225)$$

In the format of the mixed-time formalism, Eq. (224) is written as follows

$$\begin{aligned}
\left[k_\alpha k_{\alpha'}\Pi_{\mathcal{G}\mathcal{G}}\right]^{b'b\,cc'}(p_0,\vec{p},\vec{k}) &= g^2\int\frac{dk_0}{2\pi}\int_0^\beta d\tau\int_0^\beta d\tau' e^{\left[k_0-i\frac{1}{\beta}\phi^b\right]\tau}e^{\left[(k_0-p_0)-i\frac{1}{\beta}\phi^c\right]\tau'}\\
&\quad\times\left[k_\alpha k_{\alpha'}\mathcal{G}\right]^{b'b}(\tau,\vec{k})\,\mathcal{G}^{c'c}(\tau',\vec{k}-\vec{p}),\\
&= g^2\int_0^\beta d\tau e^{-\left(p_0-i\frac{1}{\beta}\phi^b+i\frac{1}{\beta}\phi^c\right)(\beta-\tau)}\\
&\quad\times\left[k_\alpha k_{\alpha'}\mathcal{G}\right]^{b'b}(\tau,\vec{k})\,\mathcal{G}^{cc'}(\beta-\tau,\vec{k}-\vec{p}),\\
&= g^2\int_0^\beta d\tau e^{\left(p_0-i\frac{1}{\beta}\phi^a\right)\tau}\left[k_\alpha k_{\alpha'}\mathcal{G}\right]^{b'b}(\tau,\vec{k})\,\mathcal{G}^{cc'}(\beta-\tau,\vec{k}-\vec{p}). \qquad (226)
\end{aligned}$$

In the above equation (i.e. Eq. (226)), the following relation is considered

$$\begin{aligned}
\int\frac{dk_0}{2\pi}\int_0^\beta d\tau\int_0^\beta d\tau' e^{\left(k_0-i\frac{1}{\beta}\phi^b\right)(\tau+\tau')} &= \frac{1}{\beta}\sum_n^{\text{even}}\int_0^\beta d\tau\int_0^\beta d\tau' e^{i\omega_n(\tau+\tau')},\\
&= \int_0^\beta d\tau\int_0^\beta d\tau'\delta(\tau+\tau'-\beta), \qquad (227)
\end{aligned}$$

besides the following identity

$$\begin{aligned}\exp\left[-\left(p_0 - i\frac{1}{\beta}\phi^b + i\frac{1}{\beta}\phi^c\right)\beta\right] &= \exp\left[-\left(p_0 - i\frac{1}{\beta}\phi^a\right)\beta\right], \\ &= 1,\end{aligned} \tag{228}$$

is adopted in the calculation. The term $[k_\alpha k_{\alpha'}\mathcal{G}]^{b'b}(\tau,\vec{k})$, which is appeared in Eq. (226), is defined in the context of the mixed-time representation. It needs a rather more sophisticated work to be calculated. It is decomposed to the Lorentz components, namely, zero, zero-vector and finally vector-vector components as follows,

$$\begin{aligned}[k_0\mathcal{G}]^{bb'}(\tau,\vec{k}) &= \frac{1}{2}\left[1 + N_G\left(\epsilon_G(\vec{k}) - i\frac{1}{\beta}\phi^b\right)\right]e^{-\tau\left(\epsilon_G(\vec{k}) - i\frac{1}{\beta}\phi^b\right)}\,\delta^{bb'} \\ &\quad -\frac{1}{2}\left[N_G\left(\epsilon_G(\vec{k}) + i\frac{1}{\beta}\phi^b\right)\right]e^{\tau\left(\epsilon_G(\vec{k}) + i\frac{1}{\beta}\phi^b\right)}\,\delta^{bb'},\end{aligned} \tag{229}$$

$$\begin{aligned}\left[k_0\vec{k}_j\mathcal{G}\right]^{bb'}(\tau,\vec{k}) &= \frac{\vec{k}_j}{2}\left[1 + N_G\left(\epsilon_G(\vec{k}) - i\frac{1}{\beta}\phi^b\right)\right]e^{-\tau\left(\epsilon_G(\vec{k}) - i\frac{1}{\beta}\phi^b\right)}\,\delta^{b'b} \\ &\quad -\frac{\vec{k}_j}{2}\left[N_G\left(\epsilon_G(\vec{k}) + i\frac{1}{\beta}\phi^b\right)\right]e^{\tau\left(\epsilon_G(\vec{k}) + i\frac{1}{\beta}\phi^b\right)}\,\delta^{bb'},\end{aligned} \tag{230}$$

and

$$\begin{aligned}\left[\vec{k}_i\vec{k}_j\mathcal{G}\right]^{bb'}(\tau,\vec{k}) &= \frac{\vec{k}_i\vec{k}_j}{2\epsilon_G(\vec{k})}\left[1 + N_G\left(\epsilon_G(\vec{k}) - i\frac{1}{\beta}\phi^b\right)\right]e^{-\tau\left(\epsilon_G(\vec{k}) - i\frac{1}{\beta}\phi^b\right)}\,\delta^{bb'} \\ &\quad +\frac{\vec{k}_i\vec{k}_j}{2\epsilon_G(\vec{k})}\left[N_G\left(\epsilon_G(\vec{k}) + i\frac{1}{\beta}\phi^b\right)\right]e^{\tau\left(\epsilon_G(\vec{k}) + i\frac{1}{\beta}\phi^b\right)}\,\delta^{bb'},\end{aligned} \tag{231}$$

respectively. The term $\mathcal{G}^{cc'}(\beta-\tau,\vec{k}-\vec{p})$, which is appeared in the last line of Eq. (226), is reduced to

$$\begin{aligned}\mathcal{G}^{cc'} &= \mathcal{G}^{cc'}(\beta-\tau,\vec{k}-\vec{p}), \\ &= \frac{1}{2\epsilon_G(\vec{k}-\vec{p})}\left[1 + N_G\left(\epsilon_G(\vec{k}-\vec{p}) - i\frac{1}{\beta}\phi^c\right)\right]e^{-(\beta-\tau)\left(\epsilon_G(\vec{k}-\vec{p}) - i\frac{1}{\beta}\phi^c\right)}\,\delta^{cc'} \\ &\quad +\frac{1}{2\epsilon_G(\vec{k}-\vec{p})}\left[N_G\left(\epsilon_G(\vec{k}-\vec{p}) + i\frac{1}{\beta}\phi^c\right)\right]e^{(\beta-\tau)\left(\epsilon_G(\vec{k}-\vec{p}) + i\frac{1}{\beta}\phi^c\right)}\,\delta^{cc'}.\end{aligned} \tag{232}$$

It can be parametrized in the following way,

$$\begin{aligned}\mathcal{G}^{cc'} &= \mathcal{G}^{cc'}(\beta-\tau,\vec{k}-\vec{p}), \\ &= \frac{1}{2\epsilon_G(\vec{k}-\vec{p})}\left[N_G\left(\epsilon_G(\vec{k}-\vec{p}) - i\frac{1}{\beta}\phi^c\right)\right]e^{\tau\left(\epsilon_G(\vec{k}-\vec{p}) - i\frac{1}{\beta}\phi^c\right)}\,\delta^{cc'} \\ &\quad +\frac{1}{2\epsilon_G(\vec{k}-\vec{p})}\left[1 + N_G\left(\epsilon_G(\vec{k}-\vec{p}) + i\,\frac{1}{\beta}\phi^c\right)\right]e^{-\tau\left(\epsilon_G(\vec{k}-\vec{p}) + i\,\frac{1}{\beta}\phi^c\right)}\,\delta^{cc'}.\end{aligned} \tag{233}$$

In the similar manner, the term $[k_0\mathcal{G}]^{cc'}\left(\beta-\tau,\vec{k}-\vec{p}\right)$ is parametrized as follows

$$\begin{aligned}[k_0\mathcal{G}]^{cc'}\left(\beta-\tau,\vec{k}-\vec{p}\right) &= \frac{1}{2}\left[N_G\left(\epsilon_G(\vec{k}-\vec{p})-i\frac{1}{\beta}\phi^c\right)\right]e^{\tau\left(\epsilon_G(\vec{k}-\vec{p})-i\frac{1}{\beta}\phi^c\right)}\,\delta^{cc'} \\ &\quad -\frac{1}{2}\left[1+N_G\left(\epsilon_G(\vec{k}-\vec{p})+i\,\frac{1}{\beta}\phi^c\right)\right]e^{-\tau\left(\epsilon_G(\vec{k}-\vec{p})+i\,\frac{1}{\beta}\phi^c\right)}\,\delta^{cc'} \quad (234)\end{aligned}$$

The term, namely, $\left[k_{\alpha'}k_{\alpha}\Pi_{\mathcal{G}\mathcal{G}}\right]^{b'b\,cc'}(p_0,\vec{p})$ is decomposed to the Foldy-Wouthuysen positive and negative energy components:

$$\left[k_{\alpha'}k_{\alpha}\Pi_{\mathcal{G}\mathcal{G}}\right]^{b'b\,cc'}(p_0,\vec{p}) \;=\; \sum_{r=\pm}\sum_{s=\pm}\left[k_{\alpha'}k_{\alpha}\Pi^{(rs)}_{\mathcal{G}\mathcal{G}}\right]^{b'b\,cc'}(p_0,\vec{p}). \quad (235)$$

The positive-positive and negative-negative energy components of the Foldy-Wouthuysen decomposition are reduced to

$$\left[k_0k_0\Pi^{(++)}_{\mathcal{G}\mathcal{G}}\right]^{bc}(p_0,\vec{p},\vec{k}) \;\approx\; \frac{g^2}{4}\frac{\left[N_G\left(\epsilon_G(\vec{k})-i\frac{1}{\beta}\phi^b\right)-N_G\left(\epsilon_G(\vec{k}-\vec{p})-i\frac{1}{\beta}\phi^c\right)\right]}{p_0-\left(\epsilon_G(\vec{k})-\epsilon_G(\vec{k}-\vec{p})\right)}, \quad (236)$$

and

$$\left[k_0k_0\Pi^{(--)}_{\mathcal{G}\mathcal{G}}\right]^{bc}(p_0,\vec{p},\vec{k}) \;\approx\; -\frac{g^2}{4}\frac{\left[N_G\left(\epsilon_G(\vec{k})+i\frac{1}{\beta}\phi^b\right)-N_G\left(\epsilon_G(\vec{k}-\vec{p})+i\frac{1}{\beta}\phi^c\right)\right]}{p_0+\left(\epsilon_G(\vec{k})-\epsilon_G(\vec{k}-\vec{p})\right)}, \quad (237)$$

respectively, where the following approximation

$$\epsilon_G(\vec{k})\,/\,\epsilon_G(\vec{k}-\vec{p}) \;\approx\; 1, \quad (238)$$

is adopted. Since, the terms $\left[k_0k_0\Pi^{(rs)}_{\mathcal{G}\mathcal{G}}\right]^{bc}(p_0,\vec{p},\vec{k})$ are located under the integral $\int\frac{d^3\vec{k}}{(2\pi)^3}$, the symmetry over the polar integration $\hat{k}\cdot\vec{p}$ can be considered. The negative-negative energy component is reduced to

$$\begin{aligned}\left[k_0k_0\Pi^{(--)}_{\mathcal{G}\mathcal{G}}\right]^{bc}(p_0,\vec{p}) &= \int\frac{d^3\vec{k}}{(2\pi)^3}\left[k_0k_0\Pi^{(--)}_{\mathcal{G}\mathcal{G}}\right]^{bc}(p_0,\vec{p},\vec{k}) \\ &\approx\; -\frac{g^2}{4}\int\frac{d^3\vec{k}}{(2\pi)^3}\frac{\left[N_G\left(\epsilon_G(\vec{k})+i\frac{1}{\beta}\phi^b\right)-N_G\left(\epsilon_G(\vec{k}+\vec{p})+i\frac{1}{\beta}\phi^c\right)\right]}{p_0+\left(\epsilon_G(\vec{k})-\epsilon_G(\vec{k}+\vec{p})\right)}. \quad (239)\end{aligned}$$

In the subsequent calculations, it is useful to consider the following approximations

$$\begin{aligned}\epsilon_G(\vec{k})-\epsilon_G(\vec{k}-\vec{p}) &\;\approx\; \hat{k}\cdot\vec{p}\;\sim\; g\,T\,\cos(\theta), \\ \epsilon_G(\vec{k})+\epsilon_G(\vec{k}-\vec{p}) &\;\approx\; 2\,|\vec{k}|\;\sim\; 2\,T, \quad (240)\end{aligned}$$

for the HTL approximation with a soft external momentum p and a hard internal momentum k. The other energy components of the Foldy-Wouthuysen decomposition, namely, $(+-)$, $(-+)$, $(--)$ can be calculated in a similar way. Using the approximations that are given in Eqns. (238) and (240), the sum of the positive-positive and negative-negative energy kernel components, with the internal loop adjoint color indexes b and c which are given by Eqns. (236) and (239), is reduced to

$$\begin{aligned}
&\left(\left[k_0 k_0 \Pi^{(++)}_{\mathcal{GG}}\right]^{bc}(p_0,\vec{p},\vec{k}) + \left[k_0 k_0 \Pi^{(--)}_{\mathcal{GG}}\right]^{bc}(p_0,\vec{p},\vec{k})\right) \\
&\quad = \frac{g^2}{4}\int \frac{d^3\vec{k}}{(2\pi)^3}\left[\frac{1}{p_0-\hat{k}\cdot\vec{p}}\right]\left[N_G\left(\epsilon_G(\vec{k})-i\frac{1}{\beta}\phi^b\right)-N_G\left(\epsilon_G(\vec{k})+i\frac{1}{\beta}\phi^b\right)\right] \\
&\quad + \frac{g^2}{4}\int \frac{d^3\vec{k}}{(2\pi)^3}\left[\frac{1}{p_0-\hat{k}\cdot\vec{p}}\right]\left[N_G\left(\epsilon_G(\vec{k}-\vec{p})-i\frac{1}{\beta}\phi^c\right)-N_G\left(\epsilon_G(\vec{k}+\vec{p})+i\frac{1}{\beta}\phi^c\right)\right].
\end{aligned} \tag{241}$$

It is approximated to

$$\begin{aligned}
&\left(\left[k_0 k_0 \Pi^{(++)}_{\mathcal{GG}}\right]^{bc}(p_0,\vec{p}) + \left[k_0 k_0 \Pi^{(--)}_{\mathcal{GG}}\right]^{bc}(p_0,\vec{p})\right) \\
&= \frac{g^2}{4}\int \frac{d\Omega_k}{4\pi}\left[\frac{1}{p_0-\hat{k}\cdot\vec{p}}\right]\int \frac{d|\vec{k}|}{2\pi^2}|\vec{k}|^2\left[N_G\left(\epsilon_G(\vec{k})-i\frac{1}{\beta}\phi^b\right)-N_G\left(\epsilon_G(\vec{k})+i\frac{1}{\beta}\phi^b\right)\right] \\
&\quad - \frac{g^2}{4}\int \frac{d\Omega_k}{4\pi}\left[\frac{1}{p_0-\hat{k}\cdot\vec{p}}\right]\int \frac{d|\vec{k}|}{2\pi^2}|\vec{k}|^2\left[N_G\left(\epsilon_G(\vec{k})-i\frac{1}{\beta}\phi^c\right)-N_G\left(\epsilon_G(\vec{k})+i\frac{1}{\beta}\phi^c\right)\right] \\
&\quad - \frac{g^2}{4}\left[1-p_0\int \frac{d\Omega_k}{4\pi}\frac{1}{p_0-\hat{k}\cdot\vec{p}}\right]\int \frac{d|\vec{k}|}{2\pi^2}|\vec{k}|^2\frac{d}{d|\vec{k}|}\left[N_G\left(\epsilon_G(\vec{k})-i\frac{1}{\beta}\phi^c\right)+N_G\left(\epsilon_G(\vec{k})+i\frac{1}{\beta}\phi^c\right)\right].
\end{aligned} \tag{242}$$

In a similar way, the sum of positive-negative and negative-positive Foldy-Wouthuysen energy components is reduced to

$$\begin{aligned}
&\left(\left[k_0 k_0 \Pi^{(+-)}_{\mathcal{GG}}\right]^{bc}(p_0,\vec{p}) + \left[k_0 k_0 \Pi^{(-+)}_{\mathcal{GG}}\right]^{bc}(p_0,\vec{p})\right) \\
&\quad = -\frac{g^2}{4}\int \frac{d|\vec{k}|}{2\pi^2}\frac{|\vec{k}|}{2}\left[N_G\left(\epsilon_G(\vec{k})-i\frac{1}{\beta}\phi^b\right)+N_G\left(\epsilon_G(\vec{k})+i\frac{1}{\beta}\phi^b\right)\right] \\
&\quad\quad - \frac{g^2}{4}\int \frac{d|\vec{k}|}{2\pi^2}\frac{|\vec{k}|}{2}\left[N_G\left(\epsilon_G(\vec{k})-i\frac{1}{\beta}\phi^c\right)+N_G\left(\epsilon_G(\vec{k})+i\frac{1}{\beta}\phi^c\right)\right].
\end{aligned} \tag{243}$$

The gluon's part of the Debye mass due to the Feynman diagrams of the gluon loop, tadpole and ghost loop, reads

$$\begin{aligned}
\left(\mathbf{m}^2_{D\,(G)}\right)^b &= -g^2\int \frac{d|\vec{k}|}{2\pi^2}|\vec{k}|^2\frac{d}{d|\vec{k}|}\left[N_G\left(\epsilon_G(\vec{k})-i\frac{1}{\beta}\phi^b\right)+N_G\left(\epsilon_G(\vec{k})+i\frac{1}{\beta}\phi^b\right)\right], \\
&= 2\,g^2\int \frac{d|\vec{k}|}{2\pi^2}|\vec{k}|\left[N_G\left(\epsilon_G(\vec{k})-i\frac{1}{\beta}\phi^b\right)+N_G\left(\epsilon_G(\vec{k})+i\frac{1}{\beta}\phi^b\right)\right].
\end{aligned} \tag{244}$$

The additional terms those appear in Eq. (242) can be parametrized by

$$\left(\Delta\,\mathbf{m}^2_{D\,(G)}\right)^b \;=\; g^2\int\frac{d|\vec{k}|}{2\pi^2}\,|\vec{k}|^2\,\left[N_G\left(\epsilon_G(\vec{k})-i\frac{1}{\beta}\phi^b\right)-N_G\left(\epsilon_G(\vec{k})+i\frac{1}{\beta}\phi^b\right)\right]. \quad (245)$$

The sum over all the Foldy-Wouthuysen energy components of the composite $[k_0k_0\Pi_{\mathcal{GG}}]^{bc}\,(p_0,\vec{p})$ becomes

$$\begin{aligned}[k_0k_0\Pi_{\mathcal{GG}}]^{bc}\,(p_0,\vec{p}) \;=\; & -\frac{1}{8}\left[\frac{1}{2}\left(\mathbf{m}^2_{D\,(G)}\right)^b+\frac{1}{2}\left(\mathbf{m}^2_{D\,(G)}\right)^c\right]\\ & +\frac{1}{8}\left[2\;-\;2\,p_0\int\frac{d\Omega}{4\pi}\frac{1}{\left(p_0-\hat{k}\cdot\vec{p}\right)}\right]\left(\mathbf{m}^2_{D\,(G)}\right)^c\\ & +\frac{1}{4}\int\frac{d\Omega}{4\pi}\frac{1}{\left(p_0-\hat{k}\cdot\vec{p}\right)}\left[\left(\Delta\mathbf{m}^2_{D\,(G)}\right)^b-\left(\Delta\mathbf{m}^2_{D\,(G)}\right)^c\right]. \quad (246)\end{aligned}$$

The same calculations are performed for the other Lorentz components such as $[k_0k_i\Pi_{\mathcal{GG}}]^{bc}\,(p_0,\vec{p})$ and $[k_ik_j\Pi_{\mathcal{GG}}]^{bc}\,(p_0,\vec{p})$ components. For instance the term $[k_ik_j\Pi_{\mathcal{GG}}]^{bc}\,(p_0,\vec{p})$ is reduced to

$$\begin{aligned}[k_ik_j\Pi_{\mathcal{GG}}]^{bc}\,(p_0,\vec{p}) \;=\; & \frac{1}{8}\left[\frac{2}{3}\left(\mathbf{m}^2_{D\,(G)}\right)^c+\frac{1}{3}\left(\frac{1}{2}\left(\mathbf{m}^2_{D\,(G)}\right)^b+\frac{1}{2}\left(\mathbf{m}^2_{D\,(G)}\right)^c\right)\right]\,\delta_{ij}\\ & -\frac{2\,p_0}{8}\int\frac{d\Omega}{4\pi}\frac{\hat{k}_i\hat{k}_j}{\left(p_0-\hat{k}\cdot\vec{p}\right)}\,\left(\mathbf{m}^2_{D\,(G)}\right)^c\\ & +\frac{1}{4}\int\frac{d\Omega}{4\pi}\frac{\hat{k}_i\hat{k}_j}{\left(p_0-\hat{k}\cdot\vec{p}\right)}\left[\left(\Delta\mathbf{m}^2_{D\,(G)}\right)^b-\left(\Delta\mathbf{m}^2_{D\,(G)}\right)^c\right], \quad (247)\end{aligned}$$

where the following tensor identity has been considered in the above calculation

$$\int\frac{d\Omega}{4\pi}\left(3\hat{k}_i\hat{k}_j-\delta_{ij}\right)=0. \quad (248)$$

The Lorentz momentum components of $\hat{k}_{\alpha'}\,\hat{k}_\alpha$ are written as follows

$$\hat{k}_{\alpha'}\,\hat{k}_\alpha \;=\; \left(1,\hat{k}_i,\hat{k}_j,\hat{k}_i\hat{k}_j\right). \quad (249)$$

The general result can be obtained by the same calculations. The result reads

$$
\begin{aligned}
\left[k_{\alpha'}k_{\alpha}\Pi_{\mathcal{G}\mathcal{G}}\right]^{bc}(p_0,\vec{p}) \;=\; & 2\,\delta^0_{\alpha'}\,\delta^0_{\alpha}\left(\frac{1}{8}\right)\left[\frac{4}{3}\left(\mathbf{m}^2_{D\,(G)}\right)^c-\frac{1}{3}\left\{\frac{1}{2}\left(\mathbf{m}^2_{D\,(G)}\right)^b+\frac{1}{2}\left(\mathbf{m}^2_{D\,(G)}\right)^c\right\}\right] \\
& -g_{\alpha'\alpha}\left(\frac{1}{8}\right)\left[\frac{2}{3}\left(\mathbf{m}^2_{D\,(G)}\right)^c+\frac{1}{3}\left\{\frac{1}{2}\left(\mathbf{m}^2_{D\,(G)}\right)^b+\frac{1}{2}\left(\mathbf{m}^2_{D\,(G)}\right)^c\right\}\right] \\
& -\frac{2\,p_0}{8}\int\frac{d\Omega}{4\pi}\frac{\hat{k}_{\alpha'}\hat{k}_{\alpha}}{\left(p_0-\hat{k}\cdot\vec{p}\right)}\,\left(\mathbf{m}^2_{D\,(G)}\right)^c \\
& +\frac{1}{4}\int\frac{d\Omega}{4\pi}\frac{\hat{k}_{\alpha'}\hat{k}_{\alpha}}{\left(p_0-\hat{k}\cdot\vec{p}\right)}\left[\left(\Delta\mathbf{m}^2_{D\,(G)}\right)^b-\left(\Delta\mathbf{m}^2_{D\,(G)}\right)^c\right]. \qquad (250)
\end{aligned}
$$

The term $\left(\Delta\mathbf{m}^2_{D\,(G)}\right)^b$ generates a quadratic order temperature term (i.e. $\propto T^3$). This term also appears in Refs. [25–27]. Although these quadratic temperature terms emerge in the internal loop segments with internal adjoint color indexes, they cancel each other in the final result for the loop with external adjoint color indexes (see Eq. (100)) when the sum over the internal adjoint color indexes is considered.

By using the symmetry over the adjoint color indexes b and c that is given by Eqns. (99) and (100), the Lorentz-Lorentz polarization tensor (e.g. Eq. (250)) is contracted as follows

$$
\begin{aligned}
& \left(\mathbf{T}^{a'}\right)_{cb}\left(\mathbf{T}^{a}\right)_{bc}\left[k_{\alpha'}k_{\alpha}\Pi_{\mathcal{G}\mathcal{G}}\right]^{bc}(p_0,\vec{p}) \\
& \quad =\tfrac{1}{8}\,\left(\mathbf{T}^{a}\right)_{cb}\left(\mathbf{T}^{a}\right)_{bc}\left(\mathbf{m}^2_{D\,(G)}\right)^c\left[(2\delta^0_{\alpha'}\,\delta^0_{\alpha}-g_{\alpha'\alpha})-2\,p_0\int\tfrac{d\Omega}{4\pi}\tfrac{\hat{k}_{\alpha'}\hat{k}_{\alpha}}{(p_0-\hat{k}\cdot\vec{p})}\right]. \qquad (251)
\end{aligned}
$$

Hence after eliminating the redundant terms, it is simplified to

$$
\left[k_{\alpha'}k_{\alpha}\Pi_{\mathcal{G}\mathcal{G}}\right]^{bc}(p_0,\vec{p}) \;=\; \frac{1}{8}\,\left(\mathbf{m}^2_{D\,(G)}\right)^c\left[\left(2\delta^0_{\alpha'}\,\delta^0_{\alpha}-g_{\alpha'\alpha}\right)-2\,p_0\int\frac{d\Omega}{4\pi}\frac{\hat{k}_{\alpha'}\hat{k}_{\alpha}}{\left(p_0-\hat{k}\cdot\vec{p}\right)}\right]. \qquad (252)
$$

The quadratic temperature terms which are generated in the internal gluon loop are eliminated when the summation over the internal adjoint color indexes is considered. These quadratic terms simply disappear from the gluon polarization tensor with the external line legs those are labeled by the adjoint indexes $a'\,a$. The 3- gluons vertex is anti-symmetry over the interchange of two adjoint color indexes. Since the internal gluon loop has two 3-gluon vertexes, it is symmetry over the interchange of two adjoint color indexes. The internal loop

gluon polarization tensor becomes

$$\begin{aligned}
\Pi_{(gp)\,\alpha'\alpha}{}^{bc}(p_0,\vec{p}) &= -4\left(\left[k_{\alpha'}\,k_{\alpha}\Pi_{\mathcal{G}\mathcal{G}}\right]^{bc}(p_0,\vec{p})-\frac{1}{2}\,g_{\alpha'\alpha}\,\left[k^2\Pi_{\mathcal{G}\mathcal{G}}\right]^{bc}(p_0,\vec{p})\right),\\
&= -4\left(\left[k_{\alpha'}\,k_{\alpha}\Pi_{\mathcal{G}\mathcal{G}}\right]^{bc}(p_0,\vec{p})+\frac{1}{2}\,g_{\alpha'\alpha}\,\left[\Pi_{\mathcal{G}}\right]^{bc}(p_0,\vec{p})\right),\\
&= \left(\mathbf{m}^2_{D\,(G)}\right)^{bc}\left[-\delta^0_{\alpha'}\,\delta^0_{\alpha}+p_0\int\frac{d\Omega}{4\pi}\frac{\hat{k}_{\alpha'}\,\hat{k}_{\alpha}}{\left(p_0-\hat{k}\cdot\vec{p}\right)}\right].
\end{aligned}\tag{253}$$

When the color charges couple with the quark and gluon kinetic degree of freedom, the Debye mass has a color charge. The gluon's part of the Debye mass is labeled by an adjoint color index. The external adjoint color indexes are given by $a'\,a$ while the internal segments for the gluon loop are given by the adjoint color indexes $b'\,b$ and $c'\,c$. The internal adjoint color indexes are reduced to $b\,c$ by the contraction of $\delta^{c'\,c}$ and $\delta^{b'\,b}$ and the summation over all the possible configurations. The integration by parts reduces the gluon's part of the Debye mass to the following result,

$$\begin{aligned}
\left(\mathbf{m}^2_{D\,(G)}\right)^{b} &= 2g^2\int\frac{d|\vec{k}|}{2\pi^2}|\vec{k}|\left[N_G\left(\epsilon_G(\vec{k})-i\frac{1}{\beta}\phi^b\right)+N_G\left(\epsilon_G(\vec{k})+i\frac{1}{\beta}\phi^b\right)\right],\\
&= \frac{g^2}{\pi^2}\left[\frac{\pi^2}{3\,\beta^2}-\frac{1}{2}\left(i\,\frac{1}{\beta}\phi^b\right)^2+i\,\frac{\pi}{\beta}\left(i\,\frac{1}{\beta}\phi^b\right)\right],\\
&\to \frac{g^2}{\pi^2}\left[\frac{\pi^2}{3\,\beta^2}-\frac{1}{2}\left(\mu_C{}^{b\equiv\underbrace{(AB)}}\right)^2+i\,\frac{\pi}{\beta}\left(\mu_C{}^{b\equiv\underbrace{(AB)}}\right)\right],\\
&\to \frac{g^2}{\pi^2}\left[\frac{\pi^2}{3\,\beta^2}-\frac{1}{2}\left(\mu_{CA}-\mu_{CB}\right)^2+i\,\frac{\pi}{\beta}\left(\mu_{CA}-\mu_{CB}\right)\right].
\end{aligned}\tag{254}$$

It is interesting to note that when the fundamental color chemicals become equal $\mu_{CA}\approx\mu_{CB}$, the adjoint color chemical becomes negligible $\mu_C{}^{\underbrace{(AB)}}=(\mu_{CA}-\mu_{CB})\approx 0$ and Eq. (254) is reduced simply to $\left(\mathbf{m}^2_{D\,(G)}\right)^{bc}=g^2\,T^2/3$. When the fundamental color potentials are not equal (i.e. $\mu_{CA}\neq\mu_{CB}$), Eq. (254) develops an imaginary part and this leads to nontrivial results. The symmetrization over the internal adjoint color indexes, namely, b and c is given by

$$\begin{aligned}
(\mathbf{T}^{a'})_{cb}\,(\mathbf{T}^{a})_{bc}\,\left(\mathbf{m}^2_{D\,(G)}\right)^{bc} &= (\mathbf{T}^{a'})_{cb}\,(\mathbf{T}^{a})_{bc}\,\left[\left(\mathbf{m}^2_{D\,(G)}\right)^{b}+\left(\mathbf{m}^2_{D\,(G)}\right)^{c}\right]/2,\\
&= (\mathbf{T}^{a'})_{cb}\,(\mathbf{T}^{a})_{bc}\,\left(\mathbf{m}^2_{D\,(G)}\right)^{b},
\end{aligned}\tag{255}$$

which is identical to Eq. (223). The term $\left(\Delta \mathbf{m}^2_{D\,(G)}\right)^b$ is determined as follows

$$\begin{aligned}\left(\Delta \mathbf{m}^2_{D\,(G)}\right)^b &= g^2 \int \frac{d|\vec{k}|}{2\pi^2}\,|\vec{k}|^2 \left[N_G\left(\epsilon_G(\vec{k}) - i\frac{1}{\beta}\phi^b\right) - N_G\left(\epsilon_G(\vec{k}) + i\frac{1}{\beta}\phi^b\right)\right], \\ &= \frac{g^2\,T^3}{\pi^2}\left[\mathrm{Li}_3\left(e^{i\phi^b}\right) - \mathrm{Li}_3\left(e^{-i\phi^b}\right)\right]. \end{aligned} \tag{256}$$

The term with Poly-Logarithm functions can be simplified as follows

$$\begin{aligned}\left[\mathrm{Li}_3\left(e^{i\phi^b}\right) - \mathrm{Li}_3\left(e^{-i\phi^b}\right)\right] &= -\frac{1}{6}(i\phi^b)\left[(i\phi^b) - i\pi\right]\left[(i\phi^b) - 2i\pi\right], \\ &\equiv -\frac{1}{6}\left(\frac{{\mu_C}^b}{T}\right)\left[\left(\frac{{\mu_C}^b}{T}\right) - i\pi\right]\left[\left(\frac{{\mu_C}^b}{T}\right) - 2i\pi\right]. \end{aligned} \tag{257}$$

Furthermore, the term $\left(\Delta \mathbf{m}^2_{D\,(G)}\right)^b$ is found to be eliminated from the final results of the gluon polarization tensor with external line legs, namely, $\Pi_{(gp)\,\alpha'\alpha}{}^{a'a}(p_0,\vec{p}) = \left(\mathbf{T}^{a'}\right)_{cb}\left(\mathbf{T}^a\right)_{bc}\Pi_{(gp)\,\alpha'\alpha}{}^{bc}(p_0,\vec{p})$.

The gluon's part of the gluon polarization tensor with the soft external momentum p and the external adjoint color indexes $a'\,a$ becomes

$$\begin{aligned}\Pi_{(gp)\,\alpha'\alpha}{}^{a'a}\,(p_0,\vec{p}) &= \Pi_{(g-l)\,\alpha'\alpha}{}^{a'a}\,(p_0,\vec{p}) + \Pi_{(tp)\,\alpha'\alpha}{}^{a'a}\,(p_0,\vec{p}) + \Pi_{(gh)\,\alpha'\alpha}{}^{a'a}\,(p_0,\vec{p}), \\ &= \left(\mathbf{T}^{a'}\right)_{c'b'}\left(\mathbf{T}^a\right)_{bc}\left[\Pi_{(gp)\,\alpha'\alpha}{}^{bc}(p_0,\vec{p})\right]\,\delta^{b'b}\,\delta^{c'c}, \\ &= \left(\mathbf{m}^2_{D\,(G)}\right)^{a'a}\left[-\delta^0_{\alpha'}\,\delta^0_{\alpha} + p_0\int\frac{d\Omega}{4\pi}\frac{\hat{k}_{\alpha'}\,\hat{k}_{\alpha}}{\left(p_0 - \hat{k}\cdot\vec{p}\right)}\right]. \end{aligned} \tag{258}$$

The gluon's part of the screening Debye mass is given by

$$\begin{aligned}\left(\mathbf{m}^2_{D\,(G)}\right)^{a'a} &= \left(\mathbf{m}^2_{D\,(G)}\right)^{a}\,\delta^{a'a}, \\ &= \left(\mathbf{T}^{a'}\right)_{c'b'}\left(\mathbf{T}^a\right)_{bc}\left(\mathbf{m}^2_{D\,(G)}\right)^{bc}\,\delta^{b'b}\,\delta^{c'c}, \end{aligned} \tag{259}$$

where the two external gluon legs are labeled by the adjoint color indexes $a'\,a$ while the hard internal loop segments are labeled by $b'\,b$ and $c'\,c$.

E. Quark-loop diagram kernel $\Pi_{ql}(p,k)$

The quark-loop part of the gluon-self energy is depicted in Fig. (2 d). The structure of the quark-loop in the gluon's self-energy is quite different from the gluon's part that is given by the gluon-loop, tadpole and the ghost-loop. The interaction kernel of the quark-loop

is a function of the soft external momentum p and the hard internal momentum k. The two soft external gluon legs are identified by the adjoint color indexes $a'\,a$ and the Lorentz polarization indexes, namely, $\alpha'\,\alpha$. It is given by

$$\begin{aligned}\Pi^{\alpha'\alpha\,a'a}_{(ql)}(p,k) &= \Pi^{\alpha'\alpha\,a'a}_{(ql)}(p_0,\vec{p},k_0,\vec{k}),\\ &= \sum_{Q}^{N_F}\Pi^{\alpha'\alpha\;\;a'a}_{(ql)\,Q}(p,k),\end{aligned}\tag{260}$$

where the sum is taken over the flavors and the kernel of quark-loop polarization tensor is given by

$$\begin{aligned}\Pi^{\alpha'\alpha\;\;a'a}_{(ql)\,Q}(p,k) &= \Pi^{\alpha'\alpha\;\;a'a}_{(ql)\,Q}(p_0,\vec{p},k_0,\vec{k}),\\ &= \mathrm{tr}\,\Big[\Big(-g\,\gamma^{\alpha'}\,\mathbf{t}^{a'\dagger}_{i'j'}\Big)\;i\,\mathcal{S}_{Q\,j'j}(k_0,\vec{k})\\ &\qquad\times\;\big(-g\,\gamma^{\alpha}\,\mathbf{t}^{a}_{ji}\big)\;i\,\mathcal{S}_{Q\,ii'}(p_0-k_0,\vec{p}-\vec{k})\Big].\end{aligned}\tag{261}$$

Eq. (261) is reduced to

$$\begin{aligned}\Pi^{\alpha'\alpha\;\;a'a}_{(ql)\,Q}(p,k) &= \mathbf{t}^{a'\dagger}_{i'j'}\,\mathbf{t}^{a}_{ji}\;\Big[\Pi^{\alpha'\alpha}_{(ql)\,Q\;j'j\,ii'}(p,k)\Big],\\ &\equiv \mathbf{t}^{a'}_{i'j'}\,\mathbf{t}^{a}_{ji}\;\Big[\Pi^{\alpha'\alpha}_{(ql)\,Q\;j'j\,ii'}(p,k)\Big].\end{aligned}\tag{262}$$

In terms of the internal loop fundamental color indexes, it is reduced to

$$\begin{aligned}\Pi^{\alpha'\alpha}_{(ql)\,Q\;j'j\,ii'}(p,k) &= \Pi^{\alpha'\alpha}_{(ql)\,Q\;j'j\,ii'}(p_0,\vec{p},k_0,\vec{k}),\\ &= g^2\,\mathrm{tr}\,\Big[\gamma^{\alpha'}\,i\,\mathcal{S}_{Q\,j'j}(k_0,\vec{k})\,\gamma^{\alpha}\,i\,\mathcal{S}_{Q\,ii'}(p_0-k_0,\vec{p}-\vec{k})\Big].\end{aligned}\tag{263}$$

The kernel of quark-loop for the gluon polarization tensor $\Pi^{\alpha'\alpha}_{(ql)\,Q\;j'j\,ii'}(p,k)$ is identified by the internal fundamental color indexes $i'\,i$ and $j'\,j$ for the two internal quark segments of the quark loop. The external adjoint color indexes $a'\,a$ for the two soft external gluon legs are coupled to the internal quark fundamental color indexes for the two hard internal segments (i.e. the upper and lower arcs) of the internal quark-loop through the fundamental matrices elements $\mathbf{t}^{a'}_{i'j'}$ and $\mathbf{t}^{a}_{ji}$. The trace (i.e. tr) is over the Dirac matrices which appear in the quark propagators. The summation is considered over all the given flavors. It will be a good approximation to take the sum only over the up, down and strange flavors since the heavy flavors are suppressed strongly because of their large masses.

F. Quark's part of gluon self-energy: $\Pi_{ql}\,(p_0,\vec{p})$

The quark loop in the gluon polarization tensor is written as follows,

$$\begin{aligned}
\Pi_{(ql)}^{\alpha'\alpha\;a'a}(p_0,\vec{p}) &= \int\frac{d^3\vec{k}}{(2\pi)^3}\int\frac{dk_0}{2\pi}\sum_{Q}^{N_F}\Pi_{(ql)\,Q}^{\alpha'\alpha\;\;a'a}(p_0,\vec{p},k_0,\vec{k}),\\
&= \sum_{Q}^{N_F}\mathbf{t}^{a'\dagger}_{i'j'}\mathbf{t}^{a}_{ji}\left[\Pi^{\alpha'\alpha}_{(ql)\,Q\;j'j\,ii'}(p_0,\vec{p})\right],\\
&\equiv \sum_{Q}^{N_F}\mathbf{t}^{a'}_{i'j'}\mathbf{t}^{a}_{ji}\left[\Pi^{\alpha'\alpha}_{(ql)\,Q\;j'j\,ii'}(p_0,\vec{p})\right],
\end{aligned}\tag{264}$$

where $\Pi_{(ql)\,Q}^{\alpha'\alpha\;\;a'a}(p_0,\vec{p},k_0,\vec{k})$ is the colored kernel of the quark loop self-energy that is defined by Eqns. (260) and (261). It is shown in Eq. (264) that the quark-loop is given in terms of the soft external gluon momentum p, the Lorentz polarization indexes $\alpha'\,\alpha$ and the adjoint color indexes $a'\,a$ as well. Furthermore, the quark-loop part of the gluon polarization tensor, which carries external adjoint color indexes $a'\,a$, is decomposed to the components those are identified by the fundamental color indexes $i'\,i$ and $j'\,j$. Those fundamental color indexes correspond the upper and lower segments of the internal quark loop. As mention below Eq. (263), the adjoint color indexes $a'\,a$ for the two soft external gluon legs are coupled to the internal quark fundamental color indexes for the two hard internal quark segments (i.e. the upper and lower arcs) of the internal quark-loop through the elements of fundamental matrices $\mathbf{t}^{a'}_{i'j'}$ and $\mathbf{t}^{a}_{ji}$. In the imaginary-time formalism, the quark-loop that is identified by the internal quark-loop's fundamental color indexes $i'\,i$ and $j'\,j$ can be written in terms of the mixed-time representation as follows,

$$\begin{aligned}
\left[\Pi^{\alpha'\alpha}_{(ql)\,Q\;j'j\,ii'}(p_0,\vec{p},k_0,\vec{k})\right] &= \int_0^\beta d\tau\int_0^\beta d\tau' e^{\left[k_0-\mu_Q-i\frac{1}{\beta}\theta_j\right]\tau}e^{\left[(k_0-p_0)-\mu_Q-i\frac{1}{\beta}\theta_i\right]\tau'}\\
&\quad\times\left[\Pi^{\alpha'\alpha}_{(ql)\,Q\;j'j\,ii'}(\tau,\vec{k};\tau',\vec{k}-\vec{p})\right].
\end{aligned}\tag{265}$$

The quark-loop kernel becomes a function of the mixed-time variables τ and τ'. It is reduced to

$$\left[\Pi^{\alpha'\alpha}_{(ql)\,Q\;j'j\,ii'}(\tau,\vec{k};\tau',\vec{k}-\vec{p})\right] = g^2\,\mathrm{tr}\left[\gamma^{\alpha'}\,i\,\mathcal{S}_{Q\,j'j}(\tau,\vec{k})\,\gamma^{\alpha}\,i\,\mathcal{S}_{Q\,ii'}(\tau',\vec{k}-\vec{p})\right].\tag{266}$$

The integration of Eq. (265) over the momentum time-component k_0 gives

$$\begin{aligned}\left[\Pi^{\alpha'\alpha}_{(ql)\,Q\;j'j\,ii'}(p_0,\vec{p},\vec{k})\right] &= \int\frac{dk_0}{2\pi}\left[\Pi^{\alpha'\alpha}_{(ql)\,Q\;j'j\,ii'}(p_0,\vec{p},k_0,\vec{k})\right],\\ &= -\int_0^\beta d\tau e^{-\left[p_0+i\frac{1}{\beta}(\theta_i-\theta_j)\right](\beta-\tau)}\\ &\quad\times\left[\Pi^{\alpha'\alpha}_{(ql)\,Q\;j'j\,ii'}(\tau,\vec{k};\beta-\tau,\vec{k}-\vec{p})\right],\end{aligned}\tag{267}$$

where following identity

$$\begin{aligned}\int\frac{dk_0}{2\pi}e^{\left[k_0-\mu_Q-i\frac{1}{\beta}\theta_j\right]\tau}e^{\left[(k_0-p_0)-\mu_Q-i\frac{1}{\beta}\theta_i\right]\tau'} &= \int\frac{dk_0}{2\pi}e^{\left[k_0-\mu_Q-i\frac{1}{\beta}\theta_j\right](\tau+\tau')}e^{-\left[p_0+i\frac{1}{\beta}(\theta_i-\theta_j)\right]\tau'},\\ &= \frac{1}{\beta}\sum_n e^{i\omega_n(\tau+\tau')}e^{-\left[p_0+i\frac{1}{\beta}(\theta_i-\theta_j)\right]\tau'},\\ &= -\delta\left(\tau+\tau'-\beta\right)e^{-\left[p_0+i\frac{1}{\beta}(\theta_i-\theta_j)\right]\tau'},\end{aligned}\tag{268}$$

is considered. Furthermore, the following useful identity

$$\exp\left(\left[p_0+i\frac{1}{\beta}(\theta_i-\theta_j)\right]\beta\right)=1,\tag{269}$$

is considered because of the Matsubara definition for the gluon time-like energy, namely,

$$\begin{aligned}p_0+i\frac{1}{\beta}(\theta_i-\theta_j) &= i\,\frac{2m\pi}{\beta},\\ &\equiv p_0+i\frac{1}{\beta}\phi^a,\quad\left(\text{given that } a=\underbrace{(ij)}\right).\end{aligned}\tag{270}$$

The standard Foldy-Wouthuysen energy decomposition simplifies the calculation of Eq. (267). Moreover, Eq. (266) is decomposed into the positive and negative energy components as follows

$$\left[\Pi^{\alpha'\alpha}_{(ql)\,Q\;j'j\,ii'}(\tau,\vec{k};\beta-\tau,\vec{k}-\vec{p})\right] = \sum_{r=\pm}\sum_{s=\pm}\left[\Pi^{(rs)\,\alpha'\alpha}_{(ql)\,Q\quad ji}(\tau,\vec{k},\vec{p})\right]\,\delta_{j'j}\,\delta_{i'i}.\tag{271}$$

Using the preceding Foldy-Wouthuysen decomposition, Eq. (267) is decomposed to the positive and negative energy components as follows

$$\begin{aligned}\left[\Pi^{\alpha'\alpha}_{(ql)\,Q\;j'j\,ii'}(p_0,\vec{p},\vec{k})\right] &= -\int_0^\beta d\tau e^{-\left[p_0+i\frac{1}{\beta}(\theta_i-\theta_j)\right](\beta-\tau)}\\ &\quad\times\sum_r^{\pm}\sum_s^{\pm}\left[\Pi^{(rs)\,\alpha'\alpha}_{(ql)\,Q\quad ji}(\tau,\vec{k},\vec{p})\right]\,\delta_{j'j}\,\delta_{i'i},\\ &= \sum_r^{\pm}\sum_s^{\pm}\left[\Pi^{(rs)\,\alpha'\alpha}_{(ql)\,Q\quad ji}(p_0,\vec{p},\vec{k})\right]\,\delta_{jj'}\,\delta_{ii'}.\end{aligned}\tag{272}$$

The positive-positive component, namely, $\Pi^{(++)\,\alpha'\alpha}_{(ql)\,Q\quad ji}(\tau,\vec{k},\vec{p})$ is reduced to

$$\begin{aligned}\left[\Pi^{(++)\,\alpha'\alpha}_{(ql)\,Q}(\tau,\vec{k},\vec{p})\right] \;&=\; g^2\,\Lambda^{(++)^{\alpha'\alpha}}_{Q}\left(\vec{k},\vec{p}\right)\left[1-n_F\left(\epsilon_Q(\vec{k})-\mu_Q-i\frac{1}{\beta}\theta_j\right)\right]\\ &\times\left[1-n_F\left(\epsilon_Q(\vec{k}-\vec{p})-\mu_Q-i\frac{1}{\beta}\theta_i\right)\right]\\ &\times\exp\left(-\tau\left[\epsilon_Q(\vec{k})-\mu_Q-i\frac{1}{\beta}\theta_j\right]\right)\\ &\times\exp\left(-(\beta-\tau)\left[\epsilon_Q(\vec{k}-\vec{p})-\mu_Q-i\frac{1}{\beta}\theta_i\right]\right),\end{aligned}\tag{273}$$

where the double Foldy-Wouthuysen energy projector is given by

$$\Lambda^{(rs)^{\alpha'\alpha}}_{Q}(\vec{k},\vec{p}) \;=\; \mathrm{tr}\left[\gamma^{\alpha'}\,\Lambda^{(r)}_{Q}(\vec{k})\,\gamma_0\gamma^{\alpha}\,\Lambda^{(s)}_{Q}(\vec{k}-\vec{p})\,\gamma_0\right],\;(\text{where } r=\pm,\,s=\pm).\tag{274}$$

The double Foldy-Wouthuysen energy projectors are identified by the double Lorentz polarization indexes $\alpha'\,\alpha$ and the double positive and negative energy channels. The Foldy-Wouthuysen energy component, namely, $(++)$ of the quark-loop part of the gluon polarization tensor in the mixed-time representation reads,

$$\begin{aligned}\left[\Pi^{(++)\,\alpha'\alpha}_{(ql)\,Q\quad ji}(\tau,\vec{k},\vec{p})\right] \;&=\; g^2\,\Lambda^{(++)\,\alpha'\alpha}_{Q}\left(\vec{k},\vec{p}\right)\left[1-n_F\left(\epsilon_Q(\vec{k})-\mu_Q-i\frac{1}{\beta}\theta_j\right)\right]\\ &\times\left[1-n_F\left(\epsilon_Q(\vec{k}-\vec{p})-\mu_Q-i\frac{1}{\beta}\theta_i\right)\right]\\ &\times\exp\left(-\tau\left[\epsilon_Q(\vec{k})-\mu_Q-i\frac{1}{\beta}\theta_j\right]\right)\\ &\times\exp\left(-(\beta-\tau)\left[\epsilon_Q(\vec{k}-\vec{p})-\mu_Q-i\frac{1}{\beta}\theta_i\right]\right).\end{aligned}\tag{275}$$

The results for Foldy-Wouthuysen energy components, namely, $(+-)$, $(-+)$ and $(--)$ are obtained in a similar manner. The approximation of the double Foldy-Wouthuysen energy projectors in the limit $(|\vec{k}|\gg|\vec{p}|)$ simplifies the calculations drastically. They are identified by the Lorentz polarization indexes $\alpha'\,\alpha$. The time-time double Foldy-Wouthuysen energy projectors are approximated to

$$\Lambda^{(rs)\,00}_{Q}(\vec{k},\vec{p}) \;\equiv\; \Lambda^{(rs)}_{Q\,00}(\vec{k},\vec{p})\approx\{(1+rs)\},\tag{276}$$

where $\{r=\pm,s=\pm\}$ are the positive and negative energy components. The time-space components are given by

$$\Lambda^{(rs)\,0m}_{Q}(\vec{k},\vec{p}) \;\equiv\; \Lambda^{(rs)}_{Q\,0m}(\vec{k},\vec{p})\approx-\,(s+r)\;\hat{k}_m.\tag{277}$$

Furthermore, the space-space components are approximated to

$$\Lambda_{Q}^{(rs)\,nm}(\vec{k},\vec{p}) \;\equiv\; \Lambda_{Q\,nm}^{(rs)}(\vec{k},\vec{p}) \approx \Big[\delta_{ij}\,(1-r\,s) + 2r\,s\,\hat{k}_n\,\hat{k}_m\Big]\,. \tag{278}$$

Therefore, the Lorentz polarization components, namely, $\alpha'\,\alpha$ of the double Foldy-Wouthuysen energy projectors are reduced to

$$\begin{aligned}
\Big\{\Lambda_{Q}^{(rs)\,00}(\vec{k},\vec{p})\Big\} &\approx \{2,0,0,2\}\,,\\
\Big\{\Lambda_{Q}^{(rs)\,0m}(\vec{k},\vec{p})\Big\} &\approx \Big\{-2\hat{k}_m,0,0,2\hat{k}_m\Big\}\,,\\
\Big\{\Lambda_{Q}^{(rs)\,nm}(\vec{k},\vec{p})\Big\} &\approx \Big\{2\hat{k}_n\,\hat{k}_m, 2\left(\delta_{nm}-\hat{k}_n\,\hat{k}_m\right), 2\left(\delta_{nm}-\hat{k}_n\,\hat{k}_m\right), 2\hat{k}_n\,\hat{k}_m\Big\}\,,
\end{aligned} \tag{279}$$

for the positive and negative $\{(++),(+-),(-+),(--)\}$ energy components, respectively. Evaluating the integral in Eq. (272) over the time variable τ in order to find the inverse transformation of the mixed-time representation, the positive-positive energy component of the quark-loop part of the gluon polarization tensor is reduced to

$$\Pi_{(ql)\,Q}^{(++)\,\alpha'\alpha}{}_{ji}(p_0,\vec{p}) \;=\; \int \frac{d^3\vec{k}}{(2\pi)^3}\left[\Pi_{(ql)\,Q}^{(++)\,\alpha'\alpha}{}_{ji}(p_0,\vec{p},\vec{k})\right], \tag{280}$$

where

$$\begin{aligned}
\Pi_{(ql)\,Q}^{(++)\,\alpha'\alpha}{}_{ji}(p_0,\vec{p},\vec{k}) \;&=\; -g^2\,\Lambda_{Q}^{(rs)\alpha'\alpha}(\vec{k},\vec{p})\\
&\times\; \left[\frac{n_F\left(\epsilon_Q(\vec{k})-\mu_Q-i\frac{\theta_j}{\beta}\right)-n_F\left(\epsilon_Q(\vec{k}-\vec{p})-\mu_Q-i\frac{\theta_i}{\beta}\right)}{p_0-\left(\epsilon_Q(\vec{k})-\epsilon_Q(\vec{k}-\vec{p})\right)}\right].
\end{aligned} \tag{281}$$

The results for the components $(+-)$, $(-+)$ and $(--)$ are obtained in a similar manner. Using the symmetry argument under the sum of the repeated index, we have the following result,

$$\mathbf{t}_{ij}^{a'}\,\mathbf{t}_{ji}^{a}\left[n_F\left(\epsilon_Q(\vec{k})-\mu_Q-i\frac{\theta_j}{\beta}\right)-n_F\left(\epsilon_Q(\vec{k})-\mu_Q-i\frac{\theta_i}{\beta}\right)\right] \;=\; 0. \tag{282}$$

Since in the HTL approximation, we have $\vec{p} << \vec{k}$ (i.e. $p/k \sim g$), then by evaluating the integration over $\vec{k}$, Eq. (281) is approximated to

$$\begin{aligned}
\Pi_{(ql)\,Q}^{(++)\,nm}{}_{ji}(p_0,\vec{p}) \;&=\; \int\frac{d|\vec{k}|}{2\pi^2}|\vec{k}|^2\int\frac{d\Omega_k}{4\pi}\left[\Pi_{(ql)\,Q}^{(++)\,nm}{}_{ji}(p_0,\vec{p},\vec{k})\right],\\
&=\; -2g^2\int\frac{d\Omega_k}{4\pi}\,\hat{k}_n\hat{k}_m\,\frac{\hat{k}\cdot\vec{p}}{p_0-\hat{k}\cdot\vec{p}}\\
&\qquad\times\left(\int\frac{d|\vec{k}|}{2\pi^2}|\vec{k}|^2\,\frac{d}{d|\vec{k}|}\left[n_F\left(\epsilon_Q(\vec{k})-\mu_Q-i\frac{\theta_j}{\beta}\right)\right]\right),\\
&\equiv\; \frac{1}{2}\left[(\cdots\theta_i\cdots)+(\cdots\theta_j\cdots)\right],
\end{aligned} \tag{283}$$

for space-space, namely, $n\,m$ Lorentz component. The last line indicates the symmetrization over the color indexes i and j. The symmetry over the polar integration leads to

$$\int \frac{d\Omega_k}{4\pi}\left(\delta_{nm}-\hat{k}_n\hat{k}_m\right)\frac{\hat{k}\cdot\vec{p}}{p_0+\hat{k}\cdot\vec{p}} \;=\; -\int \frac{d\Omega_k}{2\pi}\left(\delta_{nm}-\hat{k}_n\hat{k}_m\right)\frac{\hat{k}\cdot\vec{p}}{p_0-\hat{k}\cdot\vec{p}}. \tag{284}$$

Moreover, a similar result is obtained for $(--)$ component but replacing $n_F\left(\epsilon_Q(\vec{k})-\mu_Q-i\frac{\theta_j}{\beta}\right)$ with $n_F\left(\epsilon_Q(\vec{k})+\mu_Q+i\frac{\theta_j}{\beta}\right)$. The same approximation is considered in calculating the $(+-)$ and $(-+)$ components. The result for the sum over $(+-)$ and $(-+)$ components is reduced to

$$\begin{aligned}
\sum_{s=-r}^{r=\pm}\Pi^{(rs)\,nm}_{(ql)\,Q\quad ji}(p_0,\vec{p}) \;&=\; \left[\Pi^{(+-)\,nm}_{(ql)\,Q\quad ji}(p_0,\vec{p})+\Pi^{(-+)\,nm}_{(ql)\,Q\quad ji}(p_0,\vec{p})\right],\\
&=\; \int\frac{d|\vec{k}|}{2\pi^2}|\vec{k}|^2\int\frac{d\Omega_k}{4\pi}\left[\Pi^{(+-)\,nm}_{(ql)\,Q\quad ji}(p_0,\vec{p},\vec{k})+\Pi^{(-+)\,nm}_{(ql)\,Q\quad ji}(p_0,\vec{p},\vec{k})\right],\\
&\approx\; 2g^2\int\frac{d\Omega_k}{4\pi}\left(\delta_{nm}-\hat{k}_n\hat{k}_m\right)\left(\int\frac{d|\vec{k}|}{2\pi^2}|\vec{k}|\right.\\
&\times\;\left.\left[1+n_F\left(\epsilon_Q(\vec{k})-\mu_Q-i\frac{\theta_j}{\beta}\right)+n_F\left(\epsilon_Q(\vec{k})+\mu_Q+i\frac{\theta_j}{\beta}\right)\right]\right).
\end{aligned}\tag{285}$$

By dropping the first term inside the square bracket which is a non-thermal one and retaining only the thermal terms, Eq. (285) becomes,

$$\begin{aligned}
\sum_{s=-r}^{r=\pm}\Pi^{(rs)\,nm}_{(ql)\,Q\quad ji}(p_0,\vec{p}) \;&\approx\; -g^2\int\frac{d\Omega_k}{4\pi}\left(\delta_{nm}-\hat{k}_n\,\hat{k}_m\right)\left(\int\frac{d|\vec{k}|}{2\pi^2}|\vec{k}|^2\,\frac{d}{d|\vec{k}|}\right.\\
&\times\;\left.\left[n_F\left(\epsilon_Q(\vec{k})-\mu_Q-i\frac{\theta_j}{\beta}\right)+n_F\left(\epsilon_Q(\vec{k})+\mu_Q+i\frac{\theta_j}{\beta}\right)\right]\right).
\end{aligned}\tag{286}$$

Furthermore, by imposing the tensor identity

$$\int d\Omega_k\left(\delta_{nm}-3\hat{k}_n\hat{k}_m\right)=0, \tag{287}$$

and the relation

$$\frac{\hat{k}\cdot\vec{p}}{p_0-\hat{k}\cdot\vec{p}} \;=\; 1-\frac{p_0}{p_0-\hat{k}\cdot\vec{p}}, \tag{288}$$

the quark-loop part, namely, $\Pi_{ql}(p_0,\vec{p})$ of the gluon polarization tensor is reduced to

$$\begin{aligned}
\left[\Pi^{nm}_{(ql)\;ji}(p_0,\vec{p})\right] \;&=\; \sum_{Q=1}^{n_F}\left[\Pi^{nm}_{(ql)\,Q\;ji}(p_0,\vec{p})\right],\\
&\approx\; -2g^2\sum_{Q=1}^{n_F}\int\frac{d|\vec{k}|}{2\pi^2}|\vec{k}|^2\frac{d}{d|\vec{k}|}\left[n_F\left(\epsilon_Q(\vec{k})-\mu_Q-i\frac{\theta_j}{\beta}\right)\right.\\
&\quad\left.+n_F\left(\epsilon_Q(\vec{k})+\mu_Q+i\frac{\theta_j}{\beta}\right)\right]\left(p_0\int\frac{d\Omega_k}{4\pi}\frac{\hat{k}_n\hat{k}_m}{p_0-\hat{k}\cdot\vec{p}}\right).
\end{aligned}\tag{289}$$

Furthermore, Eq. (289) is re-expressed as follows

$$\left[\Pi^{nm}_{(ql)\,ji}(p_0,\vec{p})\right] \;\approx\; \left(\mathbf{m}^2_{D\,(Q)}\right)_{ij}\left(p_0\int\frac{d\Omega_k}{4\pi}\frac{\hat{k}_n\hat{k}_m}{p_0-\hat{k}\cdot\vec{p}}\right). \tag{290}$$

The quark-loop part of the Debye mass is symmetrized as follows

$$\left(\mathbf{m}^2_{D\,(Q)}\right)_{ij} \;\equiv\; \frac{1}{2}\left[\left(\mathbf{m}^2_{D\,(Q)}\right)_i+\left(\mathbf{m}^2_{D\,(Q)}\right)_j\right]. \tag{291}$$

It should be noted here that the fundamental color indexes, namely, i and j run over all color charges in the final calculation. The summation over the fundamental color index i is identical to that over j. Hence, the quark-loop part of the Debye mass, with the fundamental color index i, is reduced to

$$\left(\mathbf{m}^2_{D\,(Q)}\right)_i \;=\; \sum_{Q=1}^{n_F}\left(\mathbf{m}^2_{D\,(Q)Q}\right)_i, \tag{292}$$

where

$$\begin{aligned}\left(\mathbf{m}^2_{D\,(Q)Q}\right)_i \;&=\; 4g^2\int\frac{d|\vec{k}|}{2\pi^2}|\vec{k}|\left[n_F\left(\epsilon_Q(\vec{k})-\mu_Q-i\frac{\theta_i}{\beta}\right)+n_F\left(\epsilon_Q(\vec{k})+\mu_Q+i\frac{\theta_i}{\beta}\right)\right],\\ &=\; \frac{2g^2}{\pi^2}\left[\frac{\pi^2}{6\,\beta^2}+\frac{1}{2}\left(\mu_Q+i\,\frac{1}{\beta}\theta_i\right)^2\right].\end{aligned} \tag{293}$$

When the real fundamental color potential is considered, namely, $i\,\frac{1}{\beta}\theta_i\to\mu_{Ci}$, Eq. (292) is reduced to

$$\left(\mathbf{m}^2_{D\,(Q)}\right)_i \;\to\; \frac{2g^2}{\pi^2}\sum_{Q=1}^{N_F}\left[\frac{\pi^2}{6\,\beta^2}+\frac{1}{2}\left(\mu_Q+\mu_{Ci}\right)^2\right]. \tag{294}$$

The quark-loop part of the gluon polarization tensor with the Lorentz polarization indexes, namely, $\alpha\,\alpha'$ and the internal fundamental color indexes, namely, i and j is reduced to

$$\begin{aligned}\left[\Pi^{\alpha'\alpha}_{(ql)\,ji}(p_0,\vec{p})\right] \;&=\; \sum_{Q=1}^{N_F}\left[\Pi^{\alpha'\alpha}_{(ql)\,Q\,ji}(p_0,\vec{p})\right],\\ &=\; \left(\mathbf{m}^2_{D\,(Q)}\right)_{ji}\left[-\delta_{0\alpha'}\delta_{0\alpha}+p_0\int\frac{d\Omega_k}{4\pi}\frac{\hat{k}_{\alpha'}\,\hat{k}_\alpha}{p_0-\hat{k}\cdot\vec{p}}\right].\end{aligned} \tag{295}$$

Moreover, the quark-loop part with the Lorentz polarization indexes $\alpha\,\alpha'$ and the external adjoint color indexes, namely, a and a' for the two external gluon legs is transformed as follows,

$$\begin{aligned}\left[\Pi^{\alpha'\alpha\,a'a}_{(ql)}(p_0,\vec{p})\right] \;&=\; \mathbf{t}^{a'}_{i'j'}\,\mathbf{t}^{a}_{ji}\,\delta_{j'j}\delta_{i'i}\,\left[\Pi^{\alpha'\alpha}_{(ql)\,ji}(p_0,\vec{p})\right],\\ &=\; \left(\mathbf{m}^2_{D\,(Q)}\right)^{a'\,a}\left[-\delta_{0\alpha'}\,\delta_{0\alpha}+p_0\int\frac{d\Omega_k}{4\pi}\frac{\hat{k}_{\alpha'}\,\hat{k}_\alpha}{p_0-\hat{k}\cdot\vec{p}}\right].\end{aligned} \tag{296}$$

Therefore, the quark-loop part of the gluon Debye mass with the external gluon legs, which are labeled by the adjoint color indexes $a\,a'$, is related to the Debye mass with internal fundamental color indexes $i\,j$ in the following way

$$\begin{aligned}\left(\mathbf{m}^2_{D\,(Q)}\right)^{a'a} &= \mathbf{t}^{a'}_{ij}\mathbf{t}^{a}_{ji}\,\left(\mathbf{m}^2_{D\,(Q)}\right)_{ij}\,, \\ &= \mathbf{t}^{a'}_{ij}\mathbf{t}^{a}_{ji}\,\left(\mathbf{m}^2_{D\,(Q)}\right)_{i}\,,\ (\text{or } i\to j).\end{aligned} \tag{297}$$

G. The Gluon Polarization tensor and the Debye mass

The total gluon polarization tensor, namely, $\Pi^{\alpha'\alpha\,a'a}\,(p_0,\vec{p})$ is found by adding the contribution of the gluon's part which consists the gluon loop, ghost loop and tadpole and the contribution of the quark loop all together. The contribution of the gluon's part is given by Eq. (258) while the contribution from the quark loop is given by Eq. (296). Hence, the total gluon self-energy from the all Feynman diagrams which are displayed in Figs. (2 a), (2 b), (2 c) and (2 d) is given by

$$\Pi^{\alpha'\alpha\,a'a}\,(p_0,\vec{p}) \;=\; \left[\Pi^{\alpha'\alpha\;a'a}_{(gp)}\,(p_0,\vec{p}) + \Pi^{\alpha'\alpha\,a'a}_{(ql)}\,(p_0,\vec{p})\right]. \tag{298}$$

Hence, the (total) gluon polarization tensor is reduced to

$$\Pi_{\alpha'\alpha}{}^{a'a}\,(p_0,\vec{p}) \;=\; \left(\mathbf{m}^2_D\right)^{a'a}\left[-\delta_{0\alpha'}\delta_{0\alpha} + p_0\int\frac{d\Omega_k}{4\pi}\frac{\hat{k}_{\alpha'}\hat{k}_{\alpha}}{p_0-\hat{k}\cdot\vec{p}}\right]. \tag{299}$$

The gluon Debye mass with the external adjoint color indexes a and a' for the two external gluon legs is given by

$$\left(\mathbf{m}^2_D\right)^{a'a} \;=\; \left[\left(\mathbf{m}^2_{D\,(Q)}\right)^{a'a} + \left(\mathbf{m}^2_{D\,(G)}\right)^{a'a}\right], \tag{300}$$

where the first term on the right hand side comes from the quark-loop while the second one is contribution of the gluon's part of the gluon polarization tensor. The gluon Debye mass with the external adjoint color indexes a and a' is related to the internal loop Debye mass elements with the internal fundamental color indexes $i\,j$ and the internal adjoint color indexes $b\,c$ in the following way,

$$\left(\mathbf{m}^2_D\right)^{a'\,a} \;=\; \left[\mathbf{t}^{a'}{}_{ij}\,\mathbf{t}^{a}{}_{ji}\left(\mathbf{m}^2_{D\,(Q)}\right)_{ij} + \mathbf{T}^{a'}{}_{cb}\,\mathbf{T}^{a}{}_{bc}\left(\mathbf{m}^2_{D\,(G)}\right)_{bc}\right]. \tag{301}$$

It should be noted that $\left(\mathbf{m}^2_{D\,(Q)}\right)_{ij} \equiv \left(\mathbf{m}^2_{D\,(Q)}\right)_{i}$ and $\left(\mathbf{m}^2_{D\,(G)}\right)_{bc} \equiv \left(\mathbf{m}^2_{D\,(G)}\right)_{b}$. Furthermore, the adjoint color index b can be replaced by the double fundamental-like color indexes by

the notation structure $b = \underbrace{(n\,m)}$. The summation over the repeated indexes and considering the symmetry of the fundamental and adjoint indexes $i\,j$ and $b\,c$, respectively, contract the double adjoint color indexes and lead to following result

$$\left(\mathbf{m}_D^2\right)^{a'a} \;=\; \delta^{a'a}\left(\mathbf{m}_D^2\right)^{a}. \tag{302}$$

Hence, the gluon Debye mass is identified by only one external adjoint color index a in the following way,

$$\left(\mathbf{m}_D^2\right)^{a} \;=\; \left[N_c\left(\mathbf{m}_{D\,(G)}^2\right)^{a} + \frac{1}{2}\left(\mathbf{m}_{D\,(Q)}^2\right)^{a}\right], \tag{303}$$

where

$$\left(\mathbf{m}_{D\,(G)}^2\right)^{a} \;=\; \frac{\sqrt{2}}{N_c}\sum_{ij}^{N_c}\mathbf{t}^{a}{}_{in}\left(\mathbf{m}_{D\,(G)}^2\right)\underbrace{(nj)}, \tag{304}$$

and

$$\left(\mathbf{m}_{D\,(Q)}^2\right)^{a} \;=\; \sqrt{2}\sum_{ij}^{N_c}\mathbf{t}^{a}{}_{ij}\left(\mathbf{m}_{D\,(Q)}^2\right)_{i}. \tag{305}$$

Moreover, the double adjoint color indexes for the gluon polarization tensor can be contracted and the soft gluon polarization tensor is reduced to

$$\Pi_{\alpha'\alpha}{}^{a'a}\,(p_0,\vec{p}) \;=\; \delta^{a'\,a}\,\Pi_{\alpha'\alpha}{}^{a}, \tag{306}$$

where

$$\Pi_{\alpha'\alpha}{}^{a}\,(p_0,\vec{p}) \;=\; \left(\mathbf{m}_D^2\right)^{a}\left[-\delta_{0\alpha'}\delta_{0\alpha} + p_0\int\frac{d\Omega_k}{4\pi}\frac{\hat{k}_{\alpha'}\hat{k}_{\alpha}}{p_0-\hat{k}\cdot\vec{p}}\right]. \tag{307}$$

The final result of the soft gluon polarization tensor is gauge fixing independent. The gluon polarization tensor $\Pi_{\alpha'\alpha}{}^{a'a}\,(p_0,\vec{p})$ is transverse and is satisfying the relation $p^{\alpha'}\,\Pi_{\alpha'\alpha}{}^{a'a}(p_0,\vec{p}) = 0$. The soft gluon polarization tensor can be written with respect to the Lorentz polarization indexes $\alpha'\,\alpha = \{0\,0, 0\,i, i\,j\}$, respectively, for the time-time, time-space and space-space Lorentz polarization components. The time-time component of the gluon polarization reads

$$\begin{aligned}\Pi_{00}{}^{a}\,(p_0,\vec{p}) \;&=\; \left(\mathbf{m}_D^2\right)^{a}\left[-1 + p_0\int\frac{d\Omega_k}{4\pi}\frac{1}{p_0-\hat{k}\cdot\vec{p}}\right],\\ &=\; -\left(\mathbf{m}_D^2\right)^{a}\left[1-\frac{1}{2}\,p_0\int_{-1}^{1}dx\frac{1}{p_0-|\vec{p}|x}\right],\end{aligned} \tag{308}$$

while time-space component reads,

$$\begin{aligned}\Pi_{0i}{}^{a}\left(p_0,\vec{p}\right) &= \left(\mathbf{m}_D^2\right)^a\left[-p_0\hat{p}_i\int\frac{d\Omega_k}{4\pi}\frac{\left(\hat{k}\cdot\hat{p}\right)}{p_0-\hat{k}\cdot\vec{p}}\right],\\ &= \left(\mathbf{m}_D^2\right)^a\left[-p_0\hat{p}_i\frac{1}{2}\int_{-1}^{1}dx\frac{x}{p_0-|\vec{p}|x}\right].\end{aligned} \tag{309}$$

In order to compute the space-space Lorentz polarization components with space indexes, namely, $i\,j$, the following transformation

$$\vec{k}=\sum_i\left(\vec{k}\cdot\hat{p}_i\right)\hat{p}_i, \tag{310}$$

is introduced. In the spherical coordinate, it reads

$$\vec{k} = \left(\vec{k}\cdot\hat{p}_r\right)\hat{p}_r+\left(\vec{k}\cdot\hat{p}_\theta\right)\hat{p}_\theta+\left(\vec{k}\cdot\hat{p}_\phi\right)\hat{p}_\phi, \tag{311}$$

$$\equiv \left(\vec{k}\cdot\hat{p}\right)\hat{p}+\left(\vec{k}\cdot\hat{p}_\perp\right)\hat{p}_\perp. \tag{312}$$

Subsequently, the transverse projector becomes

$$\hat{p}_{\perp i}\hat{p}_{\perp j}\to\left(\delta_{ij}-\hat{p}_i\hat{p}_j\right). \tag{313}$$

Therefore, the space-space component with space polarization indexes, namely, $i\,j$ is reduced to

$$\begin{aligned}\Pi_{ij}{}^{a}\left(p_0,\vec{p}\right) &= \left(\hat{p}_i\hat{p}_j\right)\left(\mathbf{m}_D^2\right)^a\left[\frac{p_0}{2}\int_{-1}^{1}dx\frac{x^2}{p_0-|\vec{p}|x}\right]\\ &\quad+\left(\delta_{ij}-\hat{p}_i\hat{p}_j\right)\left(\mathbf{m}_D^2\right)^a\left[\frac{1}{2}\frac{p_0}{2}\int_{-1}^{1}dx\frac{1-x^2}{p_0-|\vec{p}|x}\right].\end{aligned} \tag{314}$$

The gluon polarization tensor is decomposed to longitudinal (electric) and transverse (magnetic) components as follows

$$\Pi_{ij}{}^{a}\left(p_0,\vec{p}\right) = \left(\delta_{ij}-\hat{p}_i\hat{p}_j\right)\Pi_T{}^{a}(p_0,\vec{p})-\left(\hat{p}_i\hat{p}_j\right)\frac{p_0^2}{\vec{p}^2}\Pi_L{}^{a}(p_0,\vec{p}), \tag{315}$$

where

$$\Pi_L{}^{a}(p_0,\vec{p}) = -\left(\mathbf{m}_D^2\right)^a\frac{\vec{p}^2}{p_0^2}\left[\frac{p_0/|\vec{p}|}{2}\int_{-1}^{1}dx\frac{x^2}{(p_0/|\vec{p}|)\,-\,x}\right], \tag{316}$$

and

$$\Pi_T{}^{a}(p_0,\vec{p}) = \left(\mathbf{m}_D^2\right)^a\left[\frac{1}{2}\frac{p_0/|\vec{p}|}{2}\int_{-1}^{1}dx\frac{1-x^2}{(p_0/|\vec{p}|)\,-\,x}\right]. \tag{317}$$

H. Real and imaginary parts of the gluon polarization tensor

The real and imaginary parts of the gluon polarization tensor are essential to determine the Debye screening and Landau damping phenomena, respectively. The Debye screening means that the range of the gauge interaction is reduced by the factor $e^{-\sqrt{\left(\mathbf{m}_D^2\right)^a}\,r}$ where $\left(\mathbf{m}_D^2\right)^a$ is square Debye mass. This corresponds that the gluon is acquiring an effective mass in order to soften the infrared behavior of the gluon static electric propagator component $\frac{-1}{p^2} \rightarrow \frac{-1}{p^2+\left(\mathbf{m}_D^2\right)^a}$. In this case, the the Debye mass acts as an infrared cutoff. It is known that the static magnetic field is not associated with an infrared cutoff and subsequently the transverse component is not screened.

The Landau damping stems from the imaginary part of the gluon polarization tensor. It is the mechanical energy that is transfered from the chromo-field to the plasma constituent particles. Furthermore, the imaginary part is associated with the decay rate of the gluon where the resulting energy is absorbed by the plasma constituents and subsequently, the chromo-field is damped. The Landau damping in QCD is non-trivial phenomena due to the nonlinear effects besides the Landau damping is operative in both soft gluons and quarks. The gluons with soft momentum and hard thermal loop self-energy are dynamically screened by the Landau damping.

The analytic continuation of the gluon polarization tensor is introduced as follows

$$\frac{1}{x\,-\,x_0\,\pm\,i\,\eta}\;=\;P\left(\frac{1}{x\,-\,x_0}\right)\mp\,i\,\pi\,\delta\left(x\,-\,x_0\right). \tag{318}$$

where the first term on the right hand side is the principal value while the second term is the Dirac delta function. Hence, the longitudinal and transverse components of the soft gluon polarization tensor are written, respectively, as follows

$$\Pi_L{}^a(p_0,\vec{p})\;=\;-\left(\mathbf{m}_D^2\right)^a\frac{\vec{p}^2}{p_0^2}\left(\frac{1}{2}\frac{p_0}{|\vec{p}|}\int_{-1}^{1}dx x^2\left[P\left(\frac{1}{\frac{p_0}{|\vec{p}|}\,-\,x}\right)-i\,\pi\,\delta\left(\frac{p_0}{|\vec{p}|}\,-\,x\right)\right]\right), \tag{319}$$

and

$$\Pi_T{}^a(p_0,\vec{p})\;=\;\left(\mathbf{m}_D^2\right)^a\left(\frac{1}{2}\frac{1}{2}\frac{p_0}{|\vec{p}|}\int_{-1}^{1}dx\left(1-x^2\right)\left[\frac{1}{\frac{p_0}{|\vec{p}|}\,-\,x}-i\,\pi\,\delta\left(\frac{p_0}{|\vec{p}|}\,-\,x\right)\right]\right). \tag{320}$$

Since the variable x is restricted to the range $-1\,\leq\,x\,\leq\,1$, the constraint for the principal value to avoid the singularity is the time-like energy region $p_0^2>\vec{p}^2$ while the constraint to develop the Dirac delta function is the space-like energy region $\vec{p}^2\geq p_0^2$. Therefore, the real

and imaginary parts virtually can not be generated simultaneously but rather they can be dominated either by a real part in the time-like energy domain or by an imaginary part for the space-like energy domain. The real part is suppressed in the time-like energy.

At first, when the energy runs over the time-like energy domain (i.e. physical domain $p_0 > |\vec{p}|$), the longitudinal and transverse gluon polarization tensor components turn to their real parts, respectively, as follows,

$$\begin{aligned} {\Pi_L}^a(p_0,\vec{p}) &= \Re e\,{\Pi_L}^a(p_0,\vec{p}),\ \left(\text{time-like energy } p_0^2 > \vec{p}^2\right), \\ \Re e\,{\Pi_L}^a(p_0,\vec{p}) &= \left(\mathbf{m}_D^2\right)^a \left[1 - Q_0\left(\frac{p_0}{|\vec{p}|}\right)\right], \end{aligned} \tag{321}$$

and

$$\begin{aligned} {\Pi_T}^a(p_0,\vec{p}) &= \Re e\,{\Pi_T}^a(p_0,\vec{p}),\ \left(\text{time-like energy } p_0^2 > \vec{p}^2\right), \\ \Re e\,{\Pi_T}^a(p_0,\vec{p}) &= \frac{1}{2}\left(\mathbf{m}_D^2\right)^a \left[\frac{p_0^2}{\vec{p}^2} + \left(1 - \frac{p_0^2}{\vec{p}^2}\right) Q_0\left(\frac{p_0}{|\vec{p}|}\right)\right]. \end{aligned} \tag{322}$$

On the other hand, when the energy switches to run over the space-like energy domain (i.e. $0 \leq p_0 \leq |\vec{p}|$), the gluon polarization tensor components turn to be dominated by the imaginary parts and subsequently they are reduced solely to their imaginary parts in the following way,

$$\begin{aligned} {\Pi_L}^a\left(p_0,\vec{p}\right) &= i\,\Im m\,{\Pi_L}^a\left(p_0,\vec{p}\right),\ \left(\text{space-like energy } p_0^2 \leq \vec{p}^2\right), \\ \Im m\,{\Pi_L}^a\left(p_0,\vec{p}\right) &= \left(\mathbf{m}_D^2\right)^a \left(\frac{\pi p_0}{2|\vec{p}|}\right)\theta\left(|\vec{p}| - p_0\right), \end{aligned} \tag{323}$$

and

$$\begin{aligned} {\Pi_T}^a\left(p_0,\vec{p}\right) &= i\,\Im m\,{\Pi_T}^a\left(p_0,\vec{p}\right),\ \left(\text{space-like energy } p_0^2 \leq \vec{p}^2\right), \\ \Im m\,{\Pi_T}^a\left(p_0,\vec{p}\right) &= -\frac{1}{2}\left(\mathbf{m}_D^2\right)^a \left(1 - \frac{p_0^2}{\vec{p}^2}\right)\left(\frac{\pi p_0}{2|\vec{p}|}\right)\theta\left(|\vec{p}| - p_0\right), \end{aligned} \tag{324}$$

for the longitudinal and transverse components, respectively.

I. Effective Gluon propagator

The effective gluon propagator with adjoint color indexes $a'\,a$ and Lorentz polarization indexes $\mu\,\nu$ for the gluon's two external legs is represented as follows

$${}^*\mathcal{G}_{\mu\nu}{}^{a'a}(p_0,\vec{p}) = \delta^{a'a}\,{}^*\mathcal{G}_{\mu\nu}{}^a(p_0,\vec{p}). \tag{325}$$

The adjoint color indexes $a'\,a$ are contracted by the Kronecker delta $\delta^{a'\,a}$. The gluon propagator is gauge dependent. The gluon propagator in the Coulomb gauge fixing, where the electric and magnetic components can be separated, reads

$$ {}^*\mathcal{G}_{C\mu\nu}{}^a(p_0,\vec{p}) \;=\; {}^*\mathcal{G}_{C\mu\nu}{}^a(p_0,\vec{p}) - \xi_C\,\frac{p_\mu p_\nu}{\vec{p}^2}\,\frac{1}{\vec{p}^2}. \tag{326} $$

The gluon propagator is decomposed to

$$ \begin{aligned} {}^*\mathcal{G}_{C00}{}^a(p_0,\vec{p}) \;&=\; {}^*\mathcal{G}_L{}^a(p_0,\vec{p}), \\ {}^*\mathcal{G}_{Cij}{}^a(p_0,\vec{p}) \;&=\; (\delta_{ij}-\hat{p}_i\hat{p}_j)\;{}^*\mathcal{G}_T{}^a(p_0,\vec{p}), \end{aligned} \tag{327} $$

in the strict Coulomb gauge where $\xi_C = 0$. The effective gluon propagator ${}^*\mathcal{G}_{C\,\mu\,\nu}{}^a(p_0,\vec{p})$ is determined by finding the inverse of the following quantity,

$$ {}^*\mathcal{G}_C^{-1}{}_{\mu\nu}{}^a(p_0,\vec{p}) \;=\; \mathcal{G}_C^{-1}{}_{\mu\nu}{}^a(p_0,\vec{p}) + \Pi_{\mu\nu}{}^a(p_0,\vec{p}), \tag{328} $$

where $\mathcal{G}_C^{-1}{}_{\mu\nu}{}^a(p_0,\vec{p})$ is the gluon propagator in the Coulomb gauge. The longitudinal part becomes,

$$ \begin{aligned} {}^*\mathcal{G}_L{}^a(p_0,\vec{p}) \;&=\; \frac{-1}{\vec{p}^2+\Pi_L{}^a(p_0,\vec{p})}, \\ &=\; -\frac{1}{\vec{p}^2} \;+\; \left[\frac{\Pi_L{}^a(p_0,\vec{p})}{\vec{p}^2}\right]\frac{1}{\vec{p}^2+\Pi_L{}^a(p_0,\vec{p})}, \end{aligned} \tag{329} $$

while the transverse component is reduced to

$$ {}^*\mathcal{G}_T{}^a(p_0,\vec{p}) \;=\; \frac{-1}{p_0^2-\vec{p}^2-\Pi_T{}^a(p_0,\vec{p})}. \tag{330} $$

In the time-like energy domain (i.e. $p_0^2 > \vec{p}^2$), it is possible to write the longitudinal and transverse components of the gluon propagator near the mass shell residues, respectively, as follows

$$ \begin{aligned} \mathcal{G}_L{}^a(p_0,\vec{p}) \;&=\; \frac{-1}{(\vec{p}^2+\Pi_L{}^a(p_0,\vec{p}))}, \\ &\approx\; -\frac{z_L{}^a(p_0,|\vec{p}|)}{p_0^2-\left(\overline{\omega}_L{}^a\right)^2}, \\ &\qquad \text{(mass-shell residues: } p_0^2 \approx \left(\overline{\omega}_L{}^a\right)^2, \end{aligned} \tag{331} $$

where the longitudinal residue $\overline{\omega}_L{}^a$ is the solution of

$$ \overline{\omega}_L{}^a : \quad \vec{p}^2+\Pi_L{}^a(\overline{\omega}_L{}^a,\vec{p}) \;=\; 0, \tag{332} $$

and

$$
\begin{aligned}
{}^{*}\mathcal{G}_T{}^{a}(p_0,\vec{p}) \;&\approx\; -\frac{z_T{}^{a}(\vec{p})}{\big(p_0^2-(\overline{\omega}_T{}^{a})^2\big)},\\
&\qquad\text{(mass-shell residues: } p_0^2\approx(\overline{\omega}_T{}^{a})^2\,, \qquad (333)
\end{aligned}
$$

where the transverse residue $\overline{\omega}_T{}^{a}$ is the solution of

$$
\overline{\omega}_T{}^{a}: \quad (\overline{\omega}_T{}^{a})^2-\vec{p}^2-\Pi_T^a(\overline{\omega}_T{}^{a},\vec{p}) \;=\; 0. \qquad (334)
$$

The longitudinal and transverse pre-factors $z_L{}^{a}(\vec{p})$ and $z_T{}^{a}(\vec{p})$, respectively, are positive functions. In the time-like energy domain and in the limit $|\vec{p}|\rightarrow 0$ or $p_0/|\vec{p}|\rightarrow\infty$, the longitudinal and transverse polarization components are reduced, respectively, to

$$
\begin{aligned}
\lim_{p_0/|\vec{p}|\rightarrow\text{large}}\Pi_L(p_0,\vec{p}) \;&=\; -\frac{1}{3}\frac{\vec{p}^2}{p_0^2}\big(\mathbf{m}_{\mathcal{G}}^2\big)^{a},\\
\lim_{p_0/|\vec{p}|\rightarrow\text{large}}\Pi_T(p_0,\vec{p}) \;&=\; \frac{1}{3}\big(\mathbf{m}_{\mathcal{G}}^2\big)^{a}. \qquad (335)
\end{aligned}
$$

Hence, the effective longitudinal and transverse gluon propagator components become

$$
\begin{aligned}
\lim_{\vec{p}^2<<p_0^2}{}^{*}\mathcal{G}_L{}^{a}(p_0,\vec{p}) \;&\approx\; -\frac{1}{\vec{p}^2-\frac{\vec{p}^2}{p_0^2}\big(\mathbf{m}_{\mathcal{G}}^2\big)^{a}/3},\\
&=\; -\frac{p_0^2}{\vec{p}^2}\frac{1}{p_0^2-\big(\mathbf{m}_{\mathcal{G}}^2\big)^{a}/3}, \quad\text{(time-like energy domain)}, \qquad (336)
\end{aligned}
$$

and

$$
\lim_{\vec{p}^2<<p_0^2}{}^{*}\mathcal{G}_T{}^{a}(p_0,\vec{p}) \;\approx\; -\frac{1}{p_0^2-\big(\mathbf{m}_{\mathcal{G}}^2\big)^{a}/3}, \quad\text{(time-like energy domain)}, \qquad (337)
$$

respectively. For example, the transverse gluon propagator component is re-expressed in the time-like energy domain as follows

$$
\begin{aligned}
{}^{*}\mathcal{G}_T{}^{a}(p_0,\vec{p}) \;&=\; \frac{z_T{}^{a}(\vec{p})}{2\,\overline{\omega}_T{}^{a}}\left[\frac{1}{\overline{\omega}_T{}^{a}-p_0}-\frac{1}{-\overline{\omega}_T{}^{a}-p_0}\right],\\
&=\; \frac{\pi\, z_T{}^{a}(\vec{p})}{\overline{\omega}_T{}^{a}}\int\frac{d\xi}{2\pi}\left[\frac{\delta\left(\xi-\overline{\omega}_T{}^{a}\right)}{\xi-p_0}-\frac{\delta\left(\xi+\overline{\omega}_T{}^{a}\right)}{\xi-p_0}\right]. \qquad (338)
\end{aligned}
$$

The transverse poles are restricted to the time-like dispersion relation $\overline{\omega}_T{}^{a}>|\vec{p}|$. It is can be written in the form of the spectral density formalism in the following way

$$
{}^{*}\mathcal{G}_T{}^{a}(p_0,\vec{p}) \;=\; \int\frac{d\xi}{2\pi}\frac{({}^{*}\rho_T{}^{a}(\xi,|\vec{p}|))}{\xi-p_0}. \qquad (339)
$$

The spectral density for the time-like energy domain, namely, $p_0^2 > \vec{p}^2$, is given by

$$ {}^*\rho_T{}^a\left(\xi, |\vec{p}|\right) \;=\; \frac{\pi}{\overline{\omega}_T{}^a}\, z_T{}^a(\vec{p})\, \left[\delta\left(\xi - \overline{\omega}_T{}^a\right) - \delta\left(\xi + \overline{\omega}_T{}^a\right)\right]. \tag{340} $$

Furthermore, the extrapolation from the time-like energy domain to the space-like energy domain is established by the analytic continuation and setting $p_0 \to p_0 + i\,\eta$ in following way

$$ \begin{aligned} {}^*\mathcal{G}_T{}^a\left(p_0 + i\eta, \vec{p}\right) \;&=\; \int_{-\infty}^{\infty} \frac{d\xi}{2\pi} {}^*\rho_T{}^a\left(\xi, |\vec{p}|\right)\, \frac{1}{\xi - p_0 - i\,\eta}, \\ &=\; \int_{-\infty}^{\infty} \frac{d\xi}{2\pi}\, {}^*\rho_T{}^a\left(\xi, |\vec{p}|\right)\, \left[P\left(\frac{1}{\xi - p_0}\right) + i\,\pi\,\delta(\xi - p_0)\right], \\ &=\; \left[\int_{-\infty}^{\infty} \frac{d\xi}{2\pi}\, {}^*\rho_T{}^a\left(\xi, |\vec{p}|\right) P\left(\frac{1}{\xi - p_0}\right)\right] + i\,\frac{1}{2}\,\left({}^*\rho_T{}^a(p_0, |\vec{p}|)\right). \end{aligned} \tag{341} $$

The first term on the right hand side which is enclosed by square brackets appears in the time-like energy domain and it is responsible for the transverse Debye screening while the second term, which is an imaginary one, emerges in the space-like energy domain and it causes the Landau damping. The longitudinal and transverse gluon polarization tensors are imaginary in the space-like energy domain $\vec{p}^2 \geq p_0^2$. They are calculated as follows

$$ {}^*\rho_S{}^a\left(p_0, |\vec{p}|\right) \;=\; 2\,\Im m\left({}^*\mathcal{G}_S{}^a(p_0 + i\eta, \vec{p})\right), \tag{342} $$

where the subscript $S = L, T$ refers to the longitudinal and the transverse components, respectively. They are re-written as follows

$$ \begin{aligned} {}^*\rho_S{}^a\left(p_0, |\vec{p}|\right) \;&=\; 2\,\Im m\left({}^*\mathcal{G}_S{}^a(p_0 + i\eta, \vec{p})\right)\theta\left(\vec{p}^2 - p_0^2\right), \\ &=\; \beta_S{}^a\left(p_0, \vec{p}\right)\,\theta\left(\vec{p}^2 - p_0^2\right), \qquad (\text{with } S = L, T). \end{aligned} \tag{343} $$

Hence, in the context of the spectral density formalism, the space-like longitudinal and transverse spectral densities become

$$ {}^*\rho_S{}^a\left(\xi, |\vec{p}|\right) \;=\; \beta_S{}^a\left(\xi, \vec{p}\right)\,\theta\left(\vec{p}^2 - \xi^2\right), \tag{344} $$

where

$$ \beta_S{}^a\left(\xi, \vec{p}\right) \;=\; 2\,\Im m\left({}^*\mathcal{G}_S{}^a(\xi + i\eta, \vec{p})\right), \tag{345} $$

and $S = L, T$ correspond the longitudinal and transverse components, respectively. Moreover, both longitudinal and transverse gluon propagators split to the Debye screening parts

and the Landau damping parts, respectively, as follows

$$
\begin{aligned}
{}^{*}\mathcal{G}_{L}{}^{a}\left(p_{0}+i\eta,\vec{p}\right) \;=\; & -\frac{1}{\vec{p}^{2}}+\left[\int_{-\infty}^{\infty}\frac{d\xi}{2\pi}\left({}^{*}\rho_{L}{}^{a}(\xi,|\vec{p}|)\right)P\left(\frac{1}{\xi-p_{0}}\right)\,\theta\left(\xi^{2}-\vec{p}^{2}\right)\right] \\
& +\int_{-\infty}^{\infty}\frac{d\xi}{2\pi}\frac{\left[\beta_{L}{}^{a}\left(\xi,\vec{p}\right)\,\theta\left(\vec{p}^{2}-\xi^{2}\right)\right]}{\xi-p_{0}},
\end{aligned}
\tag{346}
$$

and

$$
\begin{aligned}
{}^{*}\mathcal{G}_{T}{}^{a}\left(p_{0}+i\eta,\vec{p}\right) \;=\; & \left[\int_{-\infty}^{\infty}\frac{d\xi}{2\pi}\left({}^{*}\rho_{T}{}^{a}(\xi,|\vec{p}|)\right)P\left(\frac{1}{\xi-p_{0}}\right)\,\theta\left(\xi^{2}-\vec{p}^{2}\right)\right] \\
& +\int_{-\infty}^{\infty}\frac{d\xi}{2\pi}\frac{\left[\beta_{T}{}^{a}\left(\xi,\vec{p}\right)\,\theta\left(\vec{p}^{2}-\xi^{2}\right)\right]}{\xi-p_{0}}.
\end{aligned}
\tag{347}
$$

The first integral on the right hand side of Eqns. (346) and (347) is the Debye screening in the time-like energy domain while the second integral is the Landau damping in the space-like energy domain. It is possible to write the longitudinal and transverse gluon propagator components in the terms of the spectral density formalism in the following way

$$
{}^{*}\mathcal{G}_{L}{}^{a}\left(p_{0},\vec{p}\right) \;=\; -\frac{1}{|\vec{p}|^{2}}+\int_{-\infty}^{\infty}\frac{d\xi}{2\pi}\frac{{}^{*}\rho_{L}{}^{a}\left(\xi,\vec{p}\right)}{\xi-p_{0}},
\tag{348}
$$

and

$$
{}^{*}\mathcal{G}_{T}{}^{a}\left(p_{0},\vec{p}\right) \;=\; \int_{-\infty}^{\infty}\frac{d\xi}{2\pi}\frac{{}^{*}\rho_{T}{}^{a}\left(\xi,\vec{p}\right)}{\xi-p_{0}},
\tag{349}
$$

respectively. Furthermore, the longitudinal and transverse gluon propagator components are transformed to

$$
\begin{aligned}
{}^{*}\mathcal{G}_{L}{}^{a}\left(\tau,\vec{p}\right) \;=\; & -\frac{\sum_{l}\delta(\tau-l\beta)}{|\vec{p}|^{2}} \\
& +\int_{-\infty}^{\infty}\frac{d\xi}{2\pi}\,{}^{*}\rho_{L}{}^{a}\left(\xi-i\,\frac{\phi^{a}}{\beta},\vec{p}\right)\,e^{-\left(\xi-i\,\frac{\phi^{a}}{\beta}\right)\tau}\,\left[\theta(\tau)+N_{G}\left(\xi-i\,\frac{\phi^{a}}{\beta}\right)\right],
\end{aligned}
\tag{350}
$$

and

$$
{}^{*}\mathcal{G}_{T}{}^{a}\left(\tau,\vec{p}\right) \;=\; \int_{-\infty}^{\infty}\frac{d\xi}{2\pi}\,{}^{*}\rho_{T}{}^{a}\left(\xi-i\,\frac{\phi^{a}}{\beta},\vec{p}\right)\,e^{-\left(\xi-i\,\frac{\phi^{a}}{\beta}\right)\tau}\,\left[\theta(\tau)+N_{G}\left(\xi-i\,\frac{\phi^{a}}{\beta}\right)\right],
\tag{351}
$$

respectively, in the mixed-time representation of the imaginary-time formalism.

VII. THE EFFECTIVE VERTEXES

In order to study the effective hard thermal quark self-energy and the effective hard thermal gluon polarization tensor besides the other quantities in the ultra-relativistic heavy

ion collisions, the effective n-quarks and m-gluons vertexes become essential in addition to the effective quark and gluon propagators. The effective n-quarks and m-gluons vertexes can be calculated to any order of the coupling constant g. For only the sake of simplicity, we shall limit the approximation up to the order g^{n+m} for the vertexes with $n+m$ external gluons and quarks. The calculation of the effective vertexes for n-quarks and m-gluons is demonstrated by calculating the effective quark-quark-gluon vertex and the effective 2-quarks and 2-gluons vertex. The Feynman diagrams those contribute to the effective quark-quark-gluon vertex up to the order g^3 are displayed in Fig. (3) while those contribute to the effective 2-quarks and 2-gluons vertex up to the order g^4 are displayed in Fig. (4).

A. quark-quark-gluon vertex

The effective quark-quark-gluon vertex can be calculated to any order of the interaction coupling g. Its effective interaction is depicted in Fig. (3 a). In order to calculated the effective quark-quark-gluon vertex up to the order of g^3, the effective quark-quark-gluon vertex is given by the sum of the interactions that are given in Figs. (3 b), (3 c) and (3 d). The effective vertex is found by calculating the bar vertex and the corrections up to the order g^3. The bar quark-quark-gluon vertex is the interaction up to order g and its Feynman diagram is depicted in Fig. (3 b). It reads

$$\Gamma^{3(0)\,a\,\mu} \;=\; -g\gamma^{\mu}\mathbf{t}^{a}_{ij}. \tag{352}$$

The next lowest order corrections to the bar vertex is of order g^3. The first correction is displayed in Fig. (3 c). The kernel of the first correction is constructed as follows

$$\begin{aligned}\Gamma^{3(A)\,a\,\mu}_{\;\;ij}(P,Q;R) \;&=\; \int \frac{d^4k}{(2\pi)^4}\left[-g\gamma^{\beta}\mathbf{t}^{b}_{i'i}\right]\,\mathcal{G}^{\beta\gamma}_{bc}(k)\,\left[-g\gamma^{\gamma}\mathbf{t}^{c}_{jj'}\right]\,i\,\mathcal{S}_{j'l}(k-Q)\\ &\qquad\times\left[-g\gamma^{\mu}\mathbf{t}^{a}_{l'l}\right]\,i\,\mathcal{S}_{l'i'}(k-P),\\ &=\; -g^3\,\mathcal{T}^{3(A)\,a}_{\;\;ij\,[i'j'\,b]}\,\mathcal{V}^{3(A)\,\mu}_{\;\;[i'j'\,b]}(P,Q;R),\end{aligned} \tag{353}$$

where the momentum R is assigned for the external gluon leg while the momenta P and Q are assigned for the two external quark legs. The vertex decomposition with respect to the fundamental color indexes, namely, $i\,j$ for two quarks and the adjoint color indexes, namely, a for one gluon is given by

$$\mathcal{T}^{3(A)\,a}_{\;\;ij\,[i'j'\,b]} \;=\; \mathbf{t}^{b}_{i'i}\mathbf{t}^{b}_{jj'}\mathbf{t}^{a}_{i'j'}, \tag{354}$$

and

$$\mathcal{V}^{3(B)\mu}_{[i'j'\,b]}(P,Q;R) \;=\; \int \frac{d^4k}{(2\pi)^4}\gamma^\beta \mathcal{G}^{\beta\gamma}_{bc}(k)\delta_{bc}\gamma^\gamma\, i\,\mathcal{S}_{j'}(k-Q)\gamma^\mu\, i\,\mathcal{S}_{i'}(k-P). \tag{355}$$

The second term correction is illustrated by the Feynman diagram that is depicted in Fig. (3 d). This correction is of order g^3. Its interaction vertex is constructed as follows

$$\begin{aligned}\Gamma^{3(B)\,a\,\mu}_{ij}(P,Q;R) \;&=\; \int \frac{d^4k}{(2\pi)^4}\left[-g\gamma^\beta \mathbf{t}^b_{i'i}\right]\, i\,\mathcal{S}_{i'j'}(k+P)\left[-g\gamma^\gamma \mathbf{t}^c_{j'j}\right]\mathcal{G}^{\gamma'\gamma}_{cc'}(k+P-Q)\\ &\qquad\times\left[-igf_{ab'c'}\Gamma^{\mu\beta'\gamma'}(-R,-k,k+P-Q)\right]\mathcal{G}^{\beta'\beta}_{b'b}(k),\\ &=\; g^3\mathcal{T}^{3(B)\,a}_{ij\,[i'j'\,bc]}\mathcal{V}^{3(B)\mu}_{[i'j'\,bc]}(P,Q;R),\end{aligned} \tag{356}$$

where the fundamental and adjoint color decomposition for the two quarks with fundamental color indexes $i\,j$ and one gluon with an adjoint color index a, respectively, is given by,

$$\mathcal{T}^{3(B)\,a}_{ij\,[i'j'\,bc]} \;=\; \mathbf{t}^b_{ii'}\mathbf{t}^c_{j'j}\mathbf{T}^a_{bc}, \tag{357}$$

and

$$\begin{aligned}\mathcal{V}^{3(B)\mu}_{[i'j'\,bc]}(P,Q;R) \;&=\; \int \frac{d^4k}{(2\pi)^4}\gamma^\beta\, i\,\mathcal{S}_{i'}(k+P)\,\delta_{i'j'}\,\gamma^\gamma\mathcal{G}^{\gamma\gamma'}_{c}(k+P-Q)\\ &\qquad\times\Gamma^{\gamma'\mu\beta'}(k+P-Q,-R,-k)\,\mathcal{G}^{\beta'\beta}_{b}(k).\end{aligned} \tag{358}$$

The effective quark-quark-gluon vertex with the corrections up to the order g^3 is obtained by adding the first and second term corrections which are of order g^3 to the bar vertex which is of order g. Hence, the effective quark-quark-gluon vertex becomes

$${}^*\Gamma^{3\,a\mu}_{ij}(P,Q;R) \;=\; -g\gamma^\mu\mathbf{t}^a_{ij} \;+\; g^3\mathbf{V}^{3\,a\mu}_{ij}(P,Q;R), \tag{359}$$

where the correction up to the order of g^3 is given by

$$\begin{aligned}\mathbf{V}^{3\,a\mu}_{ij}(P,Q;R) \;&=\; -\mathcal{T}^{3(A)\,a}_{ij\,[i'j'\,b]}\,\mathcal{V}^{3(A)\mu}_{[i'j'\,b]}(P,Q;R)\\ &\qquad+\mathcal{T}^{3(B)\,a}_{ij\,[i'j'\,bc]}\mathcal{V}^{3(B)\mu}_{[i'j'\,bc]}(P,Q;R).\end{aligned} \tag{360}$$

B. 2-quarks and 2-gluons vertex

When the correction is considered up to the order g^4, the the effective 2-quarks and 2-gluons vertex becomes essential in the self-energy corrections (i.e. the radiative corrections).

When the radiative correction is considered up to the order less than g^4, the effective 2-quarks and 2-gluons vertex becomes redundant. The Feynman diagram for the effective 2-quarks and 2-gluons vertex is displayed in Fig. (4 a). The effective 2-quarks and 2-gluons vertex is calculated from three Feynman diagrams that are displayed in Figs. (4 b), (4 c) and (4 d). The first correction to the 2-quarks and 2-gluons vertex is displayed in Fig. (4 b). It consists of four quark-quark-gluon vertexes, three internal quark lines and one internal gluon line. Every internal quark line is identified by the fundamental color indexes while the gluon line has adjoint color indexes. The contribution of the first correction is of order g^4. The interaction kernel is constructed as follows

$$\begin{aligned}\Gamma^{4(A)}{}^{ab\,\mu\nu}_{ij}(P,Q;S,R) &= \int \frac{d^4k}{(2\pi)^4}\left[-g\gamma^{\mu'}\mathbf{t}^{a'}_{ni}\right]\mathcal{G}^{\mu'\nu'}_{a'b'}(k)\left[-g\gamma^{\nu'}\mathbf{t}^{b'}_{jm}\right]\, i\,\mathcal{S}_{mm'}(k-Q)\\ &\quad\times\left[-g\gamma^{\nu}\mathbf{t}^{b}_{l'm'}\right]\, i\,\mathcal{S}_{l'l}(k-Q-S)\,\left[-g\gamma^{\mu}\mathbf{t}^{a}_{n'l}\right]\, i\,\mathcal{S}_{n'n}(k-P),\\ &= g^4\,\mathcal{T}^{4(A)}{}^{ab}_{ij\,[nml\,a']}\,\mathcal{V}^{4(A)}{}^{\mu\nu}_{[nml\,a']}(P,Q;S,R). \end{aligned} \tag{361}$$

The fundamental and adjoint color indexes, namely, $i\,j$ and $a\,b$, respectively, are decomposed by the following projector

$$\mathcal{T}^{4(A)}{}^{ab}_{ij\,[nml\,a']} = \mathbf{t}^{a'}_{ni}\mathbf{t}^{b'}_{jm}\mathbf{t}^{b}_{lm}\mathbf{t}^{a}_{nl}\,\delta_{a'b'}. \tag{362}$$

This projector consists of four fundamental color generators due to the four quark-quark-gluon vertexes. The color projector is defined by

$$\begin{aligned}\mathcal{V}^{4(A)}{}^{\mu\nu}_{[nml\,a']}(P,Q;S,R) &= \int \frac{d^4k}{(2\pi)^4}\gamma^{\mu'}\mathcal{G}^{\mu'\nu'}_{a'b'}(k)\delta_{a'b'}\gamma^{\nu'}\, i\,\mathcal{S}_m(k-Q)\gamma^{\nu}\, i\,\mathcal{S}_l(k-Q-S)\\ &\quad\times\gamma^{\mu}\, i\,\mathcal{S}_n(k-P).\end{aligned} \tag{363}$$

The Feynman diagram of the second correction is depicted in Fig. (4 c). It consists three quark-quark-gluon vertexes and one 3-gluons vertex besides two internal gluon lines and two internal quark lines. The interaction kernel for the second term correction for the 2-quarks and 2-gluons vertex is constructed as follows

$$\begin{aligned}\Gamma^{4(B)}{}^{ab\,\mu\nu}_{ij}(P,Q;S,R) &= \int \frac{d^4k}{(2\pi)^4}\left[-g\gamma^{\alpha'}\mathbf{t}^{c'}_{in}\right]\, i\,\mathcal{S}_{nn'}(k)\left[-g\gamma^{\nu}\mathbf{t}^{b}_{m'n'}\right]\, i\,\mathcal{S}_{mm'}(k-R)\\ &\quad\times\left[-g\gamma^{\beta'}\mathbf{t}^{d'}_{mj}\right]\mathcal{G}^{\beta'\beta}_{d'd}(k-R-Q)\\ &\quad\times\left[g\,(\mathbf{T}^a)_{cd}\,\Gamma^{\mu\alpha\beta}\,(-S,-k+P,k-R-Q)\right]\\ &\quad\times\mathcal{G}^{\alpha\alpha'}_{cc'}(k-P).\end{aligned} \tag{364}$$

From the preceding equation, the second term correction is written as follows

$$\Gamma^{4(B)}{}_{ij}^{ab\,\mu\nu}(P,Q;S,R) \;=\; -g^4\,\mathcal{T}^{4(B)}{}_{ij\,[nm\,cd]}^{ab}\,\mathcal{V}^{4(B)}{}_{[nm\,cd]}^{\mu\nu}(P,Q;S,R), \tag{365}$$

where the decomposition of the fundamental and adjoint color indexes for quarks and gluons, respectively, is given by

$$\mathcal{T}^{4(B)}{}_{ij\,[nm\,cd]}^{ab} \;=\; \mathbf{t}^c_{in}\mathbf{t}^b_{mn}\mathbf{t}^d_{mj}\,(\mathbf{T}^a)_{cd}\,, \tag{366}$$

and

$$\begin{aligned}\mathcal{V}^{4(B)}{}_{[nm\,cd]}^{\mu\nu}(P,Q;S,R) \;=\; &\int \frac{d^4k}{(2\pi)^4}\gamma^{\alpha'}\,i\,\mathcal{S}_n(k)\gamma^{\nu}\,i\,\mathcal{S}_m(k-R)\gamma^{\beta'}\mathcal{G}^{\beta'\beta}_{d'd}(k-R-Q)\delta_{d'd}\\ &\times\Gamma^{\mu\alpha\beta}\,(-S,-k+P,k-R-Q)\,\mathcal{G}^{\alpha\alpha'}_{cc'}(k-P)\delta_{c'c}.\end{aligned} \tag{367}$$

Finally, the third correction for the 2-quarks and 2-gluons vertex is given by the Feynman diagram that is depicted in Fig. (4 d). It consists two quark-quark-gluon vertexes and two 3-gluons vertexes besides three internal gluon segments (i.e. lines) and one internal quark segment (i.e. line). The interaction kernel for the third correction is furnished by

$$\begin{aligned}\Gamma^{4(C)}{}_{ij}^{ab\,\mu\nu}(P,Q;S,R) \;=\; &\int \frac{d^4k}{(2\pi)^4}\left[-g\gamma^{\alpha'}\mathbf{t}^{c'}_{in}\right]\,i\,\mathcal{S}_{nm}(k)\left[-g\gamma^{\beta'}\mathbf{t}^{d'}_{mj}\right]\mathcal{G}^{\beta'\beta}_{d'd}(k-Q)\\ &\times\left[g\left(\mathbf{T}^b\right)_{e'd}\Gamma^{\nu\omega'\beta}\,(-R,-(k-Q-R),k-Q)\right]\mathcal{G}^{\omega'\omega}_{e'e}(k-Q-R)\\ &\times\left[g\,(\mathbf{T}^a)_{ce}\,\Gamma^{\mu\alpha\omega}\,(-S,-(k-P),k-Q-R)\right]\mathcal{G}^{\alpha\alpha'}_{cc'}(k-P).\end{aligned} \tag{368}$$

There are two fundamental color generators and two adjoint color generators to represent the quark and gluon couplings. Eq. (368) is reduced to

$$\Gamma^{4(C)}{}_{ij}^{ab\,\mu\nu}(P,Q;S,R) \;=\; g^4\,\mathcal{T}^{4(C)}{}_{ij\,[n\,cde]}^{ab}\,\mathcal{V}^{4(C)}{}_{[n\,cde]}^{\mu\nu}(P,Q;S,R), \tag{369}$$

where

$$\mathcal{T}^{4(C)}{}_{ij\,[n\,cde]}^{ab} \;=\; \mathbf{t}^c_{in}\mathbf{t}^d_{nj}\left(\mathbf{T}^b\right)_{ed}(\mathbf{T}^a)_{ce}\,, \tag{370}$$

and

$$\begin{aligned}\mathcal{V}^{4(C)}{}_{[n\,cde]}^{\mu\nu}(P,Q;S,R) \;=\; &\int \frac{d^4k}{(2\pi)^4}\gamma^{\alpha'}\,i\,\mathcal{S}_{nm}(k)\delta_{nm}\gamma^{\beta'}\mathcal{G}^{\beta'\beta}_{d'd}(k-Q)\delta_{d'd}\\ &\times\Gamma^{\nu\omega'\beta}\,(-R,-(K-Q-R),K-Q)\,\mathcal{G}^{\omega'\omega}_{e'e}(K-Q-R)\delta_{e'e}\\ &\times\Gamma^{\mu\alpha\omega}\,(-S,-(K-P),K-Q-R)\,\mathcal{G}^{\alpha\alpha'}_{cc'}(K-P)\delta_{c'c}.\end{aligned} \tag{371}$$

Therefore, the effective 2-quarks and 2-gluons vertex up to the order of g^4 is given by adding the first, second and third correction terms those are given by Eqns. (361), (365), (369), respectively. The result for the effective 2-quarks and 2-gluons vertex becomes

$$
\begin{aligned}
{}^{*}\Gamma^{4}{}_{ij}^{ab\,\mu\nu}(P,Q;S,R) \;&=\; \Gamma^{4(A)}{}_{ij}^{ab\,\mu\nu}(P,Q;S,R) + \Gamma^{4(B)}{}_{ij}^{ab\,\mu\nu}(P,Q;S,R) \\
&\quad + \Gamma^{4(C)}{}_{ij}^{ab\,\mu\nu}(P,Q;S,R), \\
&=\; g^4 \Big[\mathcal{T}^{4(A)}{}_{ij\,[nml\,a']}^{ab}\, \mathcal{V}^{4(A)}{}_{[nml\,a']}^{\mu\nu}(P,Q;S,R) \\
&\quad - \mathcal{T}^{4(B)}{}_{ij\,[nm\,cd]}^{ab}\, \mathcal{V}^{4(B)}{}_{[nm\,cd]}^{\mu\nu}(P,Q;S,R) \\
&\quad + \mathcal{T}^{4(C)}{}_{ij\,[n\,cde]}^{ab}\, \mathcal{V}^{4(C)}{}_{[n\,cde]}^{\mu\nu}(P,Q;S,R) \Big]. \qquad (372)
\end{aligned}
$$

VIII. EFFECTIVE QUARK SELF-ENERGY UP TO THE ORDER $O(g^2)$

In order to calculate the colored quark decay rate in the ultra-relativistic heavy ion collisions, the effective quark self-energy must be calculated with the HTL approximation. In this case the momentum of the external quark line is hard (i.e. of order $\sim T$) while the momentum of the internal loop is soft (i.e. of order $\sim g\,T$). The vertexes that appear in the correction loop are hard ones. The effective quark self-energy is calculated up to the order of g^2. The relevant Feynman diagrams are depicted in Fig. (5).

In Fig. (5 a), the self-energy interaction for the hard quark line is represented by an internal quark-gluon loop where the internal loop is composed of a quark segment with an effective hard thermal quark self-energy correction and a gluon segment with an effective hard thermal gluon self-energy correction. Since the quark is considered hard, the bar quark propagator is sufficient in the calculation. The quark segment is shown by the internal lower semi-circle and it is identified by fundamental color indexes while the gluon segment is identified by adjoint color indexes and it appears as an internal upper semi-circle that complements the quark lower semi-circle in order to form the internal quark-gluon loop. The internal hard thermal quark-gluon loop consists of two hard quark-quark-gluon vertexes and one internal hard quark line (i.e. the HTL is not necessary) and one internal soft gluon line segment with the HTL correction. Furthermore, the external quark momentum $(p_0, \vec{p})$ is taken to be hard one with respect to the internal momentum $(k_0, \vec{k})$ with the assumption that $|\vec{k}|\,/\,|\vec{p}| \leq g \ll 1$. Since the external momentum $|\vec{p}|$ is assumed to be of the order $|\vec{p}| \sim T$, the internal momentum becomes of order $|\vec{k}| \sim g\,p \sim g\,T$. The lowest order

correction to be considered for the effective quark self-energy is of order of g^2 in the present work. The other contribution to the hard quark line's self-energy is given by the hard quark line with a gluon tadpole which is depicted in Fig. (5 b). The tadpole consists one effective hard thermal 2-gluons and 2-quarks vertex and an internal gluon loop with an effective HTL gluon correction and two external quark legs. The lowest order correction of the tadpole for the hard quark line is of order $O(g^4)$. When the effective quark self-energy is calculated up to the order of g^2, the quark-gluon loop interaction which is displayed in Fig. (5 a) is sufficient while the tadpole interaction which is displayed in Fig. (5 b) can be neglected. The effective quark self-energy is calculated by integrating the internal soft momentum, namely, $(k_0, \vec{k})$ as follows,

$$ {}^*\Sigma_{Q_{ij}}(p_0, \vec{p}) \;=\; \int \frac{d^4k}{(2\pi)^3}\; {}^*\Sigma_{Q_{ij}}(p_0, \vec{p}, k_0, \vec{k}). \tag{373} $$

The internal momentum k appears in the interaction kernels that are displayed in Fig. (5). The effective interaction kernel with the internal thermal quark-gluon loop which is displayed in Fig. (5 b) is written as follows:

$$ \begin{aligned} {}^*\Sigma_{Q_{ij}}\left(p_0, \vec{p}, k_0, \vec{k}\right) \;&=\; {}^*\Gamma^{3\,a\,\mu}_{ii'}\; i\; {}^*\mathcal{S}_{Q_{i'j'}}(p-k)\; {}^*\Gamma^{3\,b\,\nu}_{j'j}\; {}^*\mathcal{G}^{\mu\nu}_{ab}(k), \\ &\approx\; \Gamma^{3\,a\,\mu}_{ii'}\; i\, \mathcal{S}_{Q_{i'j'}}(p-k)\, \Gamma^{3\,b\,\nu}_{j'j}\; {}^*\mathcal{G}^{\mu\nu}_{ab}(k), \end{aligned} \tag{374} $$

where

$$ \begin{aligned} {}^*\Gamma^{3\,a\,\mu}_{ii'} \;&=\; {}^*\Gamma^{3\,a\,\mu}_{ii'}(p, -p+k, -k), \\ &\approx\; -g\,\gamma^\mu\, \mathbf{t}^a_{ii'} + O(g^3), \end{aligned} \tag{375} $$

and

$$ \begin{aligned} {}^*\Gamma^{3\,b\,\nu}_{j'j} \;&=\; {}^*\Gamma^{3\,b\,\nu}_{j'j}(p-k, -p, k) \\ &\approx\; -g\,\gamma^\nu\, \mathbf{t}^b_{j'j} + O(g^3). \end{aligned} \tag{376} $$

Since the external quark line is assumed to be hard, the internal quark loop segment is assumed to carry the hard part of the external momentum. The effective internal quark propagator is approximated to the bar one. Eq. (374) is approximated up to the order of g^2 to

$$ {}^*\Sigma_{Q_{ij}}(p_0, \vec{p}, k_0, \vec{k}) \;\approx\; (\mathbf{t}^a)_{in}(\mathbf{t}^a)_{nj}\; {}^*\Sigma^a_{Q_n}(p_0, \vec{p}, k_0, \vec{k}), \tag{377} $$

where

$$
\begin{aligned}
{}^{*}\Sigma_{Q_n}^{a}(p_0,\vec{p},k_0,\vec{k}) \;&\approx\; g^2\;[\gamma_0\, i\;{}^{*}\mathcal{S}_n(p-k)\,\gamma_0\;{}^{*}\mathcal{G}_L^{a}(k)] \\
&\quad + g^2\;\sum_{l,k=1}^{3}\Big[\gamma_l\, i\;{}^{*}\mathcal{S}_n(p-k)\,\gamma_k\;\Big(\delta_{lk}-\hat{k}_l\hat{k}_k\Big)\;{}^{*}\mathcal{G}_T^{a}(k)\Big], \\
&\approx\; g^2\;[\gamma_0\, i\,\mathcal{S}_n(p-k)\,\gamma_0\;{}^{*}\mathcal{G}_L^{a}(k)] \\
&\quad + g^2\;\sum_{l,k=1}^{3}\Big[\gamma_l\, i\,\mathcal{S}_n(p-k)\,\gamma_k\;\Big(\delta_{lk}-\hat{k}_l\hat{k}_k\Big)\;{}^{*}\mathcal{G}_T^{a}(k)\Big]. \qquad (378)
\end{aligned}
$$

Furthermore, by considering Eq. (377), Eq. (374) is reduced to

$$
{}^{*}\Sigma_{Q_{ij}}(p_0,\vec{p}) \;=\; (\mathbf{t}^a)_{in}(\mathbf{t}^a)_{nj}\;{}^{*}\Sigma_{Q_n}^{a}(p_0,\vec{p}), \qquad (379)
$$

where

$$
{}^{*}\Sigma_{Q_n}^{a}(p_0,\vec{p}) \;=\; \int\frac{d^4k}{(2\pi)^3}\;{}^{*}\Sigma_{Q_n}^{a}(p_0,\vec{p},k_0,\vec{k}). \qquad (380)
$$

The Foldy-Wouthuysen energy transformation decomposes the interaction kernel ${}^{*}\Sigma_{Q_n}^{a}(p_0,\vec{p},k_0,\vec{k})$ to positive and negative energy components as follows

$$
\begin{aligned}
{}^{*}\Sigma_{Q_n}^{a}(p_0,\vec{p},k_0,\vec{k}) \;\approx\; g^2\;\Bigg[&\sum_{r=\pm}\gamma_0\, h_Q^{(r)}\Big(\vec{p}-\vec{k}\Big)\;\gamma_0\,\Delta_{Q\,n}^{(r)}(p-k)\;{}^{*}\mathcal{G}_L{}^{a}(k) \\
&+\sum_{r=\pm}\sum_{l,k=1}^{3}\gamma_l\, h_Q^{(r)}\Big(\vec{p}-\vec{k}\Big)\;\gamma_k\;\Big(\delta_{lk}-\hat{k}_l\hat{k}_k\Big)\;\Delta_{Q\,n}^{(r)}(p-k)\;{}^{*}\mathcal{G}_T{}^{a}(k)\Bigg]. \qquad (381)
\end{aligned}
$$

Performing the integration over the time-component variable k_0 reduces Eq. (381) to the following result

$$
\begin{aligned}
{}^{*}\Sigma_{Q_n}^{a}(p_0,\vec{p},\vec{k}) \;=\; g^2\;\Bigg[&\sum_{r=\pm}\gamma_0\, h_Q^{(r)}\Big(\vec{p}-\vec{k}\Big)\;\gamma_0\;{}^{*}\mathcal{K}_L^{(r)\,a}{}_{Q\,n}(p_0,\vec{p},\vec{k}) \\
&+\sum_{r=\pm}\sum_{i,j=1}^{3}\gamma_i\, h_Q^{(r)}\Big(\vec{p}-\vec{k}\Big)\;\gamma_j\;\Big(\delta_{ij}-\hat{k}_i\hat{k}_j\Big)\;{}^{*}\mathcal{K}_T^{(r)\,a}{}_{Q\,n}(p_0,\vec{p},\vec{k})\Bigg], \qquad (382)
\end{aligned}
$$

where

$$
\begin{aligned}
{}^{*}\mathcal{K}_S^{(r)\,a}{}_{Q\,n}(p_0,\vec{p},\vec{k}) \;&=\; \int\frac{dk_0}{2\pi}\;{}^{*}\Delta_{Q\,n}^{(r)}(p-k)\;{}^{*}\mathcal{G}_S{}^{a}(k), \\
&=\; \int\frac{dk_0}{2\pi}\int_0^{\beta}d\tau\int_0^{\beta}d\tau' e^{\left[(p_0-k_0)-\mu_Q-\frac{i\theta_n}{\beta}\right]\tau'}\;e^{\left[k_0-\frac{i\phi^a}{\beta}\right]\tau} \\
&\qquad\qquad \times\Delta_{Q\,n}^{(r)}(\tau',\vec{p}-\vec{k})\;{}^{*}\mathcal{G}_S{}^{a}(\tau,\vec{k}), \\
&=\; \int_0^{\beta}d\tau e^{\left[p_0-\mu_Q-\frac{i\theta_n}{\beta}-\frac{i\phi^a}{\beta}\right]\tau}\Delta_{Q\,n}^{(r)}(\tau,\vec{p}-\vec{k})\;{}^{*}\mathcal{G}_S{}^{a}(\tau,\vec{k}). \qquad (383)
\end{aligned}
$$

The subscript $S = L, T$ is referred to the longitudinal and transverse component, respectively. The integrations over the variables k_0 and τ are evaluated explicitly in Eqns. (382) and (383). The results for the positive and negative Foldy-Wouthuysen energy components of the interaction kernel are reduced to

$$
\begin{aligned}
{}^{*}\mathcal{K}_{S}^{(+)a}{}_{n}(p_0,\vec{p},\vec{k}) \;=\; & \int_{-\infty}^{\infty}\frac{d\xi_0}{2\pi}\left[\frac{1-n_F\left(\epsilon_Q(\vec{p}-\vec{k})-\mu_Q-i\frac{\theta_n}{\beta}\right)+N_G\left(\xi_0-i\frac{\phi^a}{\beta}\right)}{p_0-\epsilon_Q(\vec{p}-\vec{k})-\xi_0}\right] \\
& \times\; {}^{*}\rho_S{}^{a}\left(\xi_0-i\frac{\phi^a}{\beta},\vec{k}\right), \qquad (384)
\end{aligned}
$$

and

$$
\begin{aligned}
{}^{*}\mathcal{K}_{S}^{(-)a}{}_{n}(p_0,\vec{p},\vec{k}) \;=\; & \int_{-\infty}^{\infty}\frac{d\xi_0}{2\pi}\left[\frac{n_F\left(\epsilon_Q(\vec{p}-\vec{k})+\mu_Q+i\frac{\theta_n}{\beta}\right)+N_G\left(\xi_0-i\frac{\phi^a}{\beta}\right)}{p_0+\epsilon_Q(\vec{p}-\vec{k})-\xi_0}\right] \\
& \times\; {}^{*}\rho_S{}^{a}\left(\xi_0-i\frac{\phi^a}{\beta},\vec{k}\right), \qquad (385)
\end{aligned}
$$

respectively. By adopting the approximation of $|\vec{k}|/|\vec{p}| \approx g \ll 1$, the pole of Eq. (384) is allocated in the following position,

$$
\begin{aligned}
& |\vec{p}| \approx p_0, \\
& \epsilon_Q(\vec{p}-\vec{k}) \approx |\vec{p}| - |\vec{k}|\hat{k}\cdot\hat{p}, \qquad (386) \\
& p_0 - \epsilon_Q(\vec{p}-\vec{k}) - \xi_0 \approx |\vec{k}|\hat{k}\cdot\hat{p} - \xi_0.
\end{aligned}
$$

The conservation of color charges connects both the fundamental and the adjoint color chemical potentials for the quark-quark-gluon vertex in the following way

$$
\begin{aligned}
\phi^a \;&=\; \phi^{\overbrace{(ii')}}, \\
&=\; \theta_i - \theta_{i'}. \qquad (387)
\end{aligned}
$$

This leads to $\theta_i = \theta_n + \phi^a$ in the quark-gluon loop interaction that is depicted in Fig. (5 a). Therefore, by using the preceding results and preforming the analytic continuation over the external momentum's time-component $p_0 \to p_0 + i\,\eta$, Eq. (384) is approximated to the following result:

$$
\begin{aligned}
{}^{*}\mathcal{K}_{S}^{(+)a}{}_{n}(p_0+i\eta,\vec{p},\vec{k}) \;=\; & \int_{-\infty}^{\infty}\frac{d\xi_0}{2\pi}\left[P\left(\frac{1}{|\vec{k}|\,\hat{k}\cdot\hat{p}-\xi_0}\right)+i\,\pi\,\delta\left(\xi_0-|\vec{k}|\,\hat{k}\cdot\hat{p}\right)\right] \\
& \times\left[1-n_F\left(\epsilon_Q(\vec{p}-\vec{k})-\mu_Q-i\frac{\theta_n}{\beta}\right)+N_G\left(\xi_0-i\frac{\phi^a}{\beta}\right)\right] \\
& \times\; {}^{*}\rho_S{}^{a}\left(\xi_0-i\frac{\phi^a}{\beta},\vec{k}\right). \qquad (388)
\end{aligned}
$$

In this class of function (i.e. Eq. (388)), the real and imaginary parts do not overlap with each other and they do not enhance simultaneously in the momentum complex plane. The real part exists only in the time-like energy domain $\vec{p}^2 < p_0^2$. When the momentum turns to run over the space-like energy domain $\vec{p}^2 \geq p_0^2$, the imaginary part is developed while the real part is strongly suppressed. In the limit $\vec{p}^2 \to p_0^2$ that when $\vec{p}^2$ approaches p_0^2 from below, the time-like energy domain switches to the space-like energy domain and consequently the imaginary part is developed while the real part disappears under the present HTL approximation. Therefore, the resultant imaginary part is reduced to

$$
\begin{aligned}
{}^*\mathcal{K}_S^{(+)a}{}_n(p_0 + i\eta, \vec{p}, \vec{k}) \;=\; & \int_{-\infty}^{\infty} \frac{d\xi_0}{2\pi} \left[1 - n_F\left(\epsilon_Q(\vec{p} - \vec{k}) - \mu_Q - i\frac{\theta_n}{\beta}\right) + N_G\left(\xi_0 - i\frac{\phi^a}{\beta}\right)\right] \\
& \times\; i\,\pi\,\delta\left(\xi_0 - |\vec{k}|\,\hat{k}\cdot\hat{p}\right)\; {}^*\rho_S{}^a\left(\xi_0 - i\frac{\phi^a}{\beta}, \vec{k}\right), \\
& \qquad \text{(in space-like energy domain)}, \qquad (389)
\end{aligned}
$$

for the external hard p-momentum (i.e. the external hard quark line) and the internal soft k-momentum (i.e. the internal soft gluon line). It should be noted that the spectral density ${}^*\rho_S{}^a\left(\xi_0, \vec{k}\right)$ is given in the space-like energy domain. On the other hand, the negative Foldy-Wouthuysen energy component, that is given by Eq. (385), is approximated to

$$
\begin{aligned}
{}^*\mathcal{K}_S^{(-)a}{}_n(p_0, \vec{p}, \vec{k}) \;\approx\; & \frac{1}{2|\vec{p}|}\int_{-\infty}^{\infty} \frac{d\xi_0}{2\pi} \left[n_F\left(\epsilon_Q(\vec{p} - \vec{k}) + \mu_Q + i\frac{\theta_n}{\beta}\right) + N_G\left(\xi_0 - i\frac{\phi^a}{\beta}\right)\right] \\
& \times\; {}^*\rho_S{}^a\left(\xi_0 - i\frac{\phi^a}{\beta}, \vec{k}\right), \\
{}^*\mathcal{K}_S^{(-)a}{}_n(p_0 + i\eta, \vec{p}, \vec{k}) \;\approx\; & \text{dropped from the calculation.} \qquad (390)
\end{aligned}
$$

It is evident that the negative Foldy-Wouthuysen component has no pole and it does not develop any imaginary part for the external p-momentum even when the momentum turns to run over the space-like energy domain. This means that Eq. (390) can be dropped from the calculation since it does not develop an imaginary part in the space-like energy domain.

The relevant quantity for the quark decay rate is

$$
\frac{1}{4|\vec{p}|}\mathrm{tr}\left[p\cdot\gamma\; {}^*\Sigma\left(p_0, \vec{p}\right)\right], \qquad (391)
$$

in the limit $|\vec{p}| \to p_0 + i\,\eta$ from below (i.e. the brink of space-like energy domain). It is useful to introduce the following approximations

$$
\frac{1}{4|\vec{p}|}\mathrm{tr}\left[(p\cdot\gamma)\gamma_0 h_+\left(\vec{p} - \vec{k}\right)\gamma_0\right] \;\approx\; 1, \qquad (392)
$$

and

$$\frac{1}{4|\vec{p}|}\mathrm{tr}\left[(p\cdot\gamma)\gamma_i h_+\left(\vec{p}-\vec{k}\right)\gamma_j\right]\approx\hat{p}_i\hat{p}_j, \tag{393}$$

under the assumption of the hard external p-momentum and the soft internal loop k-momentum (i.e. $p\gg k$ and $k/p\sim g$). The decay rate for the quark line with external fundamental color indexes δ_{ij} and the hard momentum is given by

$$\begin{aligned}\gamma_{Q\,ij} &= \lim_{|\vec{p}|\to p_0}\frac{1}{4|\vec{p}|}\,\mathrm{tr}\left[(p\cdot\gamma)\ {}^*\Sigma_{Q\,ij}(p_0+i\eta,\vec{p})\right],\\ &= \sum_a\sum_n \mathbf{t}^a_{in}\,\mathbf{t}^a_{nj}\,\gamma_{Q}{}^a_n.\end{aligned} \tag{394}$$

In order to be specific, the decay rate is given by taking the imaginary part of $\gamma_{Q\,ij}$ and $\gamma_{Q}{}^a_n$. The decay rate part of the internal quark-gluon loop, namely, $\gamma_{Q}{}^a_n$ with an internal quark segment with a fundamental color index n and a gluon segment with an adjoint color index a is given by

$$\begin{aligned}\gamma_{Q}{}^a_n &= \lim_{|\vec{p}|\to p_0}\frac{1}{4|\vec{p}|}\,\mathrm{tr}\left[(p\cdot\gamma)\ {}^*\Sigma_{Q}{}^a_n(p_0+i\eta,\vec{p})\right],\\ &= \lim_{|\vec{p}|\to p_0}\frac{1}{4|\vec{p}|}\,\mathrm{tr}\left[(p\cdot\gamma)\int\frac{d^3\vec{k}}{(2\pi)^3}\,{}^*\Sigma_{Q}{}^a_n(p_0+i\eta,\vec{p},\vec{k})\right].\end{aligned} \tag{395}$$

In the limit $|\vec{p}|\to p_0$, the quark's decay rate of the effective internal thermal quark-gluon loop is reduced to

$$\begin{aligned}\gamma_{Q}{}^a_n &= \frac{1}{4|\vec{p}|}\,\mathrm{tr}\left[(p\cdot\gamma)\ {}^*\Sigma_{Q}{}^a_n(p_0+i\,\eta,\vec{p},\vec{k})\right],\\ &= g^2\left[\int\frac{d^3\vec{k}}{(2\pi)^3}\,{}^*\mathcal{K}_L^{(+)\,a}{}_n(p_0+i\,\eta,\vec{p},\vec{k})\right.\\ &\qquad\left.+\int\frac{d^3\vec{k}}{(2\pi)^3}\left(1-(\hat{p}\cdot\hat{k})^2\right)\,{}^*\mathcal{K}_T^{(+)\,a}{}_n(p_0+i\,\eta,\vec{p},\vec{k})\right].\end{aligned} \tag{396}$$

By using Eq. (389), the quark's decay rate which is given by Eq. (396) is reduced to

$$\begin{aligned}\gamma_{Q}{}^a_n &= \lim_{|\vec{p}|\to p_0}\frac{1}{4|\vec{p}|}\,\mathrm{tr}\left[(p\cdot\gamma)\ {}^*\Sigma_{Q}{}^a_n(p_0+i\,\eta,\vec{p})\right],\\ &= g^2\,(i\,\pi)\int_{-\infty}^{\infty}\frac{d\xi_0}{2\pi}\int\frac{d^3\vec{k}}{(2\pi)^3}\,\delta\left(\xi_0-|\vec{k}|\,\hat{k}\cdot\hat{p}\right)\left[{}^*\rho_L{}^a\left(\xi_0-i\frac{\phi^a}{\beta},\vec{k}\right)\right.\\ &\qquad\left.+\left(1-(\hat{p}\cdot\hat{k})^2\right)\,{}^*\rho_T{}^a\left(\xi_0-i\frac{\phi^a}{\beta},\vec{k}\right)\right]\\ &\qquad\times\left[1-n_F\left(\epsilon_Q(\vec{p}-\vec{k})-\mu_Q-i\frac{\theta_n}{\beta}\right)+N_G\left(\xi_0-i\frac{\phi^a}{\beta}\right)\right].\end{aligned} \tag{397}$$

The Dirac δ-function is transformed to

$$\delta\left(\xi_0 - |\vec{k}|\,\hat{k}\cdot\hat{p}\right) \;=\; \frac{1}{|\vec{k}|}\,\delta\left(\cos\theta - \frac{\xi_0}{|\vec{k}|}\right). \tag{398}$$

Furthermore, by transforming the δ-function using $\delta\left(\xi_0 - |\vec{k}|\,\hat{k}\cdot\hat{p}\right) \;\rightarrow\; \left[1/|\vec{k}|\right]\delta\left(\cos\theta - \xi_0/|\vec{k}|\right)$ and evaluating the integral that is given in Eq. (397) over $\hat{k}\cdot\hat{p} \;=\; \cos\theta$ where $\cos\theta \;=\; \xi_0/|\vec{k}|$, the calculation leads to the interval constraint $|\vec{k}| \;\geq\; \xi_0 \;\geq\; -|\vec{k}|$. The decay rate of the internal quark-gluon loop is reduced to

$$\begin{aligned}
\gamma_{Q_n^a} \;=\; & g^2\,(i\,\pi)\int_0^\infty \frac{d|\vec{k}|}{(2\pi)^2}\,|\vec{k}|\int_{-|\vec{k}|}^{|\vec{k}|}\frac{d\xi_0}{2\pi}\,\left[{}^*\rho_L{}^a\left(\xi_0 - i\frac{\phi^a}{\beta},\vec{k}\right)\right. \\
& \left. + \left(1 - \frac{\xi_0^2}{\vec{k}^2}\right){}^*\rho_T{}^a\left(\xi_0 - i\frac{\phi^a}{\beta},\vec{k}\right)\right] \\
& \times\left[1 - n_F\left(\epsilon_Q(\vec{p}-\vec{k}) - \mu_Q - i\frac{\theta_n}{\beta}\right) + N_G\left(\xi_0 - i\frac{\phi^a}{\beta}\right)\right]\Bigg|_{\hat{k}\cdot\hat{p}=\xi_0/|\vec{k}|}.
\end{aligned} \tag{399}$$

The spectral density is given by

$${}^*\rho_S{}^a\left(\xi_0,\vec{k}\right) = \beta_S{}^a\left(\xi_0,\vec{k}\right)\theta\left(\vec{k}^2 - \xi_0^2\right), \quad (\text{where} \quad S = T, L), \tag{400}$$

in the space-like energy domain. Therefore, the decay rate is re-written as follows

$$\begin{aligned}
\gamma_{Q_n^a} \;=\; & g^2\,(i\,\pi)\int_0^\infty \frac{d|\vec{k}|}{(2\pi)^2}\,|\vec{k}|\int_{-|\vec{k}|}^{|\vec{k}|}\frac{d\xi_0}{2\pi}\,\left[\beta_L{}^a\left(\xi_0 - i\frac{\phi^a}{\beta},\vec{k}\right)\right. \\
& \left. + \left(1 - \frac{\xi_0^2}{\vec{k}^2}\right)\beta_T{}^a\left(\xi_0 - i\frac{\phi^a}{\beta},\vec{k}\right)\right] \\
& \times\left[1 - n_F\left(\epsilon_Q(\vec{p}-\vec{k}) - \mu_Q - i\frac{\theta_n}{\beta}\right) + N_G\left(\xi_0 - i\frac{\phi^a}{\beta}\right)\right]\Bigg|_{\hat{k}\cdot\hat{p}=\xi_0/|\vec{k}|}.
\end{aligned} \tag{401}$$

The explicit expressions for the longitudinal and transverse spectral densities are given by

$$\begin{aligned}
\beta_L{}^a\left(\xi_0,\vec{p}\right) \;&=\; \frac{\Pi_L{}^a(\xi_0,\vec{p})}{\left(\vec{p}^2\right)^2 + \left[\Pi_L{}^a(\xi_0,\vec{p})\right]^2}, \\
\beta_T{}^a\left(\xi_0,\vec{p}\right) \;&=\; -\frac{\Pi_T{}^a(\xi_0,\vec{p})}{\left(\xi_0^2 - \vec{p}^2\right)^2 + \left[\Pi_T{}^a(\xi_0,\vec{p})\right]^2},
\end{aligned} \tag{402}$$

respectively, where

$$\begin{aligned}
\Pi_L{}^a(\xi_0,\vec{p}) \;&=\; (\mathbf{m}_D^2)^a\left(\frac{\pi\,\xi_0}{2|\vec{p}|}\right), \\
\Pi_T{}^a(\xi_0,\vec{p}) \;&=\; -\frac{1}{2}(\mathbf{m}_D^2)^a\left(1 - \frac{\xi_0^2}{|\vec{p}|^2}\right)\left(\frac{\pi\,\xi_0}{2|\vec{p}|}\right).
\end{aligned} \tag{403}$$

Since it is supposed that $\xi_0 - i\phi^a/\beta \leq gT \ll 1$, the gluon's partition becomes the dominant term. Hence, it is possible to assume the following approximation

$$\begin{aligned}\left[1 - n_F\left(\epsilon_Q(\vec{p}-\vec{k}) - \mu_Q - i\frac{\theta_n}{\beta}\right) + N_G\left(\xi_0 - i\frac{\phi^a}{\beta}\right)\right]\Big|_{\hat{k}\cdot\hat{p}=\xi_0/|\vec{k}|} &\approx N_G\left(\xi_0 - i\frac{\phi^a}{\beta}\right), \\ &\approx \frac{T}{\xi_0 - i\frac{\phi^a}{\beta}}, \\ &\to \frac{T}{\xi_0 - {\mu_C}^a}. \end{aligned} \tag{404}$$

This approximation simplifies the calculation of the hard quark decay rate drastically. For instance, the gluonic part of the colored fermion Landau frequency and the colored gluon's Debye mass develop nontrivial imaginary terms for the (real-) flavor and (real/imaginary-) color chemical potentials. These imaginary parts vanish when the adjoint color potentials vanish. The condition ${\mu_C}^a = (\mu_{C\,A} - \mu_{C\,B}) = 0$ (where $a = 1, \cdots, N_c^2 - 1$), means that fundamental chemical potentials become equal to each other for different color species, namely, blue, green and red colors. The equality of the fundamental color chemical potentials is possible in the $U(N_c)$ symmetry group. In the $SU(N_c)$ symmetry group, the equality constraint implies that the color chemical potentials vanish because of the unimodular condition $\sum_{i=1}^{N_c} \theta_i = 0$. Therefore, in order to set $\mu^a = 0$, either the fundamental color chemical potentials vanish or the quark lines carry all the color information in the sense that the quark segment of internal loop carries the same color charge of the external quark line. The later possibility imposes an additional color contraction $\delta_{i\,n}$ where i and n are the external and internal quark lines indexes, respectively. In the case that all the fundamental color chemical potentials vanish the system turns to be color neutral and this is equivalent to neglect the explicit color degrees of freedom for quarks and gluons. Under the extreme conditions when the the free mobile of colored quarks and gluons matter is reached, it is possible that the adjoint color chemical potentials of the internal gluon's segment become finite and subsequently the fundamental color chemical potentials turn to be finite. In this case, the Debye mass squared becomes an imaginary one. The external and internal quark lines are presumed hard while the internal gluon segment is considered to be soft then it is reasonable to imagine that in the deconfinement matter most of the energy information is carried by the hard colored quark lines. Under this assumption, the internal adjoint color potential ${\mu_C}^a$

vanishes (i.e. $\mu_C{}^a \to 0$) and Eq. (404) is reduced to

$$\left[1 - n_F\left(\epsilon_Q(\vec{p}-\vec{k}) - \mu_Q - i\frac{\theta_n}{\beta}\right) + N_G\left(\xi_0 - i\frac{\phi^a}{\beta}\right)\right]\Big|_{\hat{k}\cdot\hat{p}=\xi_0/|\vec{k}|} \to \frac{T}{\xi_0}. \tag{405}$$

The resultant decay rate with the approximation those are given by Eqns. (404) and (405) is reduced to

$$\begin{aligned}
\gamma_{Q_n^a} &= i\,\frac{g^2\,T}{4\pi^2}\int_0^\infty d|\vec{k}|\,|\vec{k}|\int_{-|\vec{k}|}^{|\vec{k}|}\frac{d\xi_0}{2\pi}\,\frac{1}{\left(\xi_0 - i\frac{\phi^a}{\beta}\right)}\left[\beta_L{}^a\left(\xi_0 - i\frac{\phi^a}{\beta},\vec{k}\right)\right. \\
&\qquad \left. + \left(1 - \frac{\xi_0^2}{\vec{k}^2}\right)\beta_T{}^a\left(\xi_0 - i\frac{\phi^a}{\beta},\vec{k}\right)\right], \\
&\approx i\,\frac{g^2\,T}{4\pi^2}\int_0^\infty d|\vec{k}|\,|\vec{k}|\int_{-|\vec{k}|}^{|\vec{k}|}\frac{d\xi_0}{2\pi}\,\frac{1}{\xi_0}\left[\beta_L{}^a\left(\xi_0,\vec{k}\right) + \left(1 - \frac{\xi_0^2}{\vec{k}^2}\right)\beta_T{}^a\left(\xi_0,\vec{k}\right)\right].
\end{aligned} \tag{406}$$

Nonetheless, the validity of these kind of approximations need to be scrutinized numerically and to be tested experimentally at LHC. The decay rate for the quark with the external fundamental color indexes, namely, $i\,j$ is determined by

$$\begin{aligned}
\gamma_{Q_{i\,j}} &= \sum_n^{N_c}\sum_a^{N_c^2-1}\left(\mathbf{t}^a\right)_{in}\left(\mathbf{t}^a\right)_{nj}\,\gamma_{Q_n^a}, \\
&= i\sum_n^{N_c}\sum_a^{N_c^2-1}\left(\mathbf{t}^a\right)_{in}\left(\mathbf{t}^a\right)_{nj} \\
&\qquad \times \frac{g^2\,T}{4\pi^2}\int_0^\infty d|\vec{k}|\,|\vec{k}|\int_{-|\vec{k}|}^{|\vec{k}|}\frac{d\xi_0}{2\pi}\,\frac{1}{\xi_0}\left[\beta_L{}^a\left(\xi_0,\vec{k}\right) + \left(1 - \frac{\xi_0^2}{\vec{k}^2}\right)\beta_T{}^a\left(\xi_0,\vec{k}\right)\right].
\end{aligned} \tag{407}$$

The decay rate is calculated by taking $\Im m\left(\gamma_{Q_{i\,j}}\right)$ where

$$\begin{aligned}
\gamma_{Q_{i\,j}} &= i\,\delta_{ij}\,\frac{1}{2N_c}\left[N_c\sum_n^{N_c}\gamma_Q\overbrace{{}^{(in)}} - \gamma_Q\overbrace{{}^{(00)}}\right], \\
&\approx i\,\delta_{ij}\,\frac{N_c^2-1}{2N_c}\,\gamma_Q\overbrace{{}^{(00)}},
\end{aligned} \tag{408}$$

and

$$\begin{aligned}
\gamma_Q\overbrace{{}^{(AB)}} &= \frac{g^2\,T}{4\pi^2}\int_0^\infty d|\vec{k}|\,|\vec{k}|\int_{-|\vec{k}|}^{|\vec{k}|}\frac{d\xi_0}{2\pi}\,\frac{1}{\xi_0}\left[\beta_L\overbrace{{}^{(AB)}}\left(\xi_0,\vec{k}\right)\right. \\
&\qquad \left. + \left(1 - \frac{\xi_0^2}{\vec{k}^2}\right)\beta_T\overbrace{{}^{(AB)}}\left(\xi_0,\vec{k}\right)\right].
\end{aligned} \tag{409}$$

The observable quantities such as the decay rate of colored quark turn to be dependent on the fundamental color chemical potentials and the interaction details. The fluid characteristic

of the quark-gluon plasma in RHIC energy support the idea of the role of the color degrees of freedom and the weakly color coupling in the quark-gluon plasma.

IX. DISCUSSION AND CONCLUSION

It is argued that the quark-gluon plasma above the tri-critical point of the phase transition from the low-lying hadronic phase to the quark-gluon plasma is not true deconfined matter but rather a weakly interacting quarks and gluons. There are strong indications from RHIC that quark-gluon plasma is a perfect fluid with a low shear viscosity and not a true deconfined matter. Hence, it is natural to assume that the explicit role of the color degrees of freedom becomes important above the deconfinement phase transition line in the phase transition diagram from the hadronic matter to the quark-gluon plasma. Furthermore, it is naive to believe that the quarks and gluons carry color charges and the color fugacities tend to vary in the medium. The color chemical potentials appear explicitly in the quark and gluon partition functions. In this case, the color degrees of freedom couple with the other degrees of freedom such as the kinematic degree of freedom because the color chemical potentials appear explicitly in the quark and gluon partition functions. The color chemical potentials for the colored quarks are represented by the fundamental color chemical potentials while color chemical potentials for the colored gluons are given by the adjoint ones. The imaginary chemical potentials for quarks and gluons are given by the Fourier variables $i\,\theta_i$ with a fundamental index, namely, i that runs over $i = 1, \cdots, N_c$ and $i\,\phi^a \equiv i\,(\theta_A - \theta_B)$ with an adjoint index, namely, $a = \underbrace{(AB)}$ that runs over $a = 1, \cdots, N_c^2 - 1$, respectively. The imaginary fundamental and adjoint color chemical potentials, namely, $i\,\theta_i/\beta$ and $i\,\phi^a/\beta$, respectively, maintain the conservation of color charges and/or project a specific internal color symmetry when they are integrated over the invariance Haar measure and an appropriate color wave-function. It is very relevant to calculate the equation of state with an expansion of the weak coupling corrections for the quark-gluon bag with a specific internal color structure in order to understand the mechanism of the deconfinement phase transition. The real fundamental and adjoint color chemical potentials, namely, $\mu_{C\,i}$ and $\mu_C{}^a = \mu_{C\,A} - \mu_{C\,B}$ for quarks and gluons, respectively, adjust the color fugacities and determine the color densities. Despite of the apparent complexity of the color construction, the calculation is found simple and straightforward. The hard thermal loops with soft and hard momenta are extended

in a straightforward manner to include the color degrees of freedom for quarks and gluons. In general, there is always a way to decompose the external fundamental and adjoint color indexes with respect to the internal loop color indexes. The Fermion plasma frequency is decomposed as follows

$$\begin{aligned}\left(\omega_{0\,Q}^2\right)_{ij} &= \left(\omega_{0\,Q}^2\right)_i\,\delta_{ij},\\ &= \sum_{a}^{N_c^2-1}\sum_{n=1}^{N_c}\mathbf{t}_{in}^a\,\mathbf{t}_{nj}^a\,\left[\left(\omega_{0\,Q(Q)}^2\right)_n+\left(\omega_{0\,Q(G)}^2\right)^a\right],\\ &\qquad\text{(there is no sum over the fundamental color indexes } i\,,\,j),\end{aligned}\tag{410}$$

where

$$\left(\omega_{0\,Q(Q)}^2\right)_n = \frac{g^2}{4\pi^2}\left[\frac{\pi^2}{6}\,T^2+\frac{1}{2}\left(\mu_Q+\mu_{C\,n}\right)^2\right],\tag{411}$$

and

$$\begin{aligned}\left(\omega_{0\,Q(G)}^2\right)^a &= \frac{g^2}{4\pi^2}\left[\frac{\pi^2}{3}\,T^2-\frac{1}{2}\left(\mu_{C\,A}-\mu_{C\,B}\right)^2+i\,\pi\,T\,\left(\mu_{C\,A}-\mu_{C\,B}\right)\right],\\ &\qquad\left(\text{given that } a=\underbrace{(A\,B)}\right).\end{aligned}\tag{412}$$

The external fundamental color indexes $i\,j$ are parametrized in terms of the internal loop's fundamental color index n and the internal loop's adjoint color index a using the matrix elements of fundamental and/or adjoint group generators. The colored gluon's Debye mass is decomposed as follows

$$\begin{aligned}\left(\mathbf{m}_D^2\right)^{a'a} &= \left(\mathbf{m}_D^2\right)^a\,\delta^{aa'},\\ &= \sum_{b,c=1}^{N_c^2-1}\sum_{i,j=1}^{N_c}\left[(\mathbf{T}^{a'})_{cb}\,(\mathbf{T}^a)_{bc}^{\dagger}\,\left(\mathbf{m}_{D\,(G)}^2\right)^b+\mathbf{t}_{ij}^{a'}\,(\mathbf{t}^{a\dagger})_{ji}\,\left(\mathbf{m}_{D\,(Q)}^2\right)_i\right],\\ &\qquad\text{(there is no sum over the adjoint color indexes } a\,,\,a'),\end{aligned}\tag{413}$$

where

$$\begin{aligned}\left(\mathbf{m}_{D\,(G)}^2\right)^b &= \frac{g^2}{\pi^2}\left[\frac{\pi^2}{3}\,T^2-\frac{1}{2}\left(\mu_{C\,A}-\mu_{C\,B}\right)^2+i\,\pi\,T\,\left(\mu_{C\,A}-\mu_{C\,B}\right)\right],\\ &\qquad\left(\text{given that } b=\underbrace{(A\,B)}\right),\end{aligned}\tag{414}$$

and

$$\left(\mathbf{m}_{D\,(Q)}^2\right)_i = \frac{2g^2}{\pi^2}\sum_{Q=1}^{N_F}\left[\frac{\pi^2}{6}\,T^2+\frac{1}{2}\left(\mu_Q+\mu_{C\,i}\right)^2\right].\tag{415}$$

The external adjoint color indexes $a'\,a$ for gluons are parameterized in terms of the internal adjoint color indexes $b\,c$ for the gluon and ghost loops and tadpole as well through the elements of adjoint generators (i.e. adjoint matrices) while they are parameterized in terms of the internal fundamental color indexes $i\,j$ for the quark-loop. The astonished result is that the gluon part of both the fermion Landau frequency and the Debye mass develop an imaginary part for the real flavor and color chemical potentials. This imaginary part is canceled when the color adjoint chemical potentials vanish. This nontrivial solution leads to the conclusion that the fundamental color potential of various color species (i.e. red, green and blue) tend to be equal to each other. However, the equality of the fundamental color potentials is possible in the $U(N_c)$ symmetry group while this equality in the $SU(N_c)$ symmetry group means that the fundamental color potentials are all identical to zero. The possible alternate solution for vanishing the adjoint color chemical potentials is that the quarks could carry all the color information and they do not violate the color species in the interaction. These phenomena enrich the physics of the quark-gluon plasma above the deconfinement phase transition.

On the other hand, the imaginary part disappears when both the imaginary flavor and the imaginary color chemical potentials are adopted in the calculation. The imaginary chemical potentials correspond Fourier variables for the grand canonical ensemble where the flavor and color charges are conserved (i.e. the charge densities are calculated by the Fourier transformation of the Fourier variables). In this case both the flavor and the color fugacities are eliminated.

The gluon polarization tensor usually generates quadratic temperature terms (i.e $\left(\Delta\,\mathbf{m}^2_{D\,(G)}\right)^b \propto T^3$ where b is any internal adjoint color index) in the virtual internal loop interaction level [25–27]. Those quadratic temperature terms are fortunately found to cancel each other in the final result of the polarization tensor for the real colored gluon in the medium. This cancellation takes place when the sum of all the internal adjoint color indexes is considered.

The decay rate for the colored hard quark is written as follows

$$\begin{aligned}\gamma_{Q_{i\,j}} &= \gamma_{Q_i}\,\delta_{ij},\\ &= \sum_{n}^{N_c}\sum_{a}^{N_c^2-1}\,\left(\mathbf{t}^a\right)_{in}\,\left(\mathbf{t}^a\right)_{nj}\,\gamma_{Q_n^a},\\ &\qquad\text{(there is no sum over the fundamental indexes } i\,,\,j),\end{aligned}\tag{416}$$

where the external fundamental color indexes $i\,j$ are coupled to the internal fundamental and adjoint color indexes of the internal loop through the matrix elements of the group generators. The color fugacities enter explicitly the quarks' and gluons' partition functions and moreover they appear explicitly in the fundamental quark and adjoint gluon propagators. They also appears in the physical quantities such as the quark's self-energy and gluon's polarization tensor. The finite color chemical potentials seem to modify the decay rate for the colored hard quarks. Therefore, it is possible at the extreme conditions to see the decay rates of the colored quarks to depend explicitly on the (fundamental-) color chemical potentials. General speaking, despite of the apparent complexity of the internal color structure, it is possible to extend the soft and hard thermal loop calculations to include the color degrees of freedom for quarks and gluons explicitly. The internal color structure of quarks and gluons above the deconfinement phase transition is rich and non-trivial one.

Acknowledgments

The early stages of this work has been supported by Alexander von Humboldt foundation. The author thanks Carsten Greiner and Robert Pisarski for the discussion.

---

[1] I. Zakout and C. Greiner (2010), 1002.3119.

[2] I. Zakout and C. Greiner, Phys. Rev. **C78**, 034916 (2008), 0709.0144.

[3] I. Zakout, C. Greiner, and J. Schaffner-Bielich, Nucl. Phys. **A781**, 150 (2007), nucl-th/0605052.

[4] V. V. Begun, M. I. Gorenstein, and W. Greiner, J. Phys. **G36**, 095005 (2009), 0906.3205.

[5] R. Abir and M. G. Mustafa, Phys. Rev. **C80**, 051903 (2009), 0905.4140.

[6] L. Ferroni and V. Koch, Phys. Rev. **C79**, 034905 (2009), 0812.1044.

[7] J. Noronha-Hostler, M. Beitel, C. Greiner, and I. Shovkovy (2009), 0909.2908.

[8] J. Noronha-Hostler, C. Greiner, and I. A. Shovkovy, Phys. Rev. Lett. **100**, 252301 (2008), 0711.0930.

[9] J. Noronha-Hostler, J. Noronha, and C. Greiner, Phys. Rev. Lett. **103**, 172302 (2009), 0811.1571.

[10] J. Noronha-Hostler, H. Ahmad, J. Noronha, and C. Greiner (2009), 0906.3960.

[11] N. P. Landsman and C. G. van Weert, Phys. Rept. **145**, 141 (1987).

[12] E. Braaten and R. D. Pisarski, Nucl. Phys. **B337**, 569 (1990).

[13] E. Braaten and R. D. Pisarski, Phys. Rev. Lett. **64**, 1338 (1990).

[14] J. Frenkel and J. C. Taylor, Nucl. Phys. **B334**, 199 (1990).

[15] E. Braaten and R. D. Pisarski, Phys. Rev. **D42**, 2156 (1990).

[16] E. Braaten and R. D. Pisarski, Phys. Rev. **D45**, 1827 (1992).

[17] E. Braaten and R. D. Pisarski, Phys. Rev. **D46**, 1829 (1992).

[18] A. V. Smilga, Phys. Rept. **291**, 1 (1997), hep-ph/9612347.

[19] J.-P. Blaizot and E. Iancu, Phys. Rept. **359**, 355 (2002), hep-ph/0101103.

[20] J. P. Blaizot, E. Iancu, and A. Rebhan, Phys. Lett. **B470**, 181 (1999), hep-ph/9910309.

[21] J.-P. Blaizot, E. Iancu, and A. Rebhan (2003), hep-ph/0303185.

[22] H. Vija and M. H. Thoma, Phys. Lett. **B342**, 212 (1995), hep-ph/9409246.

[23] T. Schafer, Nucl. Phys. **A728**, 251 (2003), hep-ph/0307074.

[24] P. Levai and U. W. Heinz, Phys. Rev. **C57**, 1879 (1998), hep-ph/9710463.

[25] Y. Hidaka and R. D. Pisarski, Phys. Rev. **D78**, 071501 (2008), 0803.0453.

[26] Y. Hidaka and R. D. Pisarski, Phys. Rev. **D80**, 036004 (2009), 0906.1751.

[27] Y. Hidaka and R. D. Pisarski (2009), 0912.0940.

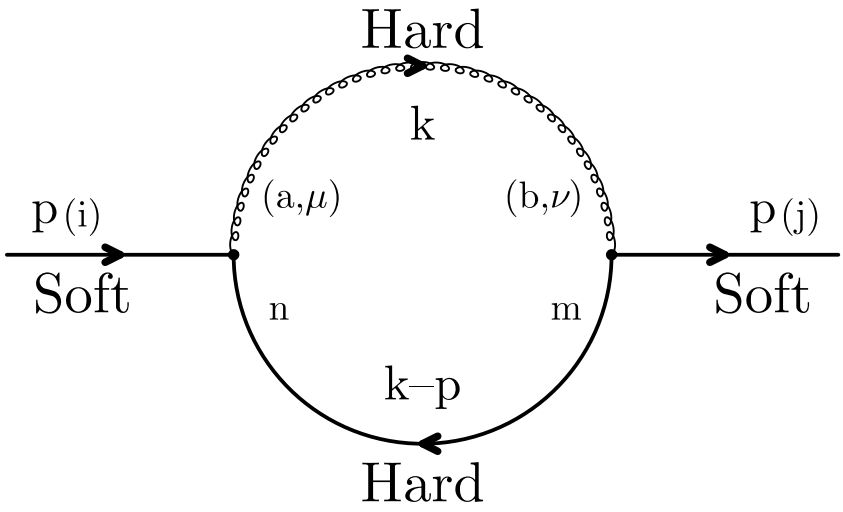

FIG. 1: The soft quark self-energy correction.

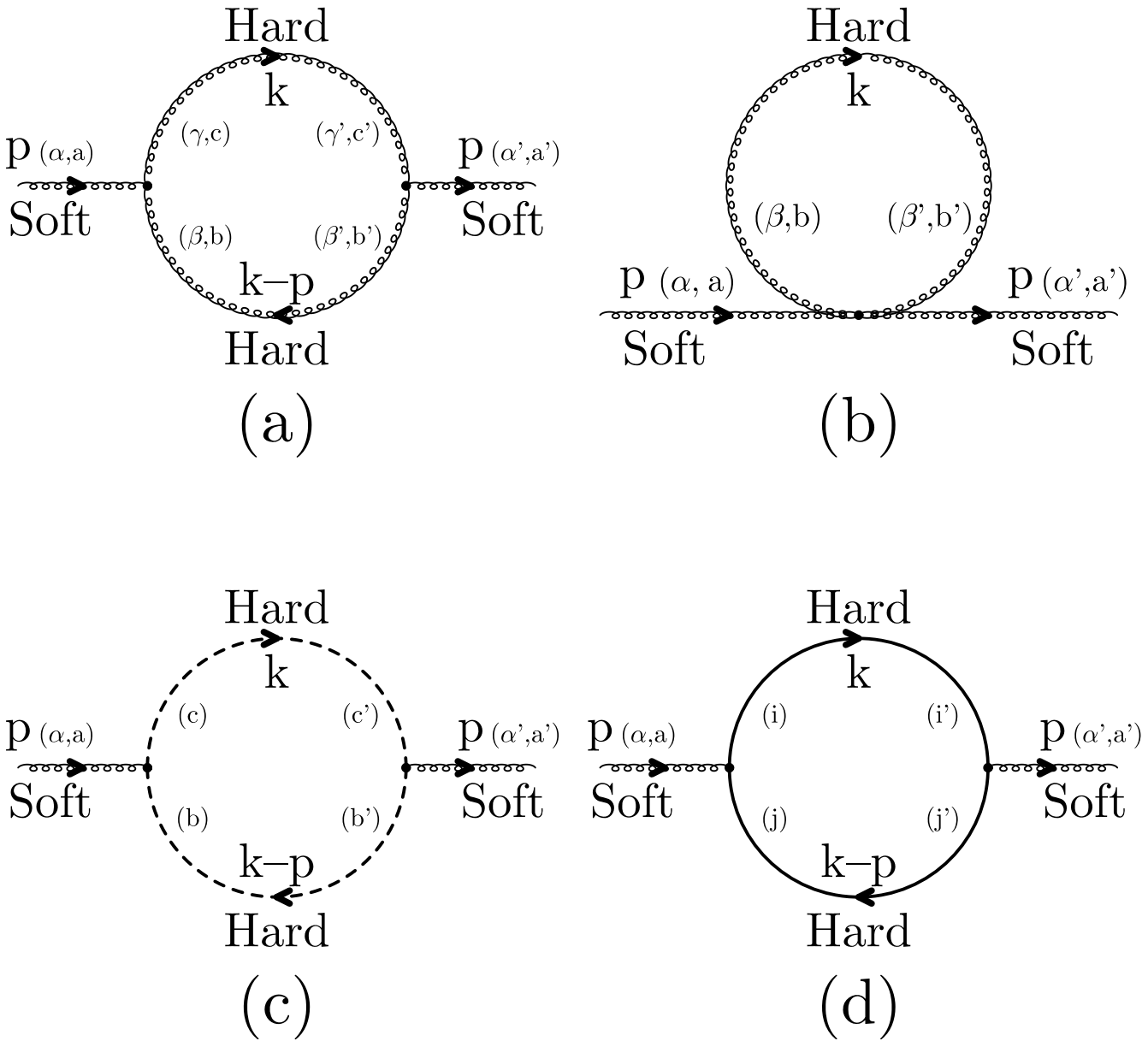

FIG. 2: The soft gluon self-energy correction.

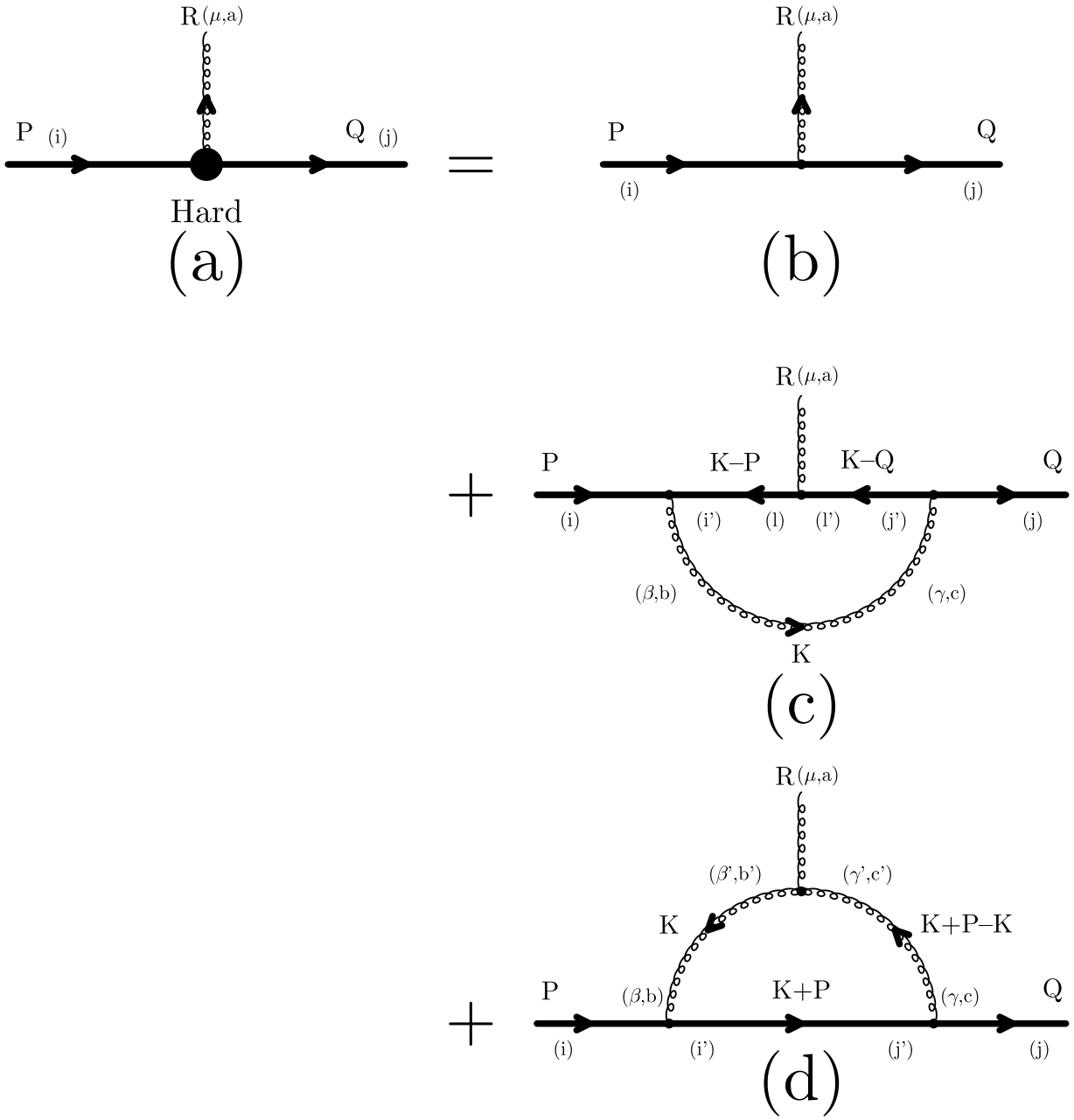

FIG. 3: The effective hard quark-quark-gluon vertex.

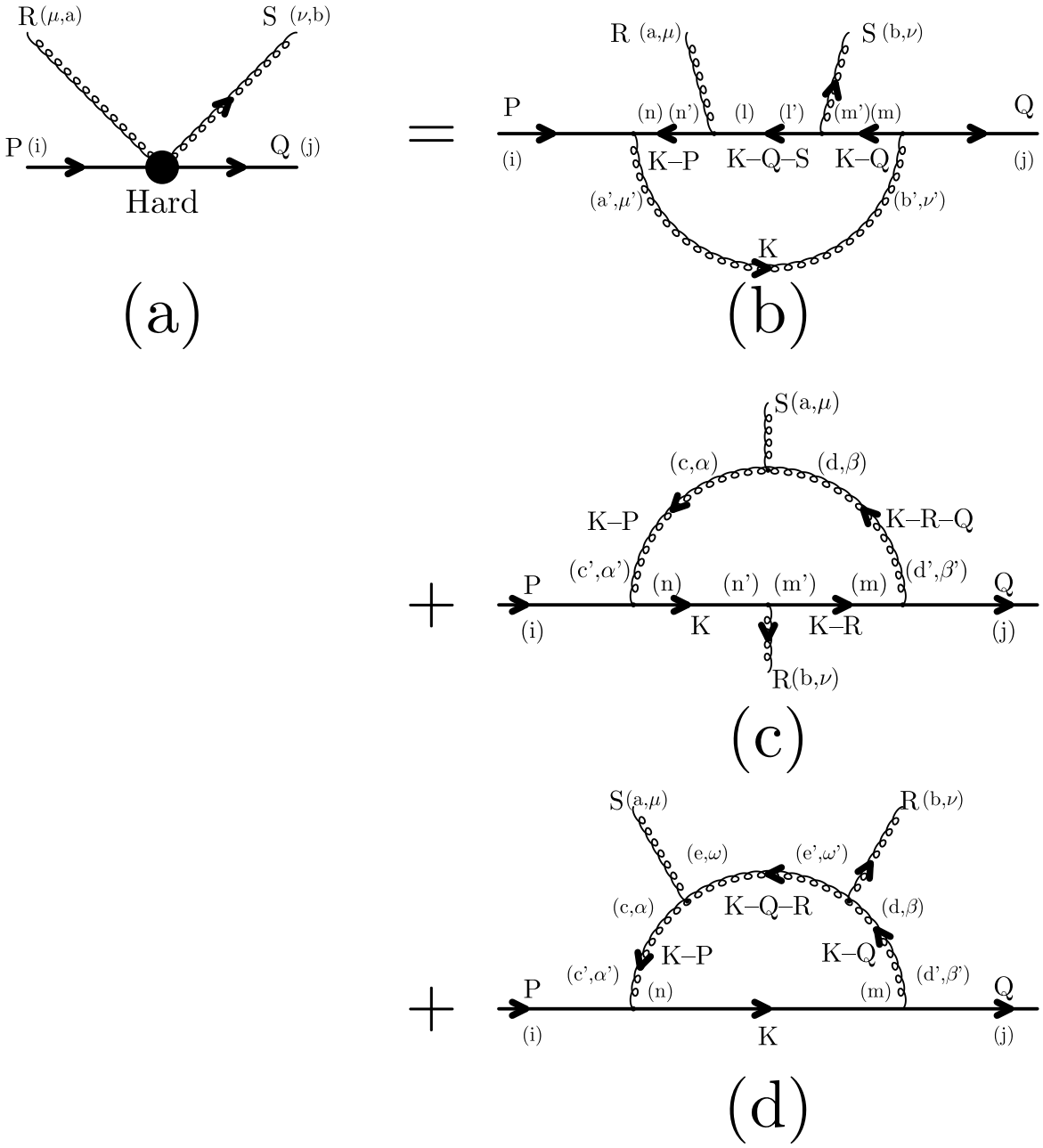

FIG. 4: The effective hard 2-quarks and 2-gluons vertex.

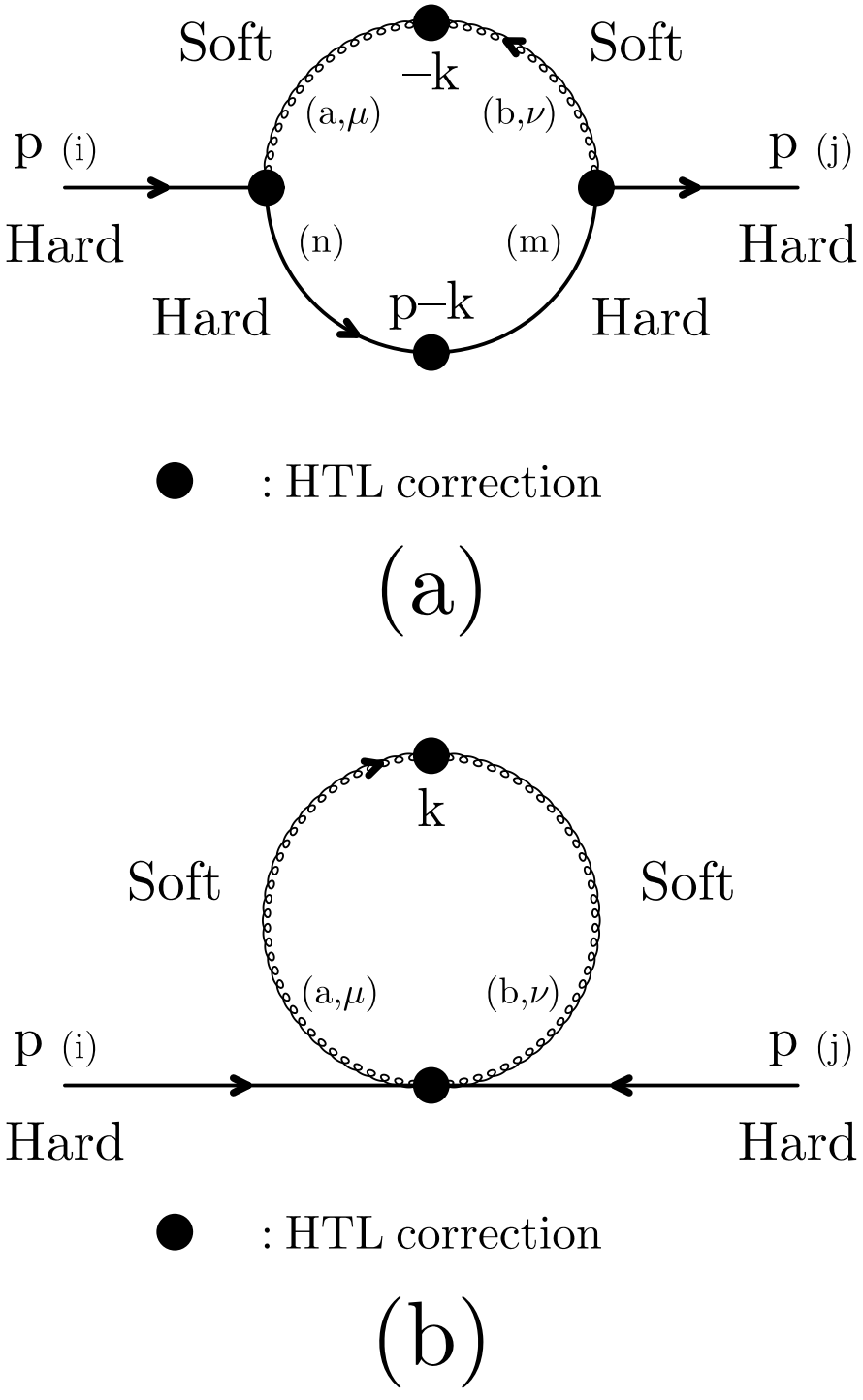

FIG. 5: Effective self-energy for the hard thermal quark.